SMA 20601.01-R1-0

SEISMIC FRAGILITIES OF STRUCTURES AND COMPONENTS AT THE MILLSTONE 3 NUCLEAR POWER STATION

prepared for

NORTHEAST UTILITIES
Hartford, Connecticut

March, 1984

STRUCTURAL MECHANICS ASSOCIATES
A Calif. Corp.
5160 Birch Street, Newport Beach, Calif. 92660 (714) 833-7552

SMA 20601.01-R1-0

SEISMIC FRAGILITIES OF STRUCTURES AND COMPONENTS AT THE MILLSTONE 3 NUCLEAR POWER STATION

by

D. A. Wesley
R. D. Campbell
P. S. Hashimoto
T. R. Kipp
W. H. Tong

prepared for

NORTHEAST UTILITIES
Hartford, Connecticut

March, 1984

STRUCTURAL MECHANICS ASSOCIATES
A Calif. Corp
5160 Birch Street, Newport Beach, Calif. 92660 (714) 833-7552

TABLE OF CONTENTS

TABLE OF CONTENTS (Continued)

TABLE OF CONTENTS (Continued)

TABLE OF CONTENTS (Continued)

TABLE OF CONTENTS (Continued)

TABLE OF CONTENTS (Continued)

TABLE OF CONTENTS (Continued)

1. INTRODUCTION

A probabilistic risk assessment (PRA) of the Millstone 3 Nuclear Power Station is being conducted by Northeast Utilities (NU). In this evaluation, system models, event trees, and fault trees are utilized to determine the frequency of radioactive release from the site due to random equipment failure and failures initiated by natural hazard events. Earthquakes are one of the extreme natural hazards being considered in this PRA. Structural Mechanics Associates, Inc. (SMA) is under contract to NU to provide the required information for earthquake (seismic) capacities of structures and equipment items that are included in the risk models.

The frequency of seismically-induced failure as a function of effective peak ground acceleration for both safety-related structures and equipment has been developed by SMA for the Millstone 3 facility. Also included is the expected variability in the frequency of failure. The determination of the seismic hazard is being conducted by others. The information for both the frequency of occurrence of different levels of effective peak ground acceleration and the frequency of failure of the safety-related systems and components will then be incorporated into the risk models by NU to determine the frequency of seismic-induced radioactive release from the site.

In order to correctly interpret the fragilities derived in this report, it is necessary to define the effective peak acceleration to which these fragilities are anchored. It is recognized that the damage potential of an earthquake depends on many factors, among which are magnitude, peak acceleration, and duration. For the Millstone site, it is estimated that the majority of seismic risk results from earthquakes that have magnitudes between 5.3 and 6.3. This is the range represented by the ground response spectra used to evaluate the fragilities. Because

the ground response spectra used in this study are centered around this magnitude range, the fragilities given in this report are to be anchored to the mean peak acceleration. This acceleration is the average of the peak accelerations from two orthogonal horizontal components. Note that if the magnitude range were different, say 6.0 to 7.0, a somewhat different set of median spectra would be required.

The Millstone 3 Nuclear Power Station was designed in the 1970's in accordance with criteria and codes in effect at that time (Reference 1). Table 1-1 lists some of the more important codes and specifications used in design of the structures. The Millstone 3 systems and components which are essential to the prevention or mitigation of consequences of accidents which could affect the public health and safety were designed to enable the facility to withstand the effects of natural forces including earthquakes. The design criteria included the effects of simultaneous earthquake and loss-of-coolant-accident (LOCA) conditions. The plant was designed to withstand both an Operating Basis Earthquake (OBE) and a Safe Shutdown Earthquake (SSE). The structural design criteria for the SSE was based on 0.17g and the OBE on 0.09g peak horizontal ground accelerations for all Seismic Category I structures. Vertical accelerations of two-thirds of the corresponding horizontal values were used for both the OBE and SSE.

The plant structures and equipment were originally divided into two categories according to their function and the degree of integrity required to protect the public. These categories are Category I and non-Category I. Millstone 3 Nuclear Power Station structures, systems and components important to safety, as well as their foundations and supports, were designed to withstand the effects of an OBE and an SSE and were, thus, designated as Seismic Category I. Seismic Category I structures include:

Containment and Internal Structure
Containment Enclosure Building
Auxiliary Building
Fuel Building (Partially)
Control Building
Cable Tunnel
Emergency Generator Enclosure and Diesel Building
Fuel Oil Tank Vault
Engineered Safety Features Building
Main Steam Valve Building
Circulating and Service Water Pumphouse (Partially)
Hydrogen Recombiner Building
Circulating Water Discharge Tunnel
and Discharge Structure
Railroad Canopy
Refueling Water Storage Tank (RWST)
Demineralized Water Storage Tank (DWST)

Not all of these structures house equipment which is important to prevent core melt. For instance, the Fuel Building, Hydrogen Recombiner Building, and Railroad Canopy were designed as Category I structures but are not essential to prevent core melt. Other structures such as the Turbine Building and the Containment Enclosure Building were evaluated only to the extent that their failure could cause damage to one of the essential structures. The structures evaluated in detail consist of:

Reactor containment building and concrete internals structures
Engineered safety features building
Auxiliary building
Control building
Emergency generator enclosure
Service water pumphouse

The Millstone 3 site is located on the Millstone Point near Niantic Bay on the south shore of Connecticut on the Long Island Sound. The site consists of competent rock overlain in some areas by ablation till and dense basal till. Plant grade is at approximately El. 24 ft. The following elastic constants were developed for use in the design analysis of the structures dynamic response:

Material	Young's Modulus, E (psi)	Shear Modulus, G (psi)	Poisson's Ratio
Rock	$4x10^6$	$1.5x10^6$	0.33
Basal Till	$4x10^5$	$1.4x10^5$	0.44
Ablation Till	$2x7x10^4$	$9.0x10^3$	0.49

Most structures important to safety are founded on bedrock with the exception of the Emergency Generator Enclosure and the Control Building. The Control Building is founded on 1 to 4 feet of structural backfill overlying 1 to 15 feet of basal till. The Emergency Generator Enclosure is founded on approximately 20 feet of structural backfill overlying a 20 foot thick layer of basal till. No evaluation of any possible soils-related failures was conducted. The Demineralized Water Storage Tank is founded on concrete fill to bedrock. The effects of the soil-structure interaction for structures founded on fill was accounted for in the design analysis using finite element methods. For structures founded on bedrock, elastic half-space springs based on the rock properties were used.

The ground response spectra used in the design of Millstone 3 are Newmark-type spectra which are similar to those recommended in USNRC Regulatory Guide 1.60 (Reference 2). The horizontal ground response spectra are anchored to 0.17g for the SSE and 0.09g for the OBE. The horizontal spectra used for design are shown in Figures 1-1 and 1-2.

Both modal response spectrum and modal time-history analyses were conducted for the Millstone 3 Category I structures. In general, the response spectrum analysis results were used for evaluation of the structure seismic loads and stresses while time-history results were used to generate in-structure response spectra for the design and evaluation of

piping and equipment. The synthetic time-histories were generated based on the ground response spectra. Comparisons of the ground response spectra generated by these artificial time-history records compared to the SSE design spectra are shown in Figures 1-3 through 1-6 for 2, 5, 7 and 10 percent damping (Reference 1).

Structures, equipment, and components which are important to plant operation, but are not essential for preventing an accident which would endanger the public health and safety and are not essential for the mitigation of the consequences of these accidents, are classified as non-Category I. An example of a non-Category I structure is the Turbine Building. Non-Category I structures were investigated in this project only to the extent their failure could damage a safety-related structure or component. Examples of non-Category I equipment include the offsite power and the station power transformers.

For the most part, results of existing analyses and evaluations of structures and equipment for the Millstone 3 plant were utilized in this study. As part of this evaluation, some limited analysis based on original design analysis loads was conducted to determine the expected seismic capacities of the important structures. The approach adopted in this study was to determine the median factor of safety and its statistical variability which exists for the SSE in order to estimate the expected response at failure. The median effective peak ground acceleration was used to define failure, rather than an instrumental peak acceleration which is not considered to be as accurate a descriptor of damage. It is known that earthquakes with only one or two high acceleration spikes are not as damaging to structures and equipment as longer duration earthquakes with multiple peaks at close to the maximum acceleration level. This is because the shorter duration earthquakes do not have sufficient energy content to develop resonances. For this reason, the fragility evaluations described in this report are keyed to an effective peak acceleration and an earthquake of the duration expected at Millstone 3. This type of earthquake is expected to develop narrow band response spectra.

An evaluation of the individual important structures and some of the equipment was conducted for specific items and failure modes. However, much of the piping and equipment were evaluated on the basis of a number of generic categories. Although inelastic energy dissipation is included in determining the factors of safety, no nonlinear analyses have been conducted for either the structures or equipment for Millstone 3, and all evaluations were based on elastic analysis and load distributions.

These results can be used together with the estimated annual frequency of occurrence of various ground motion levels to determine the frequency of seismic-induced failure for each safety-related structure or component in the plant. In the total study, these conditional component failure frequencies are used with systems models to determine the probability of core melt frequencies and radioactive release frequencies. These results are then combined with the results of the consequence analysis to determine the risks induced by earthquakes.

TABLE 1-1

CODES AND STANDARDS USED IN THE DESIGN OF CATEGORY I STRUCTURES (REFERENCE 1)

	Structural Component	Design Codes and Specifications
1.	ACI 211.1-70	Recommended Practice for Selecting Proportions for Normal Weight Concrete
2.	ACI 214-65	Recommended Practice for Evaluation of Compression Test Results of Field Concrete
3.	ACI 301-72	Specification for Structural Concrete for Buildings
4.	ACI 304-59	Recommended Practice for Measuring, Mixing, and Placing Concrete
5.	ACI 305-72	Recommended Practice for Hot Weather Concreting
6.	ACI 306-66	Recommended Practice for Cold Weather Concreting
7.	ACI 318-71	Building Code Requirements for Reinforced Concrete
8.	ACI 347-68	Recommended Practce for Concrete Formwork
9.	AISC	Specification for the Design, Fabrication and Erection of Structural Steel for Buildings Seventh Edition (February 12, 1969); Supplement No. 1 (November 1, 1970), Supplement No. 2 (December 8, 1971), and Supplement No. 3 (June 12, 1974)
10.	AISC	Specification for Structural Joints Using ASTM A325 or A490 Bolts (April 18, 1972)
11.	ASTM A 36-74	Specification for Structural Steel
12.	ASTM A 193-73	Standard Specification for Alloy Steel and Stainless Steel Bolting Materials for High-Temperature Services

TABLE 1-1 (Continued)

CODES AND STANDARDS USED IN THE DESIGN OF CATEGORY I STRUCTURES (REFERENCE 1)

Structural Component	Design Codes and Specifications
13. ASTM A 307-74	Specification for Low Carbon Steel Externally and Internally Threaded Standard Fasteners
14. ASTM A 325-74	Specification for High Strength Bolts for Structural Steel Joints Including Suitable Nuts and Plain Hardened Washers
15. ASTM A 440-74	Specification for High Strength Structural Steel
16. ASTM A 441-74	Specification for High Strength Low-Alloy Structural Manganese Vanadium Steel
17. ASTM A 490-74	Specification for Quenched and Tempered Alloy Steel Bolts for Structural Steel Joints
18. ASTM A 588-79	Specification for High-Strength Low-Alloy Structural Steel with 50,000 psi Minimum Yield Point to 4 Inches Thick
19. ASTM A 615-68	Standard Specification for Deformed Billet Steel Bars for Concrete Reinforcement including Supplement S-1 (December, 1972)
20. ASTM C 31-69	Making and Curing Concrete Compressive and Flexural Strength Test Specimens in the Field
21. ASTM C 33-71	Standard Specification for Concrete Aggregates (and 1978 Revision)
22. ASTM C 94-71	Specification for Ready-Mixed Concrete
23. ASTM C 109-1973	Method of Test for Compressive Strength of Hydraulic Mortars (using 2-inch (50 mm) Cube Specimens)
24. ASTM C 143-71	Method of Test for Slump of Portland Cement
25. ASTM C 150-73	Specification for Portland Cement
26. ASTM C227-71	Test for Potential Reactivity of Cement Aggregate Combinations (Mortar Bar Method)

TABLE 1-1 (Continued)

CODES AND STANDARDS USED IN THE DESIGN OF CATEGORY I STRUCTURES (REFERENCE 1)

Structural Component	Design Codes and Specifications
27. ASTM C 233-69	Standard Method of Testing Air-entraining Admixtures for Concrete
28. ASTM C 260-69	Air-entraining Admixtures for Concrete
29. ASTM C 289-71	Test for Potential Reactivity of Aggregates (Chemical Method)
30. ASTM C 295-1965 (1973)	Recommended Practice for Petrographic Examination of Aggregates for Concrete
31. ASTM C 586-69	Test for Potential Alkali Reactivity of Carbonate Rocks for Concrete Aggregates
32. AWS D1.1-72 Rev. 1-73	Structural Welding Code
33. AWS D12.1-61	Recommended Practices for Welding Reinforcing Steel, Metal Inserts and Connections in Reinforced Concrete Construction
34. NRC Regulatory Guides as qualified in FSAR Section 1.8 (Reference 1) on the following topics:	
a. Cadweld Splices	1.8.1.10
b. Reinforcing Bar Testing	1.8.1.15
c. Structural Acceptance Testing	1.8.1.18
d. Placement of Concrete	1.8.1.55
e. Design Response Spectra	1.8.1.60
f. Seismic Damping Values	1.8.1.61
35. BOCA	Basic Building Code of the Building Officials and Code Administrators International, Inc., 1970
36. State of Connecticut Basic Building Code, 1971	

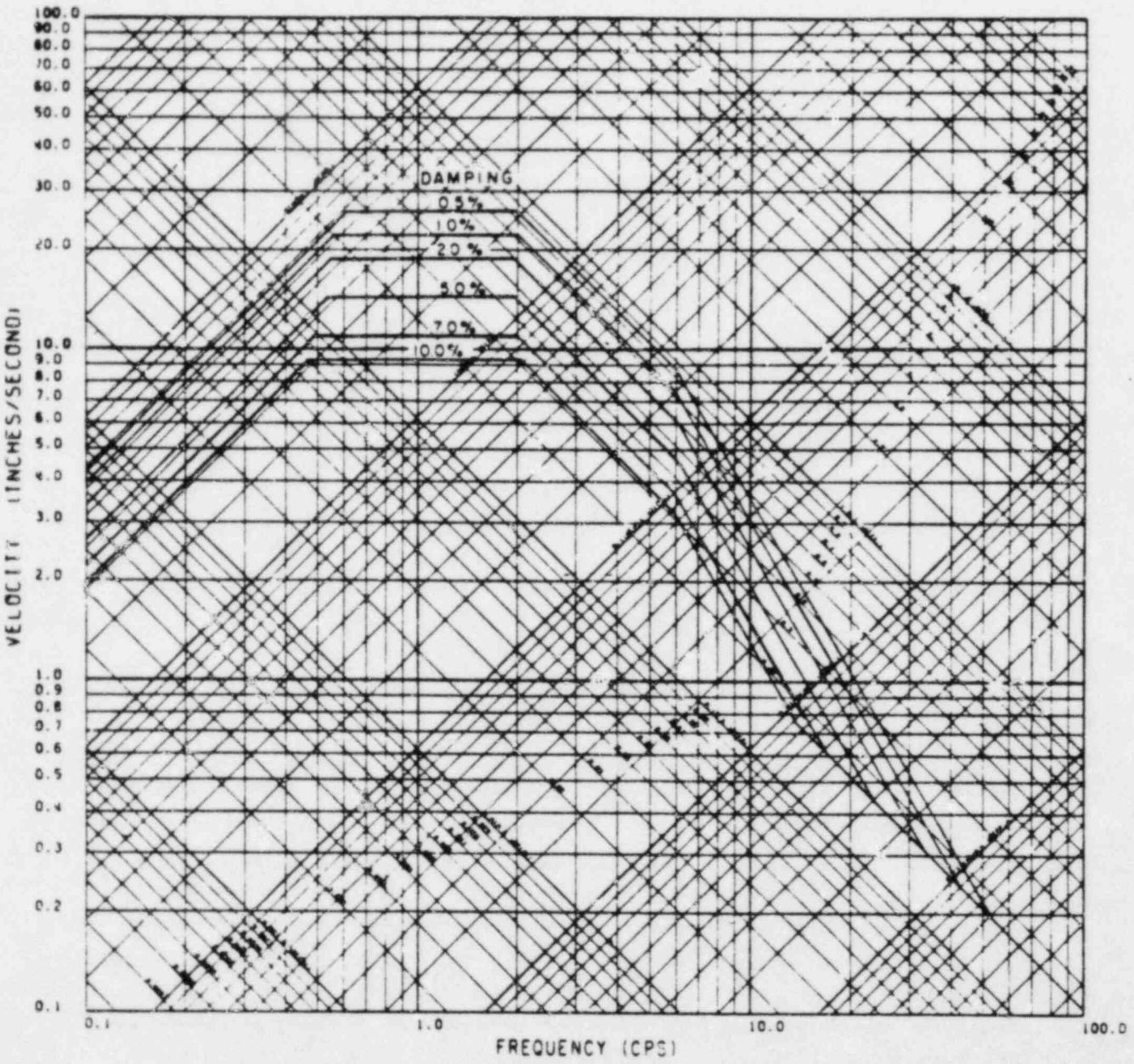

FIGURE 1-1. SSE HORIZONTAL GROUND RESPONSE SPECTRA

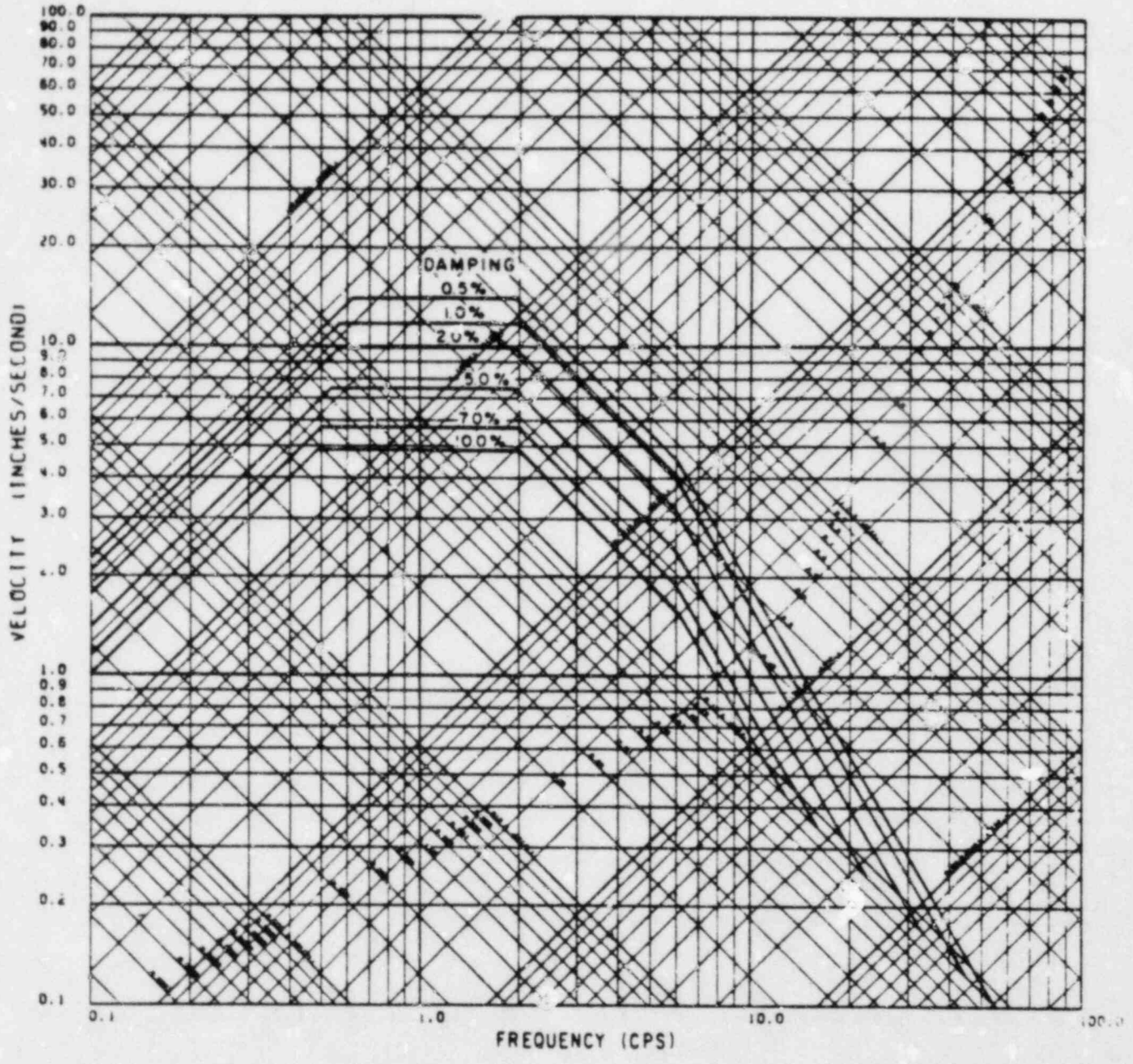

FIGURE 1-2. OBE HORIZONTAL GROUND RESPONSE SPECTRA

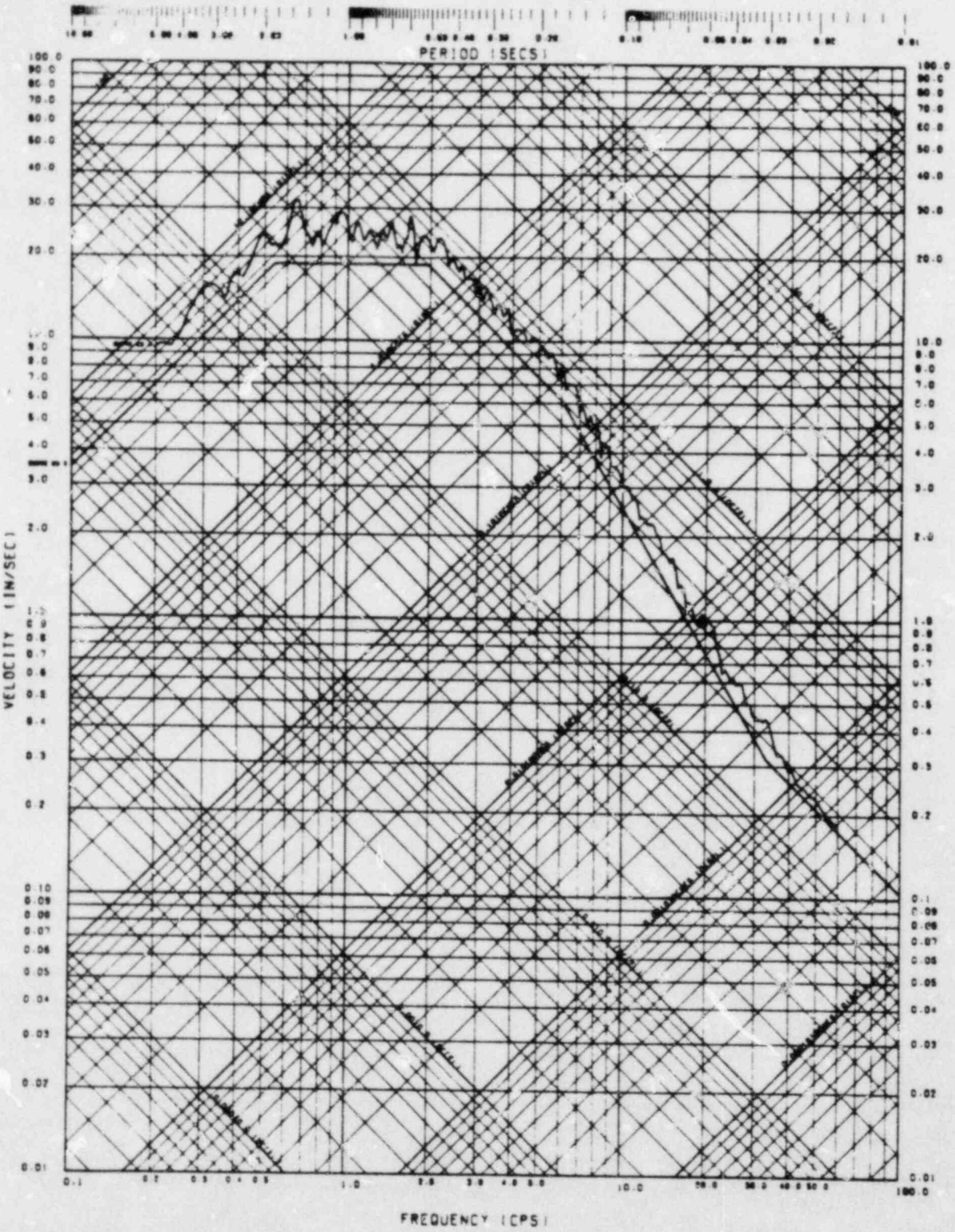

FIGURE 1-3. COMPARISON OF ARTIFICIAL EARTHQUAKE TIME HISTORY SPECTRUM WITH SSE DESIGN SPECTRUM (2% DAMPING)

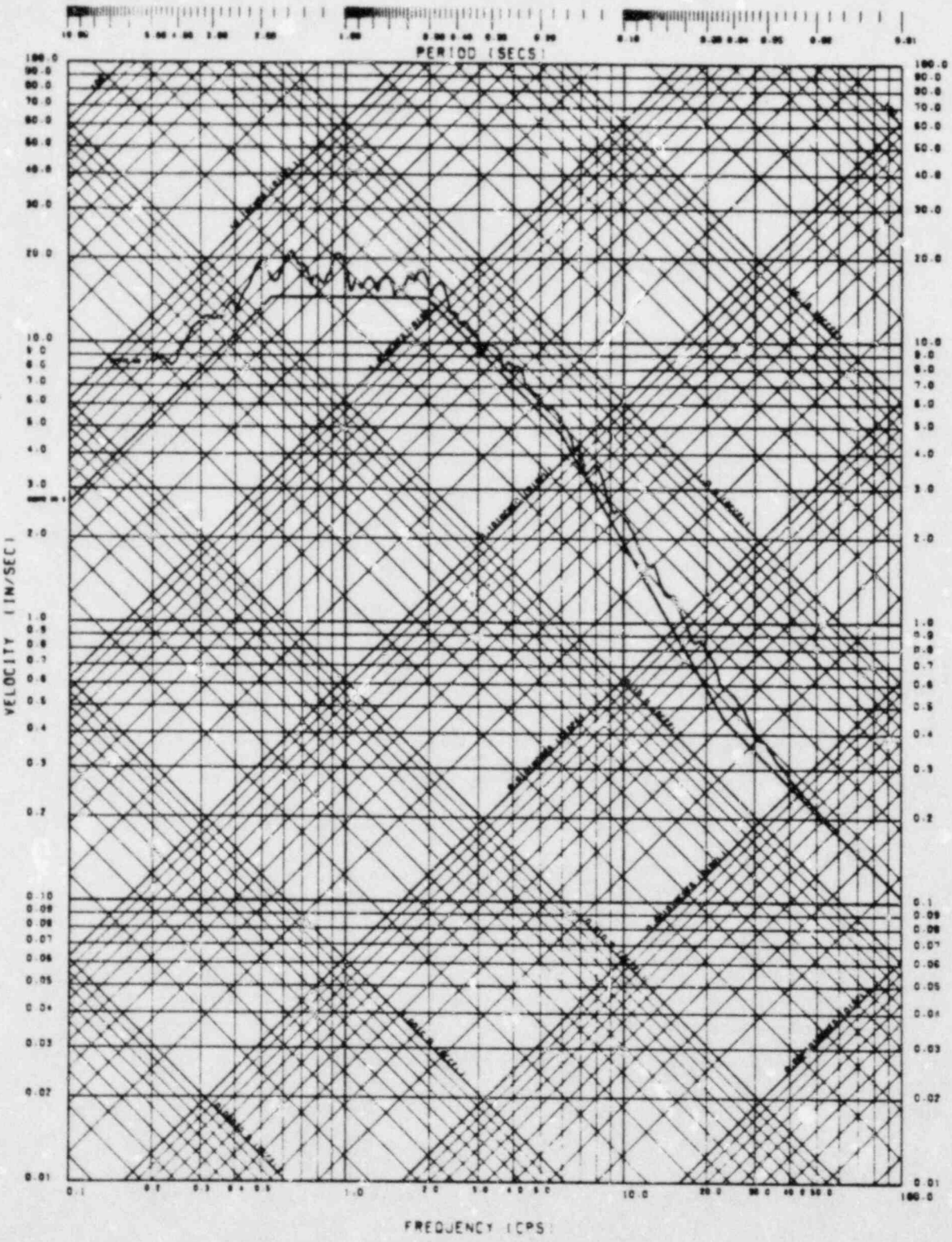

FIGURE 1-4. COMPARISON OF ARTIFICIAL EARTHQUAKE TIME HISTORY SPECTRUM WITH SSE DESIGN SPECTRUM (5% DAMPING)

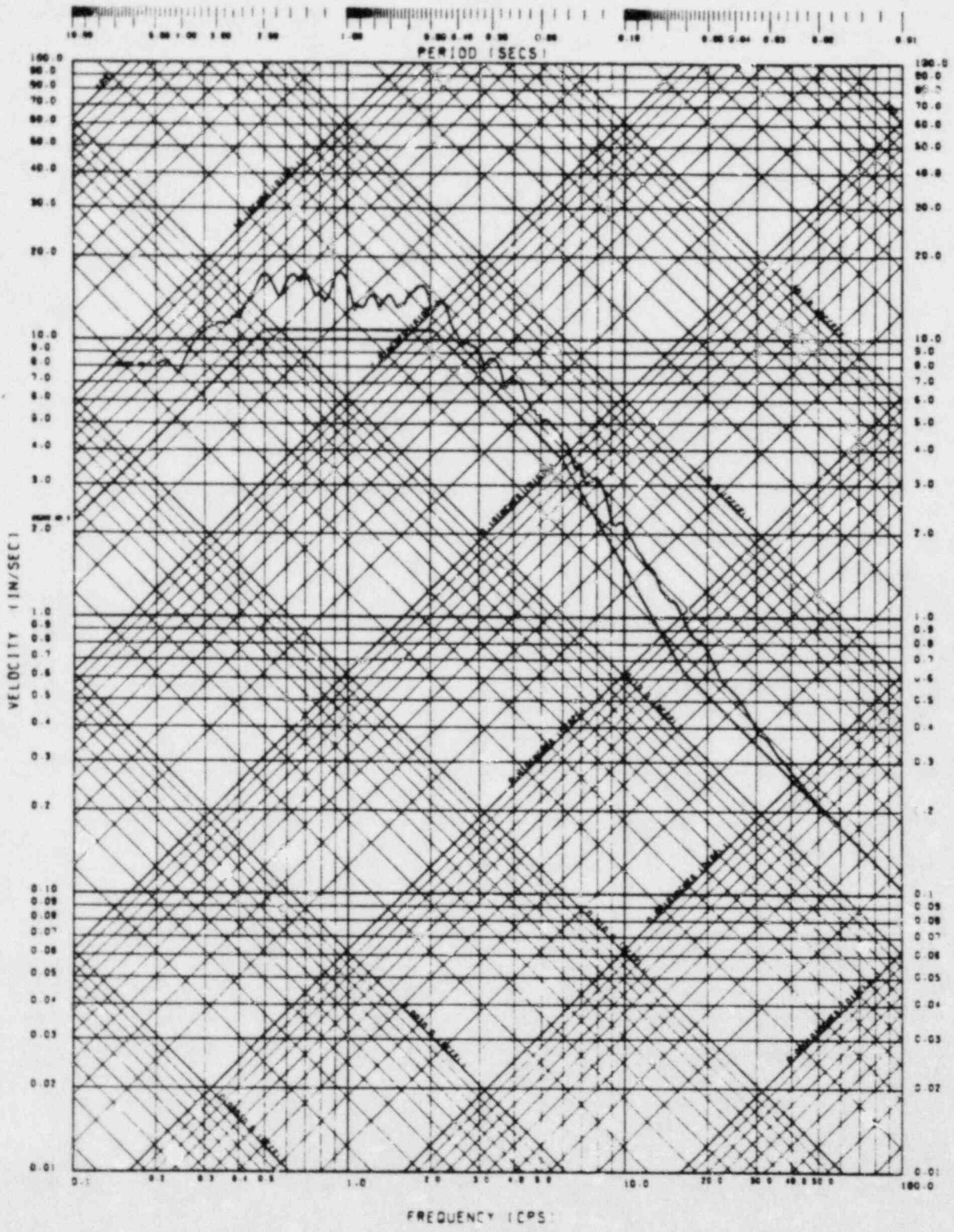

FIGURE 1-5. COMPARISON OF ARTIFICIAL EARTHQUAKE TIME HISTORY SPECTRUM WITH SSE DESIGN SPECTRUM (7% DAMPING)

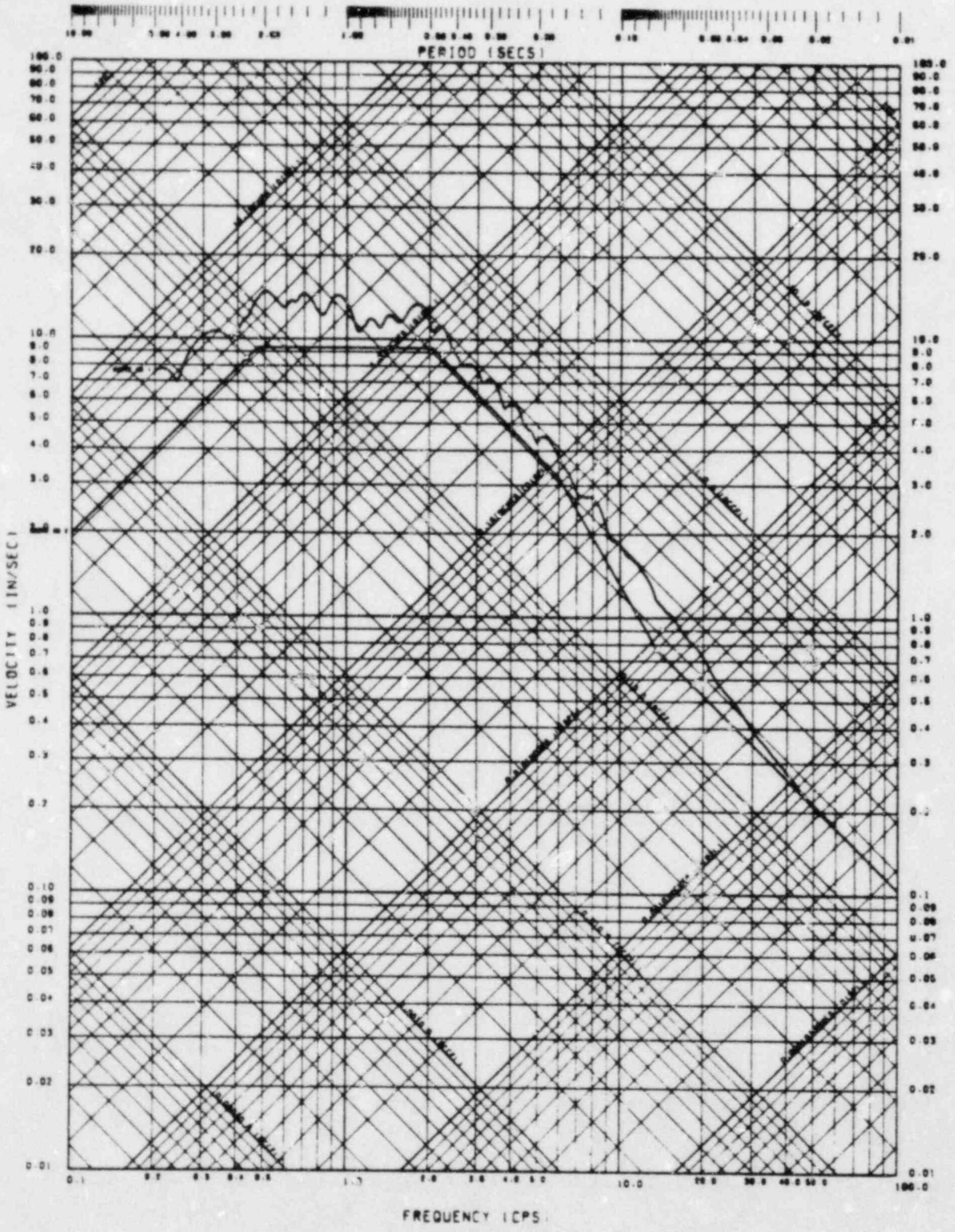

FIGURE 1-6. COMPARISON OF ARTIFICIAL EARTHQUAKE TIME HISTORY SPECTRUM WITH SSE DESIGN SPECTRUM (10% DAMPING)

2. GENERAL CRITERIA FOR DEVELOPMENT OF MEDIAN SEISMIC SAFETY FACTORS

The factor of safety of a structure or component is defined herein as the resistance capacity divided by the response associated with the Safe Shutdown Earthquake (SSE) of 0.17g effective peak acceleration. The development of seismic safety factors associated with the SSE is based on consideration of several variables. The variability of dynamic response to the specified acceleration and the strength capacity of the structure or equipment component are the two basic considerations in determining the variability in the factor of safety. Several variables are involved in determining both the structural response and the structural capacity, and each such variable, in turn, has a median factor of safety and variability associated with it. The overall factor of safety is the product of the factors of safety for each variable. The median of the overall factor of safety is the product of the median safety factors of all the variables. The variabilities of the individual variables also combine to determine that of the overall safety factor.

Variables influencing the factor of safety on structural capacity to withstand seismic-induced vibration include the strength of the equipment or structure compared to the design stress level and the inelastic energy absorption capacity (ductility) of a structure or its ability to carry load beyond yield. The variability in computed structural response for a given effective peak free-field ground acceleration is made up of many factors. The more significant factors include variability in (1) ground motion and the associated ground response spectra for a given peak free-field ground acceleration, (2) energy dissipation (damping), (3) structural modeling, (4) method of analysis, (5) combination of modes, (6) combination of earthquake components, and (7) soil-structure interaction. For structures which may be susceptible to sliding, the variability in the amount of sliding is also significant.

Equipment located inside a building acts as a secondary system and requires the previously mentioned structural response factors together with a similar set of equipment response factors which are specific to the equipment itself (see Chapter 5). The ratio between the median value of each of these factors and the value used in design of the Millstone 3 plant and the variability of each factor are quantitatively estimated in Chapters 4 and 5 for various structures and components. These estimates are based on available test data for Millstone 3 structures and equipment, limited analysis, and engineering judgment and experience in the analysis of nuclear power plants and components.

2.1 DEFINITION OF FAILURE

In order to estimate the median factor of safety against the structure or component failure for the SSE effective peak acceleration (0.17g), it is necessary to define what constitutes failure.

2.1.1 Seismic Category I Structures

For purposes of this study, Category I structures are considered to fail functionally when inelastic deformations of the structure under seismic load are estimated to be sufficient to potentially interfere with the operability of safety-related equipment attached to the structure. These limits on inelastic energy absorption capability (ductility limits) chosen for Category I structures are estimated to correspond to the onset of significant structural damage. For many potential modes of failure, this is believed to represent a conservative bound on the level of inelastic structural deformation which might interfere with the operability of components housed within the structure. It is important to note that considerably greater margins of safety against structural collapse are believed to exist for these structures than many cases reported within this study. Thus, the conditional probabilities of failure for a given free-field ground acceleration reported herein for Catetory I structures are considered appropriate for equipment operability limits and should not necessarily be inferred as corresponding to

structure collapse. Structures which are susceptible to sliding are considered to have failed when sufficient sliding deformation is incurred to fail buried or interconnecting piping or electrical duct banks.

2.1.2 Seismic Category I Equipment and Piping

Piping, electrical, mechanical and electro-mechanical equipment vital to safe shutdown of the plant or mitigation of an accident are considered to fail when they will no longer perform their designated functions. Rupture of the pressure boundary on mechanical equipment is also considered a failure. Therefore, for mechanical equipment, a dual failure definition exists: failure to function and pressure boundary rupture. Depending upon the equipment type, one or the other definition will govern. For active equipment, the functional failure definition usually governs as equipment pressure boundaries are generally very conservatively designed for equipment such as pumps and valves. For piping, failure of the support system or plastic collapse of the pressure boundary are considered to represent failure. The inelastic energy absorption limits (ductility limits) associated with these failure modes have been conservatively estimated in order to define the margins of safety.

2.1.3 Non-Category I Structures

In the Millstone 3 plant, no components identified as important to safety are located within non-Category I buildings. The non-Category I structures are separated from Category I structures. The turbine building was evaluated only for the failure modes deemed likely to damage the adjacent important structures. No other non-Category I structures were analyzed since failures in these structures were judged to have no effect on any Category I building.

2.1.4 Non-Seismic Category I Equipment and Piping

Failure of non-seismic Category I piping, electrical, mechanical and electro-mechanical equipment is defined as for Category I equipment;

i.e., failure to perform its intended function or failure of the pressure boundary. No items of non-seismic Category I equipment whose failure is likely to cause damage to safety-related equipment were identified during the plant visit.

2.2 BASIS FOR SAFETY FACTORS DERIVED IN STUDY

There was a general lack of detailed information available for this study on seismic fragility of specific Millstone 3 structures and equipment. This condition exists for all plants and occurs because existing codes and standards do not require determination of ultimate seismic capacities, either for structures or equipment qualified by analysis, or for equipment or components qualified by testing. Therefore, most median safety factors, estimates of variability, and conditional frequencies of failure estimated in this study are based on existing analyses and qualified engineering judgment and assumptions. Limited additional analyses were conducted to evaluate the expected failure capacities of the important structures. The additional analyses were based for the most part on the original design analyses which were available, however. Some additional analyses were conducted to develop structural loads and load distributions for several structures.

2.2.1 Structural Response and Capacity

The results from dynamic analyses which were used in the design of the important structures were extensively used in this study. These were supplemented as required to provide estimates of load redistributions resulting from localized failures, etc. Levels of conservatism associated with the method of analysis used in design were estimated such that safety factors reflecting this analysis could be estimated for the building structures and for the seismic excitation of equipment mounted within the building.

Detailed structural design calculations were not reviewed, but the design criteria used in design as defined in the FSAR (Reference 1) were reviewed. Some ultimate load capacity analyses were conducted which served as a basis for estimating the median factor of safety on structural resistance to the SSE.

2.2.2 Seismic Category I Piping and Equipment Response and Capacity

For most of the safety-related equipment, information on analysis methods was available in summary form in the FSAR. Seismic response information for the selected sample of safety-related equipment evaluated in this study was obtained from available vendor seismic qualification reports or design calculations for specific components. In some cases such as for piping, only the seismic analysis requirements and stress acceptance criteria were known. Safety factors for response and structural or functional capacity were estimated from existing information. No new analyses were conducted.

In-structure response spectra for all Category I structures were generated during the design process. From these typical floor response spectra and knowledge or estimates of equipment fundamental frequencies, an estimate is made of the peak equipment response. The peak equipment response estimate is then compared to the dynamic response or equivalent static coefficient used in design to determine a median safety factor on response.

Capacity factors are derived from several sources of information; plant-specific design reports, test reports, generic fragility test data from military test programs and generic analytical derivations of capacity based on governing codes and standards. Two failure modes are considered in developing capacity factors for piping and equipment: structural and functional. Equipment and piping design reports delineate stress levels for the specified seismic loading plus normal operating conditions. Where the equipment fails in a structural mode (i.e., pressure boundary rupture or loss of support), the median capacity factor and its variability are derived in the same manner as for structures considering strength and energy absorption (ductility). In cases where equipment must function, the capacity factor is derived by comparing the equipment functional failure (or fragility) level to the design level of seismic loading. Some fragility test data are available on generic classes of equipment that have been utilized in hardened military

installations. Such equipment was off-the-shelf without special shock-resistant design but is similar to nuclear power plant equipment. These data provide estimates of the fragility levels, and thus, safety factors can be developed for the specified design earthquake. Fragility levels are not normally determinable from equipment qualification reports, but the achieved test levels can be utilized to update generic fragilities derived from the military data.

2.3 FORMULATION USED FOR FRAGILITY CURVES

Seismic-induced fragility data are generally unavailable for specific plant components and are certainly unavailable for the specific Millstone 3 structures. Thus, fragility curves must be developed primarily from analysis combined heavily with engineering judgment supported by very limited test data. Such fragility curves will contain a great deal of uncertainty, and it is imperative that this uncertainty be recognized in all subsequent analyses. Because of this uncertainty, great precision in attempting to define the shape of these curves is unwarranted. Thus, a procedure which requires a minimum amount of information, incorporates uncertainty into the fragility curves, and easily enables the use of engineering judgment, was used in this study.

The entire fragility curve for any mode of failure and its uncertainty can be expressed in terms of the best estimate of the median ground acceleration capacity, $\breve{A}$, times the product of random variables. Thus, the ground acceleration, A, corresponding to failure is given by:

$$A = \breve{A}\, \varepsilon_R\, \varepsilon_U \qquad (2\text{-}1)$$

in which ε_R and ε_U are random variables with unit median representing the inherent randomness (failure fraction) about the median and the uncertainty (probability) in the median value, respectively. Equation 2-1 enables the fragility curve and its uncertainty to be represented as shown in Figure 2-1; i.e., as a set of shifted curves with attached uncertainty levels. Thus, it is assumed that all uncertainty in the fragility curves can be expressed through uncertainty in the median alone.

Next, it is assumed that both ε_R and ε_U are lognormally distributed with logarithmic standard deviations of β_R and β_U, respectively. The advantages of this formulation are:

1. The entire fragility curve and its uncertainty can be expressed by three parameters - $\breve{A}$, ε_R, and ε_U. With the very limited available data on fragility, it is much easier to only estimate three parameters rather than the entire shape of the fragility curve and its uncertainty.

2. The formulation in Equation 2-1 and the lognormal distribution are very tractable mathematically.

Another advantage of the lognormal distribution is that it is easy to convert Equation 2-1 to a deterministic composite "best estimate" fragility curve (i.e., one which does not separate out uncertainty from underlying randomness) defined by:

$$A = \breve{A}\,\varepsilon_C \tag{2-2}$$

where ε_C is a lognormal random variable with unity median and logarithmic standard deviation β_C given by:

$$\beta_C = \sqrt{\beta_R^2 + \beta_U^2} \tag{2-3}$$

This composite fragility curve (shown in Figure 2-1) can be used in preliminary deterministic safety analyses if one only needs a "best estimate" on failure fraction and does not desire an estimate of uncertainty. In this study, the guidelines used to estimate the values of β_R and β_U for each variable affecting A were based on considering the inherent randomness, β_R, to be associated with the earthquake characteristics themselves, and β_U to be associated with other lack of knowledge. Thus, such variability as resulting from earthquake response spectra shapes and amplification, earthquake duration, numbers and phasing of peak

excitation cycles, etc., together with their contributions to structure ductility and response characteristics is attributed to randomness. In general, it is not considered possible to significantly reduce randomness by additional analysis or test based on current state-of-the-art techniques. Uncertainty, on the other hand, is considered to result primarily from analytical modeling assumptions and other lack of knowledge concerning variables such as material strength, damping, etc., which could in many cases be reduced by additional study or test.

The lognormal distribution can be justified as a reasonable distribution since the statistical variation of many material properties (References 3 and 4) and seismic response variables may reasonably be represented by this distribution (Reference 5). In addition, the central limit theorem states that a distribution consisting of products and quotients of distributions of several variables tends to be lognormal even if the individual distributions are not lognormal. Use of this distribution for estimating failure fractions on the order of one percent or greater is considered to be quite reasonable. Lower fraction estimates which are associated with the extreme tails of the distributions must be considered less accurate.

Use of the lognormal distribution for estimating very low failure fractions of components or structures associated with the tails of the distribution is considered to be conservative because the low-frequency tails of the lognormal distribution generally extend farther from the median than actual structural resistance or response data might indicate. Such data generally show cut-off limits beyond which there is essentially zero failure fraction. The degree of conservatism introduced into the probability of release is dependent not only on the conservatism in the fragility description, but also on the seismic hazard description at low seismic levels. If the seismic hazard for low seismic input levels is large enough, it is apparent that very low level earthquakes can govern the seismic-induced release. This is considered unrealistic for engineered structures and equipment found in nuclear power plants. Structures and

equipment are subjected to low level dynamic loads from a number of sources including wind on a repetitive basis which have never been known to produce nuclear power plant structural failures. Similarly, for low level earthquakes, it is expected that below some threshold, there is virtually no chance of failure due to seismic excitation. Material strength data, for instance, normally does not fall to very low values compared to the median value but instead normally exhibits some lower bound (Reference 3 and 4). Other variables, such as damping, also indicate both lower and upper bounds which are not zero or infinite. Extensive studies have been conducted to develop response spectra from available earthquake records and while dispersion exists about the median values, spectra with essentially zero or infinite response do not occur (Reference 5). For these as well as other variables contributing to the seismic fragility of a given structure or component, it is apparent that some lower and upper bound cutoffs on the tails of the dispersion exist. Since the overall fragility curves are based on a combination of these variables, it is expected that a threshold exists below which no failures will occur. This is supported by experience. Although quantitative data are lacking, this threshold value is expected to be at approximately minus two lognormal standard deviations for the median curves using the "best estimate" or composite fragility variability. The composite lognormal standard deviation, β_C, is used for the basis of the cut-off rather than randomness or uncertainty since the composite value combines the effects of both dispersions.

However, it is also apparent that some variability should be associated with the cut-off. Essentially no data are available to establish the distribution of this variability or its range. A lognormal distribution is, therefore, assumed consistent with the majority of the other variables encountered in the PRA. The following approximation is recommended for establishing the cut-offs for the various fragility curves:

The cut-off on the lower tails of the median (50 percentile) fragility curve should be:

$$\breve{A}_{co} = \breve{A}\left[\exp\ (-2\beta_C)\right]$$

where $\breve{A}_{co}$ is the cut-off on the median curve, $\breve{A}$ is the median effective peak ground acceleration for failure, and β_C is the composite lognormal standard deviation.

The cut-off for the lower tails of the other fragility curves should be:

$$A_{co} = \breve{A}_{co}\left[\exp\ (-x\beta_C/1.65)\right]$$

where x is the ratio of the deviation divided by the standard deviation. For instance, for the median curve, x = 0; for the 25 percentile curve, x = -0.67; for the 5 percentile curve and below, x = -1.65; and for the 95 percentile curve and above, x = 1.65.

It is recommended that the cut-off on the upper tails be established as $+3\beta_C$ for all fragility curves. Similarly, for fragility curves involving only uncertainty, it is recommended that the cut-offs be set at $-3\beta_U$ for the lower bound and $+3\beta_U$ for the upper bound, respectively.

Some characteristics of the lognormal distribution as applied to seismic capacities are discussed in Appendix A of this report.

2.4 DESIGN AND CONSTRUCTION ERRORS

An inadequate data base exists upon which to determine explicitly the contributions of design and construction errors to most Millstone 3 structures and equipment seismic capacities. In one exception to this, the possibility of a large throughwall flaw was considered as a lower bound for generic piping. In general, for a plant as new as Millstone 3

with current design and QA procedures, the possibility is considered remote that design and construction errors may exist which can significantly affect the seismic capacity of a component. Although some discrepencies have been identified and others may be in the future, these items have been modified as necessary or shown to have no safety implications. Thus, these items are not expected to significantly affect the seismic capacity of the equipment or structures after they have been identified. However, there is a possibility that unidentified design and construction errors may exist which can affect the seismic capacity.

It should be recognized that design and construction errors do not necessarily always result in a decrease in capacity. It is possible to install higher strength bolts than specified, larger reinforcing bars or more closely-spaced bars than required, or slip a decimal point in the conservative as well as in the unconservative direction in the analysis. Some additional confidence exists in that structures and equipment are subjected to normal operating loads continually. In many cases, these loads may be large; as for instance, in the case of pressure, water hammer, and thermal loads in fluid systems when compared to seismic loads. In other cases, as for instance the wind forces on structures, the loads may be less than seismic loads but occur on a much more frequent basis. Pressure tests of containment vessels, while producing different types of response than seismic, would likely provide an indication if significant construction errors exist in these structures. Thus, although data on which to quantify accurate estimates of the effects of design and construction errors are not available, these are expected to affect a minimal number of components.

2.5 CORRELATION BETWEEN FAILURE MODES

Many of the potential failure modes discussed in the following sections are not considered to be completely independent. The most obvious examples involve failure of one item caused by failure of a separate component. For instance, if a potential mode of failure is the collapse of a structure, failure of the equipment and piping located in

that structure is also expected. Similarly, failure of relatively heavy equipment may often be expected to fail lighter equipment in the immediate vicinity. Some degree of correlation exists for all items and for all modes of failure since they are all excited by the same earthquake. An example of very high dependency of failure modes of components and structures include two identical items located very close to each other in the same structure. For two components which are identical but located in different structures or different locations in the same structure, some degree of correlation is expected but less than 100%.

For different modes of failure in a given structure, or in similar structures, some degree of correlation between modes is also expected. For instance, if the capacity of the lateral force resisting system (i.e., the shear walls) is actually higher or lower than the value used in the analysis, the acceleration capacities of all failure modes (including different structures) governed by the shear walls would be expected to be proportionately higher or lower. The actual capacity of the force resisting system may be different from that used in the evaluation due to differences in strength or modeling assumptions. These effects are of course included in the variabilities associated with each mode of failure for a given structure or component. However, different degrees of correlation may exist from mode-to-mode. For instance, for a given structure with given concrete and reinforcing steel strengths, the variability on strength from mode-to-mode may be strongly correlated, while different modeling assumptions may result in little correlation for different failure modes.

There is also a certain degree of interdependency between structural and sliding modes of failure that could be considered. In Section 4, fragilities are presented for failure modes associated with structure sliding or failure of the structure itself (i.e., shear wall failure). These fragilities were developed assuming that the sliding and structural failure modes were completely independent. That is, structural failure acceleration capacities were based upon seismic loads with the

structure bonded to the supporting rock (or soil), even if sliding was expected at lesser acceleration levels. In reality, the occurrence of sliding will limit the structure inertial loads since accelerations in excess of those corresponding to sliding cannot be transmitted through the structure/rock (or soil) interface. Treatment of the structure fragilities which incorporate the probability that sliding does occur would likely result in higher structure capacities.

For failure modes with little contribution to risk, consideration of correlation between modes is probably unimportant. However, consideration should be given to possible correlation between controlling seismically-induced failure modes.

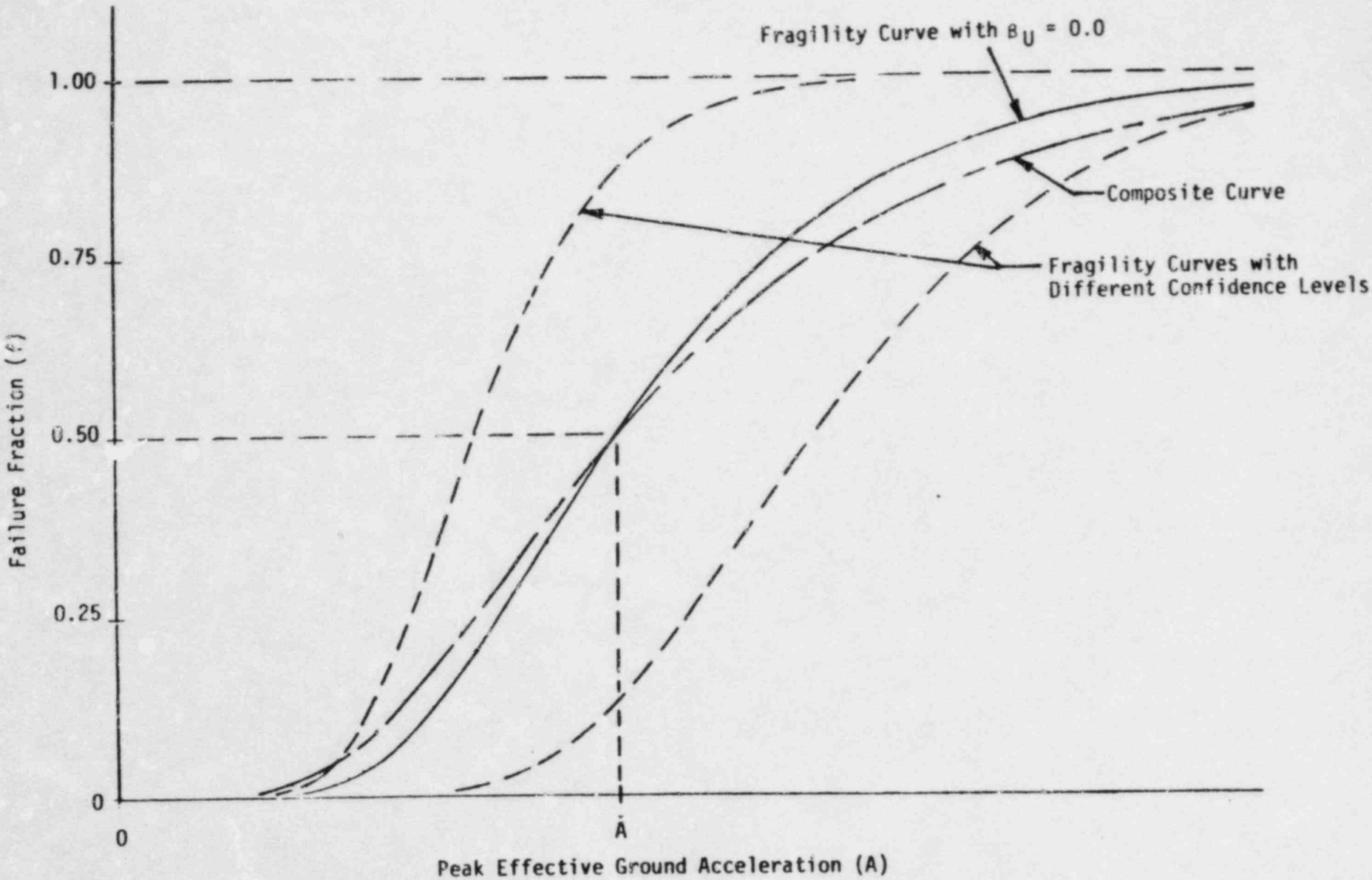

FIGURE 2-1. FRAGILITY CURVE REPRESENTATIONS

3. DIFFERENCES BETWEEN CRITERIA USED FOR DESIGN OF MILLSTONE 3 AND PARAMETERS USED IN THE EVALUATION OF THE SEISMIC CAPACITY

The seismic design of the Millstone 3 structures and equipment was based for the most part part on currently accepted methodology and criteria in conformance with NRC licensing requirements. Some differences exist in the use of the Newmark-type ground spectra, in the directional combination and in the damping ratios used. Also, some differences exist between the design and analysis of the Millstone 3 Nuclear Steam Supply System (NSSS) and non-NSSS Category I components. However, these criteria and methods together with the design codes in use at the time of the design form a conservative design basis and ensure that substantial factors of safety are introduced at various stages in the design procedure. The exact magnitude of many of these safety factors is still a matter of considerable discussion. Nevertheless, in order to establish a realistic value of the actual seismic capacity of a structure or equipment component, the amount of conservatism along with its variability must be established as accurately as possible. In this chapter, the design basis of the most important parameters affecting seismic capacity are identified, and the general methods used in obtaining more realistic values associated with very high seismic response levels are discussed. The detailed determination of these parameters is described in Chapters 4 and 5 for structures and equipment, respectively. The estimated seismic capacities of the most probable failure modes are also developed in Chapters 4 and 5.

The general approach used in the evaluation of the Millstone 3 seismic capacities is to develop the overall factor of safety associated with each important potential failure mode. Based on the governing design parameters, a median seismic capacity is then obtained in terms of some representative seismic input such as free-field acceleration. The

overall factor of safety is typically composed of several important contributions such as strength, allowance for inelastic energy dissipation (ductility), and differences in median structure response compared to design values resulting from such parameters as earthquake characteristics, damping, and directional load components.

3.1 STRENGTH

The design strength of a structure or an equipment component is typically determined from applicable codes and standards such as the ACI building codes for concrete or the ASME boiler and pressure vessel code for mechanical equipment. Inherent in these design codes is a factor of safety on material strength. Sometimes this factor is known reasonably accurately, such as the design allowable being one-half the minimum yield strength or some similar relationship. At other times, it is less well defined or may be a function of the geometry or other physical characteristics of the component such as for reinforced concrete shear walls. For metal structures and components, the safety factor included in the codes is usually fairly accurately known as are the relationships between minimum and mean or median strengths. For concrete structures, the factor of safety is normally less accurately known. In this case, the strength of the element is a function of the concrete strength, the amount and strength of the reinforcing steel, and the configuration of the element including the element geometry and reinforcing steel details. In establishing the strength and seismic capacity of concrete components, the results of concrete compression tests and reinforcing steel strength and elongation tests provide a valuable basis for establishing the element strength capacity. However, the increase in concrete strength with age together with the specific details of the element must also be considered. These effects are discussed in more detail in Chapter 4 for structures and Chapter 5 for the piping and equipment.

3.2 DUCTILITY

In order to establish realistic seismic capacity levels for most structures and components, an assessment of the inelastic energy absorption must usually be considered. Exceptions to this are some modes involving brittle failure, functional failure or elastic buckling. However, most failures due to seismic response involve at least some degree of yielding. This is true of reinforced concrete as well as the somewhat more ductile metal structures and components.

Consideration of structure ductility typically results in the ability of the structure to withstand greater seismic excitation than would be predicted using linear elastic techniques. In the design analysis of the Millstone 3 structures, all design analyses were based on linear elastic analyses although both cracked and uncracked properties were considered for the containment. No nonlinear analyses of the structures were conducted. Although inelastic analysis would be desirable in order to more accurately quantify the inelastic effects, the dissipation of inelastic energy may be adequately accounted for without the time and expense of performing nonlinear analyses. This can be accomplished by the use of the ductility-modified response spectrum approach (References 6 and 7) together with a knowledge of the elastic model results and the expected ductility ratios of the critical elements of the structure or component. This approach is based on a series of nonlinear time-history analyses using single-degree-of-freedom models with various nonlinear resistance functions and levels of damping. For different levels of ductility, the reduction in seismic response for the nonlinear system compared to the equivalent elastic system response is calculated. This reduction has been shown to be a function of the frequency and damping of the system as well as the ductility. However, a reasonably accurate assessment of the reduction in response of a structure or component can be made provided the results of the elastic analysis are available and a realistic evaluation of the system ductility can be made. In the current evaluation, the effective ductility was also considered to be a function of the earthquake magnitude.

3.3 SYSTEM RESPONSE

A number of parameters must be evaluated when considering the expected system response near failure compared to the design conditions. Among these are the expected compared to the design earthquake characteristics, directional combinations, system damping, load combinations, and system modeling approaches and assumptions. In addition, the duration of the earthquake must be considered since short duration earthquakes do not possess sufficient energy to fully excite the structural systems. Some of these parameters may be essentially median centered and introduce little change in the expected seismic capacity while other design criteria may be quite conservative. Several of the more important parameters required in evaluating the system seismic response are discussed below. The factors of safety associated with these parameters are developed in the following chapters for the specific failure modes identified.

3.3.1 Earthquake Characteristics

The Millstone 3 Seismic Category I structures are founded on rock or soil deposits overlying the rock. Equipment within the structures was designed for an SSE of 0.17g defined by the Newmark-type free-field ground response spectra shown in Figure 1-1. These spectra were developed from a number of earthquakes that occurred on both soil and rock sites. They were developed for design purposes and are smoothed envelopes of the actual earthquake spectra from which they were developed. Site-specific spectra are not available for Millstone 3. The spectra chosen as representative broadband spectra for the site were derived from Reference 8. A comparison between these spectra and the design spectra is presented in Figure 3-1. A comparison of the design spectrum at 5% design damping with the site-specific spectrum at 10% damping is shown in Figure 3-1. As noted in Section 3.3.2 and Table 3-1, 10% damping is estimated to be a median value for reinforced concrete structures approaching yield. A comparison of these spectra indicates that the design spectrum typically exceeds the site-specific spectrum except at frequencies in excess of 20 Hz.

3.3.2 System Damping

Damping values used for the design analysis of the Millstone 3 plant are shown in Tables 3-1 and 3-2 for the non-NSSS and NSSS SSE design, respectively. For the non-NSSS design, the damping ratios were specified in terms of stress level for the component rather than explicitly for the SSE or OBE as listed in US NRC Reg. Guide 1.61 (Reference 9). Damping in the rock springs used for the structures founded on bedrock was assumed to be 10 percent of critical for translation and 5 percent for rocking degrees of freedom. These values are considered to be conservative but since the overall rock spring stiffnessess are so high, the damping assumptions are not expected to significantly affect the response of the structures. The soil-structure interaction design values are generally considered to be essentially median centered for structures founded on a layer of till. At response levels of structures and equipment near failure levels, the damping ratios based on stress levels used for design are considered conservative when used in conjunction with the ductility factors used in this evaluation. Very little actual test data for damping ratios exist at failure levels, particularly for structures. However, the damping values used for design, even at the higher stress levels, are generally lower compared with median centered values recommended in References 6, 10 and 11. These damping values for structures and equipment at or near yield are shown in Tables 3-1 and 3-2 in comparison with those used for design analysis. In accordance with the recommendations in Reference 10, the lower levels of the pairs of values shown in Tables 3-1 and 3-2 are considered to be lower bounds while the upper levels are considered to be essentially average values. The values of damping used for this evaluation were taken from Tables 3-1 and 3-2 assuming the upper level to be a median value. Review of piping damping values derived from experiments support the use of 5 percent of critical (Reference 11).

3.3.3 Load Combinations

The load combinations on which the design of the Millstone 3 station Category I structures were based are shown in Tables 3-3 through 3-5 (Reference 1). These load combination criteria define a large number

of load combinations that must be considered in design. For the reactor building structure and much of the equipment contained within the reactor building, these load combinations include a combination of a loss of coolant accident (LOCA) and the SSE loads. Random LOCA events have an extremely low frequency of occurrence as do seismic events such that the frequency of both events occurring simultaneously is so small that their inclusion is judged to be not important to the risk analysis results.

3.3.4 Modal Combination

The Millstone 3 seismic design analysis was conducted on the basis of loads determined by the square-root-of-the-sum-of-the-squares (SRSS) method for both the NSSS and non-NSSS structures and equipment. Closely spaced modes were considered in accordance with USNRC Regulatory Guide 1.92 (Reference 12). SRSS methods are considered to give approximately median centered results. Although some frequency shifts are expected as structures approach failure, these shifts in frequency are normally not large unless very high ductility ratios exist. Also, the relationship between loads developed from individual modes may be expected to change once nonlinear response levels are reached. In the absence of a nonlinear analysis, the changes in the modal ratios are unknown. For the seismic evaluation of Millstone 3, it is assumed that the load response relationships between modes does not change significantly once the structures reach the yield point. For systems where most of the response results from one mode, this assumption introduces negligible possibility for error. For systems with a large number of modes with significant response levels, some additional uncertainty is introduced. The resulting assumed dispersion is discussed in Chapter 4 for structures.

3.3.5 Combination of Responses for Earthquake Directional Components

With the exception of the auxiliary building, the design of the essential Millstone 3 structures was based on loads developed from the absolute sum of the accelerations in one direction due to the simultaneous responses from all three directions of input. For the design of

the auxiliary building, the dynamic forces of the members were computed by the square-root-of-the-sum-of-the-squares (SRSS) method. Structure loads were computed using response spectra methods and a comparison was made with time history loads. Where torsion was significant, the structure was analyzed by a three-dimensional model which included the effects of torsion.

Depending on the degree of coupling in the structures, the absolute sum of the three-directional components may be very conservative. Current design procedures are specified in Regulatory Guide 1.92 (Reference 12). This approach requires that the effects of two horizontal directional responses be combined with the vertical response by the SRSS, and, thus, does not require that the maximum response in each direction occur at the same instant as the maximum response in the other two directions. Other methods of combining directional components such as delineated in Newmark and Hall (Reference 10) also yield realistic results. This approach recommends adding 100% of one directional component to 40% of the remaining components. This method has the advantage of being easy to use and retains a consistent relationship between loads and stresses. Both the SRSS and the 100%, 40%, 40% method yield similar results and are considered to be essentially median centered. Therefore, no increase in the factor of safety to account for earthquake directional components was included for the auxiliary building. Generic earthquake component response factors were developed for components of different geometries by comparing resulting acceleration vectors for the applicable design criteria to median response vectors as defined by either the SRSS methodology or the 100%, 40%, 40% methodology.

3.3.6 Structure Modeling Considerations

In the seismic design analysis of Millstone 3 structures, both two-dimensional and three-dimensional, lumped-mass models were developed for the Category I structures. Two-dimensional finite element models were developed for structures founded on a layer of soil above the bedrock. To reflect the rock foundation, the design models for

structures founded on rock have base flexibilities developed from elastic half-space theory. For these buildings, no stiffnesses were included to represent the embedment of the structures. For rock founded structures, this will generally have very little effect on the frequencies that were calculated using no embedment effects. The remaining details of the models are consistent with state-of-the-art seismic analysis and do not appear to introduce significant degrees of either conservatism or unconservatism into the results.

Some aspects of the analysis procedure yield variations which can be quantifiably assessed compared to the design results. For instance, the increase in the actual concrete strength compared to the design values may be used to evaluate the change in stiffness and, hence, the change in frequencies of the concrete structures compared to the design values. The modified frequencies may, in turn, be used to reevaluate the modal responses. Another area where modified responses are considered is in the load distribution for structures where local yielding occurs in some elements before others or through diaphragms containing relatively large cut-outs. Neglecting the cut-outs typically overestimates the stiffness of the diaphragm and may consequently overestimate the seismic loads calculated. For a single stick model, typically no diaphragm loads are computed. However, an estimate of the stiffness of the diaphragm with cut-outs, and, if necessary, in the failed condition, may be used to redistribute the seismic loads if redundant load paths are available and, thus, provide a more realistic ultimate seismic capacity. The details of these and similar evaluations necessary to account for change between parameter design values and values more representative of seismic response levels near failure are discussed in the following chapters.

TABLE 3-1

COMPARISON OF CRITICAL DAMPING FOR NON-NSSS STRUCTURES AND EQUIPMENT

Stress Level	Type of Condition of Structure, System or Component	Percent Critical Damping: Millstone 3 Design (Ref. 1)	Percent Critical Damping: Fragility Evaluation* (Refs. 6, 11)
1. Low stress, well below proportional limit. Stresses below 0.25 yield point stress	Steel, reinforced concrete; no cracking and no slipping at joints, piping or components	0.5 to 1	NA
2. Working stress limited to 0.5 yield point stress	a. Welded steel, well reinforced concrete (with only slight cracking)	2	NA
	b. Bolted steel	5	NA
3. At or just below yield point	a. Welded steel	5	5 to 7
	b. Reinforced concrete	5	7 to 10
	c. Bolted steel	7	7 to 15
4. At all stress levels	a. Rock (translation)	10	10
	b. Rock (rotation)	5	5

* Lower values are considered to be approximately lower bounds; upper values are considered to be essentially median centered.

TABLE 3-2

COMPARISON OF CRITICAL DAMPING FOR NSSS EQUIPMENT

Item	Percent Critical Damping: Millstone 3 SSE Design (Ref. 1)	Percent Critical Damping: Fragility Evaluation* (Refs. 6, 11)
Primary coolant loop system components	4	5
Welded steel structures	4	5 to 7
Bolted and/or riveted steel structures	7	7 to 15
Fuel assemblies	10	10
CRDM's/CRDM supports	5	7

* Lower values are considered to be approximately lower bounds; upper values are considered to be essentially median centered.

TABLE 3-3

LOADING CONDITIONS - LINER PLATE AND ACCESS OPENINGS (REF. 1)

Category	Load Conditions	Design Allowables (per ASME III Nomenclature)	
Emergency	$D+P_D+T_D+SSE$	$P_m+P_b+Q<3S$	
Test	$D+1.15P$	$P_m<0.9S_y$ $P_m+P_b<1.35S_y$ +"CAT" curve considerations	
Normal	100 cycles of ΔP 400 cycles of ΔT 100 cycles of 1/2-SSE	NB-3222.4 (d) or (e)	
Severe Operational	$D+P_{min}+T_{min}$ 1/2-SSE	$P_m<S_m$ $P_m+P_b<1.5S_m$ $P_m+P_b+Q<3S_m$	Without temperature
	ANCHORS		
Emergency	$D+P_D+T_D$ + SSE	Max. shear < $.425\ S_u$	
Severe Operational	$D+P_{min}+T_{min}$ + 1/2-SSE	Max. tensile $<0.45\ S_u$	

NOTE:

The normal and test load combinations are producing negligible effects.

Where:

D = Dead load effect of reinforced concrete structure acting on the liner plus dead load of the liner

P_D = Design pressure (pressure resulting from design basis accident and safety margin)

T_D = Load due to thermal expansion, resulting when the liner is exposed to the design temperature

SSE = Stresses in the liner derived from applying the effect of the safe shutdown earthquake

TABLE 3-3 (Continued)

LOADING CONDITIONS - LINER PLATE AND ACCESS OPENINGS (REF. 1)

ΔP = Differential pressure between operating pressure and atmospheric pressure (100 cycles are assumed on the basis of 2.5 hr refueling cycles per year on a 40 year span)

ΔT = Load due to thermal expansion, resulting when the liner is exposed to the differential temperature between operating and seasonal refueling temperatures (400 cycles are assumed on the basis of 10 such variations per year, on a 40 year span (100 cycles of 1/2-SSE is an assumed number of cycles for this type of earthquake.)

P_{min} = Minimum pressure resulting during operation of the containment

T_{min} = Load due to thermal expansion resulting when the liner is exposed to the minimum pressure

S_y = Yield strength of the material

S_m = The smaller of 1/3-ultimate strength or 2/3-yield strength

S_u = Ultimate strength of the stud material.

TABLE 3-4

LOADING CONDITIONS, PENETRATIONS (REF. 1)

Areas of Analysis (See Figures 3.8-5 thru 3.8-9 and 3.8-15 thru 3.8-22)	Category	Stress Allowables (per ASME III Load Combinations)	Nomenclature)
1	Design	M_p or T_p or J_{ax} or J_{sh}	$P_m < 0.9\ S_y$ $P_m + P_b < 0.9\ S_y$ P concrete bearing < 2,400 psi
	Emergency	$P_d + T_d + R_o$	$P_m + P_b + Q < 3\ S_m$
2	Design(1)	M_p or T_p or J_{ax} or J_{sh}	$P_m < 0.9\ S_y$* $P_m + P_b < 0.9\ S_y$*
	Design(2)	$P_g + T_g$ + Design(1)	$(P_m + P_b) + (P_m + P_d + Q) < 3\ S_m$ Design 1 $P_g + T_g$
	Normal	$P_g + T_g + R_e$	ASME III Table NC3611.1(b)(3)-1 or Para. NB3222.4(d) or (e)

NOTES:

*For the pipe portion, refer to Section 3.7.3.1.

Where:

M_p = Yielding moment = Required bending moment to produce stresses equal to the yield strength of the pipe material

T_p = Yielding torque = Required torsional moment to produce stresses equal to the yield strength of the material

J_{ax} = Axial jet force = Load equal to the piping design pressure times the inside area of the pipe, acting in the axial direction of the piping

J_{sh} = Shear jet force = Load equal to the piping design pressure times the inside area of the pipe acting transversely to the pipe

TABLE 3-4 (Continued)

LOADING CONDITIONS, PENETRATIONS (REF. 1)

P_d = Containment design pressure

T_d = Containment design temperature

P_g = Piping design pressure

T_g = Piping design temperature

R_o = Piping reactions due to normal operation (including SSE effects)

R_e = Piping reactions due to normal operation (including 1/2 - SSE)

Design(1) - Applies to the sizing of the sleeve and attachment plate

Design(2) - Applies to the evaluation of stresses in the area of Analysis 2 due to the given load combinations

TABLE 3-5

LOADS AND LOADING COMBINATIONS (REF. 1)

1. Concrete Structures (Containment Internal Structures and Category I Structures, other than the containment mat, shell, and dome).

Loads and loading combinations are based on ACI 318, and "AEC Enclosure 3 - Structural Design Criteria for Evaluating Effects of High Energy Pipe Breaks on Category I Structures Outside the Containment," Structural Engineering Branch, Directorate of Licensing.

1. $U = 1.4D + 1.7L$

2. $U = 1.4D + 1.7L + 1.7H$
2a. $U = 0.9D + 1.7H$

3. $U = 1.4D + 1.7L + 1.4F$
3a. $U = .9D + 1.4F$

4. $U = 0.75 (1.4D + 1.7L + 1.7W)$
4a. $U = 0.90D + 1.3W$

5. $U = 0.75 (1.4D + 1.7L + 1.7 \times 1.1 (1/2\ SSE)$
5a. $U = 0.90D + 1.3 \times 1.1 (1/2\ SSE)$

6. $U = 1.1\ D + 1.1\ L + 1.1\ SSE$
6a. $U = 0.9D + 1.1\ SSE$

7. $U = 1.1\ D + 1.1\ L + 1.1\ Wt$
7a. $U = 0.9D + 1.1\ Wt$

8. $U = D + L + Ta + Ra + 1.5Pa$

9. $U = D + L + Ta + Ra + 1.25Pa + 1.25\ OBE + 1.0 (Yr + Yj + Ym)$

10. $U = D + L + Ta + Ra + Pa + SSE + 1.0 (Yr + Yj + Ym)$

Notes - Concrete Structures

(1) U is the required section strength based on strength design methods described in ACI 318-71.

(2) In combinations 8, 9, and 10, the maximum values of Pa, Ta, Ra, Yj, Yr, and Ym, including an appropriate dynamic load factor, shall be used unless a time-history analysis is performed to justify otherwise.

(3) For load combinations 9 and 10, local section strengths and stresses may be exceeded under the concentrated loads Yr, Yj,

LOADS AND LOADING COMBINATIONS (REF. 1)

and Ym, provided there will be no loss of function of any safety related system.

(4) For load combinations 7 and 7a, local section strengths and stresses may be exceeded under the tornado missile load provided there will be no loss of function of any safety related system.

2. Steel Structures

A. Elastic Working Stress Design Service Load Conditions

1. $S = D + L$

2. $1.33\ S = D + L + OBE$

3. $1.33\ S = D + L + W$

Factored Load Conditions

4. $1.6\ S = D + L + SSE$

5. $1.6\ S = D + L + Wt$

6. $1.6\ S = D + L + Ta + Ra + Pa$

7. $1.6\ S = D + L + Ta + Ra + Pa + OBE + 1.0\ (Yr+Yj+Ym)$

8. $1.6\ S = D + L + Ta + Ra + Pa + SSE + 1.0\ (Yr+Yj+Ym)$

B. Plastic Design

Factored Load Conditions

9. $0.9Y = D + L + Ta + Ra + 1.5\ Pa$

10. $0.9Y = D + L + Ta + Ra + 1.25\ Pa + 1.25\ OBE + 1.0\ (Yr+Yj+Ym)$

11. $0.9Y = D + L + Ta + Ra + Pa + SSE + 1.0\ (Yr+Yj+Ym)$

Notes - Steel Structures

(1) S is the required section strength based on the elastic design methods and allowable stresses defined in Part 1 of the AISC "Specification for the Design, Fabrication, and Erection of Structural Steel for Buildings."

(2) Y is the section strength required to resist design loads based on plastic design methods described in Part 2 of the AISC

LOADS AND LOADING COMBINATIONS (REF. 1)

"Specification for the Design, Fabrication, and Erection of Structural Steel for Buildings."

(3) Both cases of L having its full value or being completely absent are checked for load combinations 1, 2, 3, 4, and 5.

(4) In combinations 4 to 8 and 9 to 11, thermal loads are neglected when it can be shown that they are secondary and self-limiting in nature, or where the material is ductile.

(5) In combinations 6, 7, and 8, and 9, 10, and 11, the maximum values of Pa, Ta, Ra, Yr, Yj, and Ym, including an appropriate dynamic factor, are used unless a time-history analysis is performed to justify otherwise.

(6) Combination 5 shall be satisfied without the tornado missile load. Combinations 7, 8, 10 and 11 shall be first satisfied without Yr, Yj, and Ym. When considering these loads, however, local section strengths may be exceeded under the effect of these concentrated loads, provided there will be no loss of function of any safety related system. Furthermore, in computing the required section strength, S, the plastic section modulus of steel shapes may be used for combinations 7 and 8.

Loads, Definition of Terms, and Nomenclature

1. Normal Loads - Those loads encountered during normal plant operations and shutdown. They include the following:

D - Dead loads or their related internal moments and forces including any permanent equipment loads

L - Live loads or their related internal moments and forces, including any movable equipment loads and other loads which vary with intensity and occurrence

F - Lateral and vertical pressure of liquids, or their related internal moments and forces (included in D above)

H - Lateral earth pressure, or its related internal moments and forces (included in L above)

To - Thermal loads during normal operating or shutdown conditions, based on the most critical transient or steady-state condition (included in L above)

Ro - Pipe loads during operating or shutdown conditions, based on the most critical transient or steady-state condition (included in D above)

TABLE 3-5 (Continued)

LOADS AND LOADING COMBINATIONS (REF. 1)

2. Severe Environmental Loads - Those loads that could infrequently be encountered during the plant life. They include:

   OBE - Loads generated by the operating basis earthquake

   W - Loads generated by the design wind specified for the plant site (Section 3.3.1)

3. Extreme Environmental Loads - Those loads which are credible but highly improbable. They include:

   SSE - Loads generated by the safe shutdown earthquake

   Wt - Loads generated by the design tornado specified for the plant site (Section 3.3.2)

4. Abnormal Loads. Those loads generated by a postulated high-energy pipe break accident within a building and/or compartment thereof. Included in this category are the following:

   Pa = Maximum differential pressure load generated by a postulated break

   Ta = Thermal loads under accident conditions generated by a postulated break

   Ra = Pipe and equipment reactions under accident conditions generated by a postulated break

   Yr = Loads on the structure generated by the reaction on the broken high-energy pipe during a postulated break

   Yj = Jet impingement load on a structure generated by a postulated break

   Ym = Missile impact load on a structure generated by or during a postulated break, such as pipe whipping.

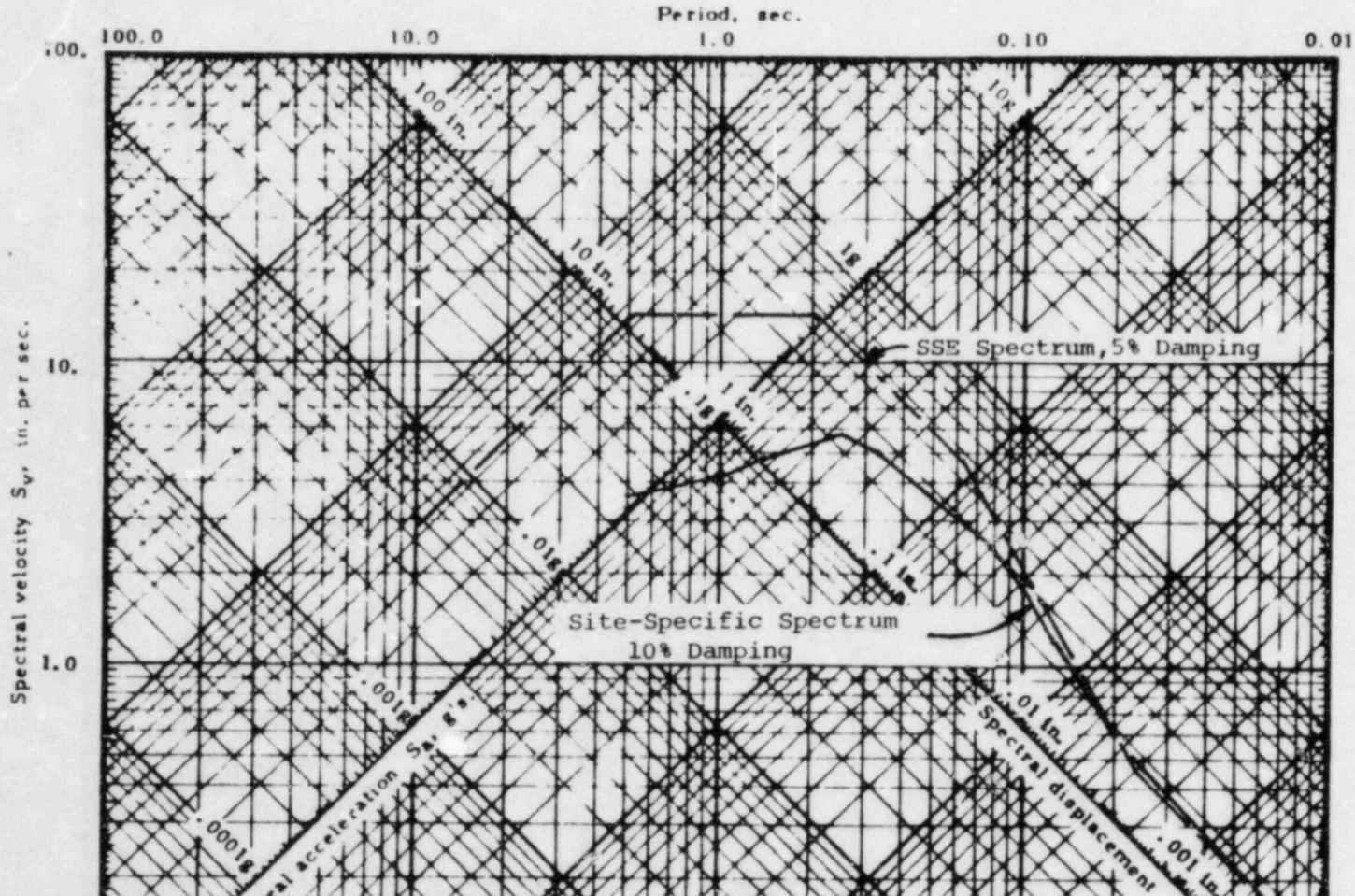

FIGURE 3-1. COMPARISON OF SSE SPECTRUM TO SITE-SPECIFIC SPECTRUM

4. STRUCTURES

In this chapter, the median factors of safety and logarithmic standard deviations for the important structures are developed. Based on these factors of safety, median acceleration levels associated with seismic failure are presented. For most of these structures, the original design dynamic models were used when available to generate seismic response characteristics in order to determine the median factors of safety and logarithmic standard deviations for each of the variables associated with structure response. All seismic analyses were based on linear response model results, but some seismic design loads were modified to more closely approximate the expected inelastic response at the high acceleration levels expected for failure.

4.1 MEDIAN SAFETY FACTORS AND LOGARITHMIC STANDARD DEVIATIONS

As discussed in Section 2.3, the seismic fragilities of structures and components are described in terms of the median ground acceleration, $\breve{A}$, and random and uncertainty logarithmic standard deviations, β_R and β_U. In estimating these fragility parameters, it is computationally attractive to work in terms of an intermediate random variable called the factor of safety, F. The factor of safety is defined as the ratio of the ground acceleration capacity, A, to the Safe Shutdown Earthquake (SSE) acceleration used in design. For equipment and structures qualified by analysis, it is easier to estimate the median factor of safety, $\breve{F}$, and variability parameters, β_R and β_U, based upon the original SSE stress analysis than it is to directly estimate the fragility parameters. Thus,

$$\breve{A} = \breve{F} \cdot A_{SSE} \qquad (4\text{-}1)$$

From the existing analyses of the important structures together with a knowledge of the deterministic design criteria utilized, median factors of safety associated with the SSE ground acceleration of 0.17g

can be estimated. These are most conveniently separated into those factors associated with the seismic strength capacity and inelastic energy absorption capability of the structure and those factors associated with the expected building response.

The factor of safety for the structure seismic capacity consists of the following parts:

1. The strength factor, F_S, based on the ratio of actual member strength to the design forces.

2. The inelastic energy absorption factor, F_μ, related to the ductility of the structure and to the magnitude range that is believed to contribute to most of the seismic risk.

Associated with the median strength factor, $\breve{F}_S$, and the median ductility factor, $\breve{F}_\mu$, are the corresponding logarithmic standard deviations, β_S and β_μ. The structure strength factors of safety and logarithmic standard deviations vary from structure to structure and according to the different failure modes of a given structure. Factors of safety for the most important modes of failure are summarized in subsequent sections.

The factor of safety, F_R, related to building response is determined from a number of variables which include:

1. The response spectra used for design compared to the median centered spectra for rock sites from multiple seismic events.

2. Damping used in the analysis compared with damping expected at failure.

3. Modal combination methods.

4. Combination of earthquake components.

5. Modeling accuracy.

6. Soil-structure interaction effects.

Based on the characteristics of the lognormal distribution, median factors of safety and logarithmic standard deviations for the various contributing effects can be combined to yield the overall estimates. For instance, the capacity factor of safety of a structure, F_{cap}, is obtained from the product of the strength and ductility factors of safety which, in turn, may include effects of more than one variable.

$$F_{cap} = F_s \times F_\mu \tag{4-2}$$

The methods of determining these safety factors are discussed in the following sections. The logarithmic standard deviation on capacity, β_{cap}, is found by:

$$\beta_{cap} = \sqrt{\beta_s^2 + \beta_\mu^2} \tag{4-3}$$

As discussed in Section 2.3, the logarithmic standard deviations are composed of both an inherent randomness and uncertainty in the median value.

Median factor of safety, $\breve{F}$, and variability, β_R and β_U, estimates are made for each of the parameters affecting capacity and response. These median and variability estimates are then combined using the properties of the lognormal distribution (described in Section 2) in the same manner as Equations 4-2 and 4-3 to obtain the overall median factor of safety and variability estimates required to define the fragility curve for the structure.

For each variable affecting the factor of safety, the random variability, β_R, and the uncertainty, β_U, must be estimated separately. The random variability, β_R, represents those sources of dispersion in the factor of safety which cannot be reduced by more detailed evaluation or

by gathering more data. Thus, β_R is due primarily to the variability of an earthquake time-history and, therefore, to a structure's response when the earthquake is only defined in terms of the peak effective ground acceleration. The uncertainty, β_U, represents those sources of dispersion which could be reduced only through better understanding or more knowledge. β_U is associated with such items as our lack of ability to predict the exact strength of materials (concrete and steel) and of structures (shear walls and diaphragms); errors in calculated response due to inaccuracies in mass and stiffness representations as well as load distributions; and use of engineering judgment in the absence of plant specific data on fragility levels.

Each of the factors presented in Chapter 3 will be discussed in more detail in the following sections. Examples are included to assist in the understanding of the application of the methodology.

4.1.1 Structure Capacity

The primary lateral load carrying systems of the Category I structures that were analyzed are of reinforced concrete construction with the exception of the refueling water storage tank which is fabricated of steel. For lateral load carrying systems which are composed of reinforced concrete, the structure strength is a function of material strengths associated with the concrete and the reinforcing steel. The determinations of these strengths are presented in the following two sections.

4.1.1.1 Concrete Compressive Strength

The evaluation of the strength of most concrete elements, whether loaded in compression or shear, is based on the concrete compressive strength, f'_c. Concrete compressive strength used for design is normally specified as some value at a specific time from mixing (for example, 28 or 60 days). This value is verified by laboratory testing of mix samples. The strength must meet specified values allowing a finite number of

failures per number of trials. As previously stated, there are two major factors which justify the selection of a median value of concrete strength above the design strength.

1. To meet the design specifications, the contractor attempts to create a mix that has an "average" strength above the design strength.

2. As concrete ages, it increases in strength.

Results of concrete compression testing were available for the Millstone 3 structures (Reference 13). Table 4-1 summmarizes these results.

As concrete ages, its strength increases. This must also be accounted for in determining the median strength compared to the design strength. Figure 4-1 from Reference 14 shows the increase of the concrete compressive strength with time assuming the concrete poured in the field is adequately represented by the curve designated as "air cured, dry at test." At 28 days, the concrete has a relative strength of 50 percent which approaches 60 percent asymptotically. The median factor relating the strength of aged concrete to the 28-day strength is, therefore, 1.2. Similarly, the median aging factor for concrete tested at 60 days was estimated to be 1.11. No information is available on the standard deviation expected for aging. Logarithmic standard deviations associated with the aging factors were estimated to be 0.10 and 0.05 for concrete tested at 28 and 60 days, respectively. Median concrete compressive strengths and variabilities used in the fragility evaluations for the Millstone 3 structures are listed in Table 4-2.

Other effects which could conceivably be included in the concrete strength evaluation include some decrease in strength in the in-place condition as opposed to the test cylinder strength, and some increase in strength resulting from rate of loading at the seismic response frequencies of the structures. The variation in the strength of in-place concrete compared with the test cylinder strength is accounted

for to a large degree in the use of empirical representations of shear wall capacities. These empirical capacities are typically developed by comparing actual wall strengths to the cylinder test strengths of the wall's concrete. Although experimental data on the in-place and rate effects are limited, that which is available would tend to indicate these effects are relatively small and of the same order magnitude. Since the two effects are opposite, they were neglected.

4.1.1.2 Reinforcing Steel Yield Strength

Grades 40, 50, and 60 reinforcing steel were used in the construction of the Millstone 3 structures. The results of tensile testing conducted on the reinforcement were reported in Reference 13. Median reinforcement yield strengths and logarithmic standard deviations used in the structure fragilities calculations were based on these data and are listed in Table 4-3. Grade 60 reinforcement was substituted for Grade 40 at some locations through the structures. This was accounted for in the fragility evaluations based on information contained in Reference 13.

Two other effects must be considered when evaluating the yield strength of reinforcing steel. These are the variations in the cross-sectional areas of the bars and the effects of the rate of loading. A survey of information (Reference 16) determined that the ratio of actual to nominal bar area has a mean value of 0.99 and a coefficient of variation of 0.024. The same reference notes that the standard test rate of loading is 34 psi/sec. Accounting for the rate of loading anticipated in seismic response of structures results in a slight decrease in yield strength of reinforcing steel in tension. This effect is neglected in concrete compression.

4.1.1.3 Shear Strength of Concrete Walls

Recent studies have shown that the shear strength of low-rise concrete shear walls with boundary elements are conservatively predicted by the ACI 318-71 code provisions (Reference 17). This is particularly true for walls with height to length ratios in the order of 1 or less. Barda (Reference 18) determined that the ultimate shear strength of low-rise walls tested could be represented by the following relationship:

$$v_u = v_c + v_s$$

$$= 8.3\sqrt{f'_c} - 3.4\sqrt{f'_c}\left(\frac{h_w}{\ell_w} - 0.5\right) + \rho_u f_y \qquad (4\text{-}4)$$

where:

v_u = Ultimate shear strength, psi

v_c = Contribution from concrete, psi

v_s = Contribution from steel reinforcement, psi

f'_c = Concrete compressive strength, psi

h_w = Wall height, in

ℓ_w = Wall length, in

ρ_u = Vertical steel reinforcement ratio

f_y = Steel yield strength, psi

The contribution of the concrete to the ultimate shear strength of the wall as a function of h_w/ℓ_w is shown in Figure 4-2. Also shown in Figure 4-2 are the available test values (References 18 through 21) and the corresponding ACI 318-71 formulation. The tests included load

reversals and varying reinforcement ratios and h_w/ℓ_w ratios. Web crushing generally controlled the failure of the test specimens. Testing was performed with no axial loads, but an increase in shear capacity of $N/4\ell_w h$ was recommended, where N is the axial load in pounds, and h is the wall thickness in inches.

The contribution of the steel to the ultimate shear strength according to ACI 318-71 is:

$$V_s = \rho_h f_y \qquad (4\text{-}5)$$

where ρ_h = horizontal steel reinforcement ratio.

Furthermore, one of the conclusions reached by Oesterle (Reference 21) is that for low-rise shear walls (specifically $h_w/\ell_w = 1$), vertical steel has no effect, and the entire contribution to shear strength is due to the horizontal steel.

In order to estimate the effects that the horizontal and vertical steel have, the steel contribution to wall shear strength was determined from test values for the range of $0.5 < h_w/\ell_w < 2$. Test data from the above references were used. The effective steel shear strength was assumed to be in the form:

$$V_{se} = AV_{su} + BV_{sh} \qquad (4\text{-}6)$$

where A, B are constants and

$V_{su} = \rho_u f_y$ = vertical steel contribution to shear strength

$V_{sh} = \rho_h f_y$ = horizontal steel contribution to shear strength

The constants A and B were then calculated assuming the concrete contribution to the ultimate strength is given as shown in Equation 4-4. Based on the results of this evaluation, the constants A and B can be shown to be:

$A = 1$	$B = 0$	$h_w/\ell_w \leq 0.5$
$= -2.0\ (h_w/\ell_w) + 2.0$	$= 2.0\ (h_w/\ell_w) - 1.0$	$0.5 \leq h_w/\ell_w \leq 1.0$
$= 0$	$= 1$	$1.0 \leq h_w/\ell_w$

and the median ultimate shear strength is given by:

$$v_u = v_c + v_{se}$$

$$= 8.3\sqrt{f_c'} - 3.4\sqrt{f_c'}\left(\frac{h_w}{\ell_w} - 0.5\right) + \frac{N}{4\ell_w h} + \rho_{se} f_y \qquad (4\text{-}7)$$

where $\rho_{se} = A\rho_u + B\rho_h$ with A and B determined as shown above. Based on an evaluation of the same experimental data, the logarithmic standard deviation was estimated to be 0.15.

The data used to substantiate the median shear strength equations presented above were derived from tests conducted on cantilever walls. The height h_w for these walls is known. However, the walls evaluated in this study typically span more than one story. For these walls, the equivalent cantilever wall height, h_{we} was taken as the ratio of the in-plane moment to the in-plane shear at the section under consideration.

The equivalent heignt h_{we} was used to determine the median wall shear strength and provides a more accurate representation of the moment-shear interaction.

4.1.1.4 Example of Shear Wall Failure in Shear

The determination of the median shear strength of the north exterior wall of the auxiliary building for the story from El. 4'-6" to El. 24'-6" is selected as an example. This wall is 2 feet thick, 102 feet long, and reinforced by #11 bars spaced at 10 inches at each face and in each direction. From Table 4-2, the median concrete compressive strength corresponding to the specified 3000 psi design strength was taken to be 5000 psi. Grade 60 reinforcement steel was substituted for Grade 40 steel in the construction of this wall. From Table 4-3, this reinforcement has a median yield strength of 69 ksi. The equivalent cantilever wall height was determined to be 71 feet. The median concrete shear strength was found to be:

$$v_c = 8.3\sqrt{5000} - 3.4\sqrt{5000}\ (71/102 - 0.5)$$

$$= 540 \text{ psi}$$

$$= 77.8 \text{ ksf}$$

The steel reinforcement ratios in the horizontal and vertical directions are the same:

$$\rho_{se} = \rho_u = \rho_h$$

$$= \frac{2(1.56)}{10(24)}$$

$$= 0.0130$$

The steel shear strength was found to be:

$$v_{se} = 0.0130\ (69{,}000)$$

$$= 897 \text{ psi}$$

$$= 129.2 \text{ ksf}$$

The increase in shear strength provided by axial compression is typically small and was neglected. For rectangular walls with uniformly distributed vertical reinforcement, the effective depth, d, from the extreme compressive fiber to the resultant of the tension force was taken to be $0.6\ \ell_w$ from Reference 21. This approximation neglects the increase in the effective depth provided by transverse, intersecting walls which behave as flanges. The median wall shear strength was found to be:

$$V_u = (77.8 + 129.2)(2)\ \left[0.6\ (102)\right]$$

$$= 25{,}300 \text{ k}$$

The applied shear load based on an elastic load distribution was found to be 4090 k. The median strength factor corresponding to shear failure of this wall was then determined to be 6.2.

4.1.1.5 Strength of Shear Walls in Flexure Under In-Plane Forces

Data on reinforced concrete shear walls failing in flexure under in-plane forces can be found in Reference 21. Equations found in Reference 20 may be used to calculate the moment capacity for walls without chord steel. However, chord steel can be accounted for by increasing the depth from the extreme compressive fiber to the neutral axis to account for the yield strength of the tensile chord steel. The compression chord steel is neglected since it is near the neutral axis, and its effect on the moment capacity is small. The total moment capacity of reinforced concrete shear walls in flexure under in-plane forces is then:

$$M = \frac{A_s f_y \ell_w}{2}\left(1 + \frac{N}{A_s f_y}\right)\left(1 - \frac{\beta_1 c}{\ell_w}\right) + A_{ch} f_y \left(d - \frac{\beta_1 c}{2}\right) \quad (4\text{-}8)$$

where:

c = Depth to neutral axis from extreme compression fiber

A_s = Area of distributed steel

A_{ch} = Area of chord steel

ℓ_w = Wall length

f_y = Steel yield strength

N = Axial load

d = Distance from the extreme compressive fiber to the centroid of tensile chord steel

β_1 = Ratio of depth of equivalent rectangular concrete stress block to depth to neutral axis (c)

4.1.1.6 Example of Shear Wall Failure in Flexure

The same wall that was analyzed for shear in Section 4.1.1.4 will be analyzed for flexure. The values to be used in Equation 4-8 are as follows:

$A_s = 2(1.56)\frac{102(12)}{10} = 191 \text{ in}^2$

$A_{ch} = 0$

$\ell_w = 102'$

$f_y = 69 \text{ ksi}$

N = (as with shear strength)

$\beta_1 = 0.85 - 0.05\frac{5000-4000}{1000} = 0.8$

From balancing the tensile and compressive forces, c = 26.9'. Using the values in Equation 4-8, the median in-plane moment capacity for this wall was found to be 1,060,000 k-ft. From the elastic load distribution, the applied in-plane moment was determined to be 289,000 k-ft. The median strength factor corresponding to flexural failure of this wall was calculated to be 3.7.

4.1.1.7 Structure Sliding

Resistance to structure sliding is provided by static friction between the structure foundation and the rock (or soil) below, lateral earth pressures from backfill placed against exterior walls, and shear keys embedded into rock (or soil). Gross structure sliding initiates when the base shear acting at the foundation-rock (or soil) interface equals the available resistance. Initiation of sliding does not constitute structure or equipment failure. As a structure slides as a rigid body, its accelerations and relative story drifts cannot exceed those values occurring at the initiation of sliding. Failure modes resulting from structure sliding are displacement-dependent. For example, piping attached at one end to the structure that is sliding and at the other end to some adjacent structure may fail under relative end displacement. Also, impact with adjacent structures may cause concrete spalling and subsequent damage to equipment or piping mounted near the localized spalling regions. However, the sliding displacements necessary to cause these failure modes are substantial and can occur only under peak ground accelerations well in excess of acceleration levels initiating sliding.

An approach recommended by Newmark (Reference 15) was used to predict structure sliding displacements. This approach is simple and results in conservative estimates of the sliding displacement. Figure 4-3 summarizes the features of Newmark's approach. The ground beneath the structure experiences a single horizontal acceleration pulse Ag that lasts for a time duration t_1, and results in a velocity V. The structure is represented as a rigid body that begins to slide relative to the ground when its rigid body acceleration reaches Ng, where N is a coefficient

relating the net sliding resistance to the total structure weight. Since the ground acceleration is conservatively assumed to be a square pulse, sliding initiates instantaneously. Structure sliding ends at time t_m when the structure has achieved the ground velocity V. The relative displacement between the ground and the structure is determined by integrating the relative velocity between the ground and the structure from time t = 0 to time t = t_m.

With estimates of the net sliding resistance coefficient, N, and the peak ground acceleration, V, as a function of the peak ground acceleration, Equation 4-9 (see Figure 4-3) can be used to determine the ground acceleration resulting in sufficient relative sliding displacement, u_m, to cause the failure mode under consideration. Newmark's approach is conservative since the ground acceleration is actually a reversing function rather than a single pulse which would greatly reduce the sliding time duration and thus the relative sliding displacement.

Due to the highly uncertain nature of structure behavior past the initiation of sliding, the logarithmic standard deviation associated with Newmark's approach was estimated to be 0.4. Because no relative displacement can occur until sliding initiates, the acceleration capacity corresponding to the initiation of sliding can be treated as a cutoff on the fragility curve for sliding-induced failure in a manner similar to that described in Section 2.3.

4.1.1.8 Example of Sliding-Induced Failure

Determination of the ground acceleration causing sliding-induced failure of piping attached to the auxiliary building will be presented as an example of the application of Newmark's approach. Accounting for sliding resistances provided by static friction from the net structure weight, the shear keys embedded in rock, and at-rest lateral earth pressure, the sliding resistance coefficient was found to be:

$$N = 1.118 - 0.1734\ A$$

The second term above accounts for the reduction in sliding resistance associated with a vertical seismic acceleration acting upward. The peak bedrock velocity corresponding to a peak ground acceleration of 1g was estimated to be 28 in/sec based on Reference 5. Typically, two inches clearance exists around the periphery of the pipe and the penetration so that contact between the pipe and the penetration does not occur during the first 2 inches of sliding, and additional motion is required before failure can occur. Because piping systems are very ductile, the median relative end displacement necessary to cause piping failure was taken to be 4 inches. The acceleration capacity was found by solving for A using Equation 4-9:

$$u_m = 4 \text{ inches}$$

$$V = 28 \text{ in/sec/g}$$

$$= 28A$$

$$u_m = \frac{V^2}{2gN}\left(1 - \frac{N}{A}\right) \qquad (4\text{-}9)$$

$$0 = \frac{V^2}{2gN} - \frac{V^2}{2gA} - u_m$$

$$= \frac{(28A)^2}{2(386.4)(1.118-0.1734A)} - \frac{(28A)^2}{2(386.4)A} - 4$$

$$A = 2.13$$

$$F_S = \frac{2.13}{0.17}$$

$$\approx 13$$

4.1.2 Structure Ductility

A much more accurate assessment of the seismic capacity of a structure can be obtained if the inelastic energy absorption of the structure is considered in addition to the strength capacity. One tractable method involves the use of ductility modified response spectra to determine the deamplification effect resulting from the inelastic energy dissipation. Early studies indicated the deamplification factor was primarily a function of the ductility ratio, μ, defined as the ratio of maximum displacement to displacement at yield. More recent analytic studies (Reference 7) have shown that for single-degree-of-freedom systems with resistance functions characterized by elastic-perfectly plastic, bilinear, or stiffness-degrading models, the shape of the resistance function is, on the average, not particularly important. However, as opposed to the earlier studies, more recent analyses have shown the deamplification factor is also a function of the system damping. For systems in the amplified acceleration region of the spectrum (i.e., between 2 Hz and 8 Hz), Figure 4-4 from Reference 7 shows the deamplification factor for several damping values as a function of the ductility ratio.

One drawback to using the Riddell-Newmark formulation from Reference 7 as it currently exists is that it does not reflect the correlation between earthquake magnitude and system ductility. It is well known that the fewer the number of strong motion cycles that a structure has to withstand, the greater the structure ductility for a given peak ground acceleration since the structure can absorb more energy per cycle. There is a rough correlation between magnitude and number of strong motion cycles. As the magnitude increases, the number of strong motion cycles tends to increase. Thus, at higher magnitudes, a structure will exhibit less ductility at failure than at lower magnitudes.

To include this relationship in the Riddell-Newmark formulation, results from Reference 22 will be employed. As part of this analysis, four different shear wall elements, with frequencies between 2.14 and

8.54 Hz and 7 percent damping, were subjected to different earthquake acceleration records. Two different ductility levels were used to define failure. The lower one, $\mu = 1.85$, represented the best estimate of inelastic deformations which would occur in a shear wall designed to remain essentially elastic for the design earthquake. The higher ductility, $\mu = 4.27$, represented a conservative lower bound for the onset of significant structural damage. The structural model yield capacities were determined from the elastic spectral acceleration of each earthquake at 7 percent damping for each frequency. The input ground motion was then scaled by a factor, F, and the maximum inelastic response was computed by time history nonlinear structural response analyses. The scale factors from Reference 22 necessary to achieve the ductility ratios of 1.85 and 4.27 are presented in Tables 4-4 and 4-5, respectively. For each table, the factors are separated into two groups: those derived from earthquakes in the 6.5-7.5 Richter magnitude range and those derived from earthquakes in the 4.5-6.0 Richter magnitude range. The mean, the median, and the range are also given for each group. Note that the distribution as represented by the median and the range is not lognormal. However, it will suffice to create an approach that approximately predicts the median F values at the low end of range.

The Riddell-Newmark method for computing the ductility factor, F_μ, is as follows:

$$F_\mu = [(q+1)\mu - q]^r$$

where: $q = 3.0\gamma^{-0.30}$ in the amplified acceleration region.

$= 2.7\gamma^{-0.40}$ in the amplified velocity region.

$r = 0.48\gamma^{-0.08}$ in the amplified acceleration region.

$= 0.66\gamma^{-0.04}$ in the amplified velocity region.

γ = percent of critical damping to be used.

Thus, for the frequency range of interest, only the q and r values for the acceleration region apply. For 7 percent damping, q = 1.67 and r = 0.411. For μ = 1.85, F_μ = 1.63; for μ = 4.27, F_μ = 2.55. Comparing these F_μ values to the four median F values taken from Tables 4-4 and 4-5, the Riddell-Newmark method overpredicts the median scale factor for the 6.5-7.5 Richter magnitude range and underpredicts the median scale factor for the 4.5-6.0 Richter magnitude range. Thus, to more accurately predict F, the ductility used in the Riddell-Newmark formula needs to be an effective ductility, μ^*. The following formulation was developed to calculate the effective ductility:

$$\mu^* = 1.0 + C_D\ (\mu - 1.0)$$

where C_D varies depending on the magnitude range. It was found that the following values for C_D produced scale factors that were in good agreement with the median factors from Tables 4-4 and 4-5:

$$C_D = 1.40 \text{ for } 4.5 < M < 6.0$$

$$= 0.70 \text{ for } 6.5 < M < 7.5$$

In calculating the variabilities due to uncertainty, β_U, and randomness, β_R, the actual scale factor was said to have only a 1 percent probability of being less than 1.0. Thus, the combined variability, β_C, was determined as follows:

$$\beta_C = \frac{1}{2.33} \ln (F_\mu)$$

β_C is the result of β_U and β_R being combined by the square-root-of-the-sum-of-the-squares method. β_R is a measure of the dispersion that is represented by the range in F values as shown in Tables 4-4 and 4-5. It was decided to let $\beta_R = 0.8\ \beta_C$ and $\beta_U = 0.6\ \beta_C$. With this value for β_R, the ranges of $\pm 2\ \beta_R$ formed around F_μ are similar to those shown in Tables 4-4 and 4-5, especially at the low end. Values at the high end are of no

concern, since only the low end contributes significantly to the risk. A comparison of the analytic results from Reference 22 with the results derived from the amended Riddell-Newmark procedure are shown in Table 4-6.

As stated in Chapter 1, the majority of seismic risk for Millstone 3 is estimated to result from earthquakes that have Richter magnitudes between 5.3 and 6.3. This range slightly exceeds that for which $C_D = 1.40$. Therefore, for the Millstone 3 evaluation, a value of 1.30 was used for C_D.

4.1.2.1 Example of Ductility Factor

Typical values used for Millstone 3 structures were 10 percent damping and a system ductility of 4. Thus, from Section 4.1.2:

$$\mu^* = 1.0 + 1.30\ (4-1) = 4.9$$

$$q = 3.0\ (10)^{-0.30} = 1.504$$

$$r = 0.48(10)^{-0.08} = 0.399$$

These values give:

$$\check{F}_\mu = [(1.504 + 1)(4.9)-1.504]^{0.399} = 2.58$$

$$\beta_C = \frac{1}{2.33} \ln (2.58) = 0.407$$

$$\beta_R = 0.8(0.407) = 0.33 \qquad \beta_U = 0.6(0.407) = 0.24$$

These values are appropriate for structures having fundamental frequencies corresponding to the amplified acceleration region of the response spectrum (approximately between 2 Hz and 8 Hz). For structures having fundamental frequencies associated with the transition region of the response spectrum (approximately between 8 Hz and 20 Hz), $\check{F}_\mu$ was interpolated between the value above and that appropriate for the rigid response region (see Reference 7).

4.1.3 Structure Response Used for Structure Fragility Evaluations

Determination of the structure response factors and their variabilities in fragility evaluations is typically performed using structure responses predicted by the original design dynamic analyses. The available design information regarding the Millstone 3 structure loads was reviewed and determined to be described in insufficient detail to permit an accurate assessment of the median structure loads. As an alternative, details of the original design dynamic models and eigensolutions were obtained. Eigensolutions predicted using the model information supplied were generated and compared to the original design eigensolutions to verify that the dynamic model information was correctly interpreted. Median-centered overall structure loads were then developed using the median-centered methods described in Section 3. These structure loads were then used to determine the median strength factors in the structures fragilities evaluations.

Because median structure responses were used directly, median response factors were taken to be unity in the structures fragility evaluations. An exception is the emergency generator enclosure. The original design response was used in the fragility evaluation since it was based on a finite element representation of the soil-structure interaction effects that could not be improved upon within the limitations of this study. Also, equipment fragility evaluations were typically performed on the basis of the original design in-structure response spectra since generation of median-centered, in-structure spectra would require greater effort than warranted.

The following discussion describes the determination of the median structure response factors based upon comparison of the median versus design responses. This convention is retained for the benefit of understanding the structure response factors used in the emergency generatory enclosure and equipment fragility evaluations.

4.1.4 Spectral Shape, Damping, and Modeling Factors

As previously discussed, the important Millstone 3 structures were designed using the ground response spectra shown in Figure 1-2. For the SSE, five percent of critical damping was used for the reinforced concrete structures. For the reinforced concrete comprising the lateral load carrying structures for Millstone 3, ten percent of critical damping is considered to be the median value expected at response levels near failure (Reference 10). As shown in Figure 3-1, the ten percent damped median-centered response spectrum exceeds the five percent damped SSE spectrum except at frequencies in excess of about 20 Hz. The frequencies predicted by the Millstone 3 original design dynamic models were available. The spectral shape factor for each structure was based on the mode or modes contributing to most of the seismic response. The spectral shape factor at the frequency under consideration is given by:

$$F_{SS} = \frac{S_{D_{\zeta = 5\%}}}{S_{M_{\zeta = 10\%}}} \qquad (4\text{-}10)$$

where $S_{D_{\zeta = 5\%}}$ represents the 5 percent damped design spectral acceleration and $S_{M_{\zeta = 10\%}}$ represents the estimated spectral acceleration associated with the median site-specific response spectrum for 10 percent damping. As noted in Section 4.1.3, structure loads used in the structure fragility evaluations of all structures except the emergency generator enclosure were derived from the median-centered response spectrum. The median spectral shape factors for these structures are therefore unity.

In computing the spectral shape factor of safety, it is convenient to combine the damping and ground response spectrum effects. In the development of logarithmic standard deviations on spectral shape, however, it is informative to consider the damping effects separately. This implies a factor of safety of unity on damping alone since it has already been included in the factor of safety on spectral shape.

The logarithmic standard deviation on spectral acceleration, β_{SA}, may be estimated from References 8 and 10. Reference 8 provided the mean site-specific spectrum and associated variabilities for five percent damping. It also presents a procedure by which mean spectra at other damping values could be calculated, but does not give the variabilities for these other spectra. These variabilities were estimated with the aid of Reference 10.

The deviation on spectral acceleration resulting from damping, β_ζ, can be estimated from:

$$\beta_\zeta \approx \ln \frac{S_{M_{\zeta = 7\%}}}{S_{M_{\zeta = 10\%}}} \qquad (4\text{-}11)$$

where $S_{M_{\zeta = 7\%}}$ is the spectral acceleration from the median site-specific spectrum at seven percent damping, and $S_{M_{\zeta = 10\%}}$ is the spectral acceleration from the ten percent damped median site-specific spectrum. Seven percent damping is estimated by Reference 10 to be one standard deviation below the median damping value of ten percent. The randomness and uncertainty components of β_ζ are judged to be approximately equal. Thus,

$$(\beta_R)_\zeta = (\beta_U)_\zeta = \frac{\beta_\zeta}{\sqrt{2}}$$

The original design dynamic models of the Millstone 3 structures were typically determined to be adequate to predict the seismic response. In generating loads for the structures fragility evaluations, model modifications were incorporated if necessary. Modeling factors of unity typically were used.

Variability in modeling predominantly influences the calculated mode shapes and modal frequencies. Since the concrete strength and, consequently, the stiffness of the structures is above the design values, calculated frequencies would be expected to be somewhat less than actual values, at least for low to moderate levels of response. At response levels approaching failure, softening of the structures due to concrete cracking occurs, and for structures analyzed using uncracked section properties, some decrease in the actual frequencies compared to the calculated values is expected. Calculated frequencies were generally assumed to be median centered unless material properties used in the original analyses differed from the material properties calculated from test data enough to significantly change the calculated frequencies. The mode shapes were assumed to stay the same regardless of whether or not frequencies changed.

Modeling uncertainties from both the mode shapes and modal frequencies enter into the uncertainty on calculated modal response as defined by β_M. Thus,

$$\beta_M = \sqrt{\beta_{MS}^2 + \beta_{MF}^2} \qquad (4\text{-}12)$$

where β_{MS} and β_{MF} are estimated logarithmic standard deviations on structural response of a given point in the structure due to uncertainties in mode shape and due to uncertainties in modal frequency, respectively. Based upon experience in performing similar analyses, β_{MS} was estimated to be typically about 0.15. The modal frequency variability shifts the frequency at which spectral accelerations are to be determined, so that:

$$\beta_{MF} = \ln\left(\frac{S_{M_{f=f_\beta}}}{S_{M_{f=f_M}}}\right) \qquad (4\text{-}13)$$

where f_M is the median frequency estimate, and f_β is the 84 percent exceedance probability frequency estimate. The logarithmic standard deviation on frequency was estimated to be approximately 0.30 for the structures evaluated.

4.1.4.1 Example of Spectral Shape, Damping, and Modeling Factors

As an example, determination of the spectral shape, damping, and modeling factors and variabilities appropriate for failure modes associated with E-W response of the auxiliary building will be presented. Review of the modal responses indicated that nearly all of the response quantities in the E-W direction are associated with the fundamental E-W mode. This mode was found to have a median elastic frequency of 8.8 Hz compared to the original design frequency of 7.8 Hz. This frequency shift can be attributed to the increase in structure stiffness associated with the median rather than design concrete compressive strength.

As noted in Section 4.1.3, evaluations of the structural failure modes for the auxiliary building were tyically based on median-centered structure loads. The median spectral shape factor for these failure modes is therefore unity. For failure modes whose fragilities were derived from the original design basis, the median spectral shape factor would be based on a comparison of the original design spectral acceleration of 0.38g at the original design frequency of 7.8 Hz for five percent design damping with the median spectral acceleration of 0.301g at the median frequency of 8.8 Hz for ten percent median damping:

$$\breve{F}_{SA} = \frac{0.38}{0.301} = 1.3$$

From information defining the median-centered spectrum for the Millstone 3 site, the variability associated with randomness was estimated to be 0.20 at the median frequency. The uncertainty was estimated to be 2/3 of the randomness.

$$\beta_R = 0.20$$

$$\beta_U = 0.13$$

The composite variability associated with damping was based on a comparison of the median spectral acceleration of 0.322g for seven percent damping at the median frequency at 8.8 Hz with the median spectral acceleration of 0.30g for ten percent damping.

$$\beta_\zeta = \ln\left(\frac{0.322}{0.301}\right)$$

$$= 0.07$$

$$(\beta_R)_\zeta = (\beta_U)_\zeta = \frac{\beta_\zeta}{\sqrt{2}} = 0.05$$

For this structure, uncertainty on frequency was estimated to be 0.30. The -1β frequency was found to be:

$$f_{-1\beta} = 8.8\, e^{-0.30}$$

$$= 6.5 \text{ Hz}$$

The modeling uncertainty associated with frequency was then based on the maximum spectral acceleration for the ten percent damped median response spectrum of 0.311g which falls within the $\pm 1\beta_f$ range.

$$\beta_{mf} = \ln\left(\frac{0.311}{0.301}\right)$$

$$= 0.03$$

This value was combined with the estimated modeling uncertainty associated with mode shape of 0.15 to give the total modeling uncertainty:

$$\beta_M = \sqrt{0.03^2 + 0.15^2}$$

$$= 0.15$$

4.1.5 Modal Combination

The seismic design analysis of Millstone 3 structures was performed by response spectrum analysis; therefore, phasing of the individual modal responses was unknown. Most current design analyses are normally conducted using response spectra techniques. The current recommended practice of the USNRC as given in Regulatory Guide 1.92 (Reference 12) is to combine modes by the square-root-of-the-sum-of-the-squares (SRSS). This was the approach used in the Millstone 3 analyses. Many studies have been conducted to determine the degree of conservatism or unconservatism obtained by use of SRSS combination of modes. Except for very low damping ratios, these studies have shown that SRSS combination of modal responses tends to be median centered. The coefficient of variation (approximate logarithmic standard deviation) tends to increase with increasing damping ratios. Figure 4-5 (taken from Reference 23) shows the actual time-history calculated peak response versus SRSS combined modal responses for structural models with four predominant modes. Based upon these and other similar results, it is estimated that for ten percent structural damping, the SRSS response is median-centered. The median modal combination factor of safety was therefore taken to be 1.0 for structural and equipment fragilities based on the original design information. Similarly, the SRSS method of modal combination was used to develop the median structure loads described in Section 4.1.3. The median modal combination factor for structural fragilities based on these loads was also taken to be 1.0. Where individual modal responses were known, the absolute sum of these

responses was used to estimate the coefficient of variation. The absolute sum is an upper bound estimated to be three standard deviations above the median SRSS response.

4.1.6 Combination of Earthquake Components

The design of the essential Millstone 3 structures with the exception of the auxiliary building was based on loads developed from the absolute sum of the accelerations in one direction due to the simultaneous responses from all three directions of input. For the design of the auxiliary building, the dynamic forces of the members were computed by the square-root-of-the-sum-of-the-squares (SRSS) method. Current licensing requirements consist of the SRSS combination of responses from three principal directions (Reference 12). Alternatively, it is recommended (Reference 10) that directional effects be combined by taking 100 percent of the effects due to motion in one direction and 40 percent of the effects from the two remaining principal directions of motion. This was considered the median condition for the current evaluation.

Depending on the geometry of the particular structure under consideration together with the relative magnitude of the individual load or stress components, the expected stresses due to the 100, 40, 40 percent method of load combinations are decreased when compared with those calculated using the original design method. For shear wall structures where the shear walls in the two principal directions act essentially independently and are the controlling elements, the two horizontal loads do not combine to a significant degree except for the torsional coupling. Thus, only the vertical component affects the individual shear wall stress. A moderate amount of vertical load slightly increases the ultimate shear load carrying capacity of reinforced concrete walls. However, there is an equal probability that the vertical seismic component will add to or subtract from the dead-weight loads at the time of maximum horizontal loads. Thus, while the dead load is sometimes included in the analyses, the vertical seismic component is ignored. Consequently, the factor of safety is not strongly influenced by the directional component assumptions.

The coefficient of variation is calculated in the same manner as it was for the modal combination factor. The absolute sum of the three components is an upper bound, estimated to be three standard deviations above the median.

4.1.7 Soil-Structure Interaction Effects

Two types of soil-structure effects are considered in the analysis of nuclear power stations. The first involves the variation in frequency and response of the structure due to the flexibility of the soil and the dissipation of energy into the soil by radiation (geometric) damping. For structures founded on competent bedrock such as most of the Millstone 3 Category I structures, these effects are usually small and are typically neglected in current design analyses. A second effect is the amplification of the bedrock motion through the soil. Again, for structures founded directly on the bedrock, essentially no amplification occurs, and the motion is normally specified at the foundation level as was done in the design of the Millstone 3 structures. Thus, the design of the Millstone 3 structures founded on rock was conducted using current state-of-the-art assumptions and methods of analysis in regard to the soil-structure interaction effects.

The original design analysis of the emergency generator enclosure, which is founded on soil, was performed using a finite element representation of the structure and the supporting media. The soil material properties were treated as being linearly viscoelastic. Nonlinear behavior of the soil properties was accounted for by the use of the Program SHAKE. The bottom boundary of the finite element model was established at bedrock while the side boundaries were represented as being energy transmitting. Seismic input consisted of the design time-history input at bedrock.

The finite element model of the emergency generator enclosure described above directly accounts for the stiffness and radiation damping representation of the major soil-structure interaction effects normally considered in seismic analysis. Also, because the design time-history was input at the bedrock boundary, amplification of the bedrock motion up through the soil to the structure foundation was directly accounted for in the seismic analysis. Based upon a review of the soil-structure interaction representation of the emergency generator enclosure, the median soil-structure interaction factor was estimated to be 1.0, with logarithmic standard deviations associated with randomness and uncertainty of 0.06 and 0.22, respectively.

The original design seismic analysis of the control building was conducted using a fixed-base representation of the soil-structure interaction effects. It appears that the seismic analysis was later revised using a finite element soil-structure interaction model similar to the emergency generator enclosure model. A comparison of the fundamental frequencies predicted by both models indicated very little frequency shift when soil-structure interaction effects were accounted for. This is consistent with the presence of the very shallow layer of stiff basal till separating the structure from bedrock. For control building fragilities based on loads generated by the original design model, the median soil-structure interaction factor was estimated to be 1.0, with logarithmic standard deviations associated with randomness and uncertainty of 0.02 and 0.10, respectively.

One other possible area of concern is the slab uplift of the structures at high input acceleration levels. For structures founded on competent rock, there is insufficient energy in the low frequency earthquake waves to sustain overturning motion of the structure at the very long response periods required to overturn an auxiliary building or containment structure. At the frequencies of maximum input energy content, although a very small amount of uplift may occur, the direction of input motion is reversed before any significant rocking motion can occur. So long as significant rock or concrete crushing does not occur,

relative motion sufficient to cause piping or electrical conduit failure is not considered a possible failure mode. The bedrock at the Millstone 3 site is considered to be of adequate strength to preclude failures resulting from base slab uplift.

4.2 STRUCTURE FRAGILITIES

The significant failure modes for each of the Millstone 3 structures included in this study were evaluated. The resulting fragilities for each of these structures are discussed in the following sections.

4.2.1 Containment and Internal Structures

The containment structure is a reinforced concrete structure consisting of a circular cylindrical wall capped by a hemispherical dome. The containment wall is supported by a base mat bearing on rock. Principal dimensions of the containment structure are:

Mat	Radius	79'-0"
	Thickness	10'-3"
	Liner plate thickness	1/4"
Cylinder	Inside radius	70'-0"
	Wall thickness	4'-6"
	Liner plate thickness	3/8"
	Height to springline	131'-3"
Dome	Inside radius	70'-0"
	Wall thickness	2'-6"
	Liner plate thickness	1/2"

The controlling mode of failure for the containment structure was found to be shear failure of the wall near the base. Concrete with a design compressive strength of 3000 psi at 28 days was used to construct the wall. Reinforcement in the meridional and hoop directions were

provided with additional reinforcement included at the discontinuities to resist increased stresses imposed by LOCA loading. Diagonal reinforcement was also provided in the wall for additional resistance against horizontal seismic shear forces.

Horizontal shear forces due to seismic response of the containment structure introduce tangential shear stresses in the wall. The median shear strength of the wall was determined using empirical relationships derived from testing conducted on models of prestressed and reinforced containment structures. Resistance to horizontal seismic shear is provided by the concrete and the four-way reinforcement pattern. This failure mode was found to have a median acceleration capacity of approximately 4.9g. Median factors of safety and variabilities for this failure mode are listed in Table 4-7. This mode of failure results in loss-of-liner integrity, failure of the reactor coolant pressure boundary, and failure of most of the safety systems and components.

The containment internal structure consists of walls and floors supporting the equipment housed within the containment structure. The internal structure also provides biological shielding and missile protection. Towards the base of the internal structure, the main load-carrying elements are the crane wall, the primary shield wall, the in-core instrumentation tunnel walls, and the steam generator columns. These elements are founded on the base mat common with the containment structure. Dimensions at the crane wall and primary shield wall are:

Crane wall	Outer radius	57'-6"
	Thickness	2'-6" above El. 46'-10"
	Height	132'-10"
Primary shield wall	Inner radius	12'-6"
	Thickness	4'-6"
	Height	51'-9"

Review of the internal structure indicated that failure due to seismic response will obviously occur towards the base of the structure. At this location, the crane wall is perforated by several large openings that create a series of wall segments typically 3'-0" by 10'-0" spanning from the top of the base mat to El. (-)0'-9". Internal structure failure is expected towards the base mat due to the reduction in material available to resist seismic loading. Because the walls above El. 3'-0" are essentially interconnected, it is appropriate to treat the walls and columns below El. 3'-0" as being tied together.

To provide a more refined evaluation of the seismic load distributions to the individual members, a more detailed static model of the structure below El. 3'-0" was created. The walls and columns were represented by individual elements and were rigidly connected at El. 3'-0". Applied loading was based upon overall seismic loads acting on the internal structure predicted by the median response spectrum analysis.

Capacity of the internal structure was found to be controlled by seismic loads acting primarily in the E-W direction. Structural yielding was found to initiate in the 3'-0" by 10'-0" crane wall columns at the west side of the structure due to tension resulting from the overall structure overturning moment. Because of redundancy, initiation of yielding at these columns does not imply structural failure of the internal structure. After adjusting the static model for local nonlinearities, failure of the internal structure was found to be controlled by in-plane shear failure of the long crane wall column at the south side of the structure. Crane wall failure was determined to have a median acceleration capacity of approximately 2.2g. Median factors of safety and variabilities for this failure mode are listed in Table 4-8. This structural failure is expected to result in failure of the reactor coolant pressure boundary. Also, the integrity of the liner cannot be guaranteed following failure of the concrete internals.

Other failure modes investigated for the containment and internal structures included flexural failure of the containment wall and sliding at the foundation. Flexural failure of the containment wall due to the overturning moment generated by horizontal seismic response was estimated to have a median acceleration capacity of approximately 6.1g. Although structure sliding is expected to initiate at a median acceleration of approximately 1.1g, damage to the structure or equipment is not expected as a result. The containment base mat is embedded in bedrock with a ± 6" gap provided between the vertical base mat and rock forces. This gap is filled with concrete sealer and hollow concrete block. Even if the concrete block is crushed, the maximum sliding displacement that can occur is expected to be only slightly more than one inch. This upper bound displacement is believed to be insufficient to fail piping attached to the structure. Overturning of the containment structure is not considered to be a credible mode of failure. The periods required to result in overturning are so large compared to the rigid body rotation periods of the structure that the earthquake input is reversed in direction before significant base slab uplift can occur.

4.2.2 Auxiliary Building

The auxiliary building is a reinforced concrete structure housing equipment related to the chemical and volume control, component cooling water, and reactor protection systems. It is founded on a base mat at El. 4'-6" which bears on bedrock and spans four stories up to the roof at El. 93'-6". The primary resistance to lateral loading is provided by shear walls. These walls also serve as bearing walls along with steel and concrete columns to support vertical loads.

The controlling failure mode leading to gross structure failure of the auxiliary building is expected to be shear wall failure. Based upon an elastic load distribution of the overall median structure loads, yielding due to in-plane overturning moment is expected to initiate at the south exterior wall between El. 4'-6" and El. 24'-6". Similar to the containment internal structure as described in Section 4.2.1, the lateral

load-carrying system for the auxiliary building is redundant so that yielding of one wall does not imply gross structural failure. The seismic load distribution was modified to account for this load redistribution. Shear wall failure was found to be controlled by failure of the north exterior wall between El. 4'-6" and El. 24'-6" at a median acceleration capacity of approximately 1.4g. Median factors of safety and variabilities for this failure mode are listed in Table 4-9. Shear wall failure is expected to lead to damage to the critical equipment located in the auxiliary building.

Other failure modes leading to localized structure damage include diaphragm failure, steel and concrete column failure, and structure sliding. The concrete floor slabs serve as diaphragms transmitting structure inertial forces to the walls and redistributing shear wall loads due to changes in wall stiffnesses from story-to-story. The slab at El. 43'-6" adjacent to the east exterior wall is perforated by a series of several openings with removable slab covers. Failure of this portion of the slab is expected at a median acceleration capacity of approximately 1.2g. Damage only to equipment or piping mounted to the slab at El. 43'-6" between Lines F.8 and F.9 is expected at this capacity. Although sufficient damage is expected to the floor slab in this location to result in possible loss of equipment anchorage, no failure of any fluid or electrical systems passing through the openings in the slab is expected. Remaining diaphragms are expected to have acceleration capacities in excess of this value. Median factors of safety and variabilities are listed in Table 4-10.

Many of the steel and concrete columns in the auxiliary building must provide vertical support for shear walls that are not continuous to the base mat. In-plane overturning moments acting on these walls must be resisted by axial loads on the columns. Evaluation of the columns was conducted on the basis of design dead, live, and SSE loads. Typically, capacities of the columns were found to be controlled by tension due to seismic uplift rather than compression. The median acceleration capacity

of 0.29g for Steel Column N9 was differentiated from the median acceleration capacity of 0.71g for Steel Columns N5, N8 and N11 because Column N9 was anchored to the slab by high-strength bolts while the other columns were anchored by Hilti bolts. The initial damage to Column N9 is expected to occur as a result of tensile failure in the bolts at the top of the column. However, the detail of the column will prevent the bolts from falling out and, together with the shear lugs in the top plate, these bolts will provide sufficient lateral support that the column will retain its compressive capacity once the earthquake load reverses. The capacity of the column in compression is significantly greater than tension, and no failure of equipment attached to or adjacent to this column is expected as a result of fracture of the upper bolts. A similar condition exists for the columns anchored by Hilti bolts except that the bolts are expected to yield rather than fracture. The amount of bolt distortion is small since the overall structure displacements result in deformation-controlled loads into the columns. The bolts and shear lugs in the column end plates will assure the columns cannot displace laterally, so their compressive capacity is not lost. The median compressive capacity is over 2g peak effective ground acceleration for these columns.

The median acceleration capacity for initial damage to the concrete columns was estimated to be approximately 0.68g. The concrete column tensile capacity was found to be limited by pullout of the dowels from the base mat. These dowels are not hooked to develop the full median yield strength. Because the columns are not part of the primary lateral-load resisting system, gross structural failure is not expected to result from column dowel pull out. The column earthquake loads are deformation controlled by the overall structure, and the dowels will provide sufficient lateral capacity to assure the concrete columns will function in compression after load reversal. Column uplift is not expected to result in failure of any piping or equipment attached to the column or in the immediate vicinity. The concrete columns have significantly higher capacity in compression and even after compression damage occurs in the columns, although some pipe anchorage may be lost, the

pipes are expected to have sufficient flexibility that failure will not occur. Based on the expected damage to both the steel and concrete columns and a site investigation of the equipment attached to the columns, failure to the equipment is not expected prior to the overall structure failure which is governed by the shear walls.

In addition to the failure modes described above, the possibility of structure sliding was evaluated. Resistance to structure sliding is provided by static friction between the base mat and the gravel layer on which it bears, shear keys embedded in bedrock, and lateral earth pressure. Although structure sliding is expected to initiate at a median acceleration capacity of approximately 0.68g, damage to piping attached to the auxiliary building and running to other structures is not expected until a median acceleration capacity of approximately 2.2g.

4.2.3 Control Building

The control building is composed of reinforced concrete floor slabs and shear walls with structural steel framing provided for additional vertical load support. The structure is founded on a base mat which bears on a thin layer of backfill overlying 1 foot to 15 feet of basal till. Equipment related to the reactor protection and electric power systems is contained within this structure. The cable spreading area and the control room are located on the floors at El. 24'-6" and El. 47'-6", respectively.

The controlling failure mode for the control building was found to be the diaphragm at El. 64'-6" adjacent to the west exterior wall. This region of the floor slab is perforated by openings for a stairwell and ducting, thus reducing the material available to resist seismic shear. The applied load consists of floor inertial forces as well as load from the discontinuous east wall at the story above, which is redistributed to the west exterior wall. The median acceleration capacity for this failure mode was estimated to be approximately 1.0g. Median factors of safety and variabilities are listed in Table 4-11. Due to the lack of redundancy

in the lateral load-resisting system, diaphragm failure is expected to lead to gross structural failure of the control building with resulting damage to the equipment housed within.

Other control building failure modes investigated included structure sliding, shear wall failure, and failure of the control room block wall. Resistance to structure sliding is provided by shear keys embedded in the soil below and static friction imposed at the base mat-soil interface. Structure sliding is expected to initiate in the west direction at a median acceleration capacity of approximately 0.43g. As noted in Section 4.1.1.7, the initiation of sliding does not necessarily imply damage to critical equipment. Should the control building slide 2 inches and impact with the adjacent building, there is a possibility of concrete spalling with subsequent damage to equipment located on or very near the west exterior wall. This failure mode was found to have a median acceleration capacity of approximately 1.2g. Median factors of safety and variabilities for this failure mode are listed in Table 4-12.

Median acceleration capacities for shear wall and control room block wall failure were estimated to be approximately 1.5g and 2.0g, respectively. Review of the control room ceiling specification indicated that the ceiling was required to be safety-wired. Inspection of available drawings indicated that the light fixtures above the control room were braced. Failure of either of these systems are expected at acceleration levels in excess of the controlling failure mode.

4.2.4 Emergency Generator Enclosure

The emergency generator enclosure (EGE) contains the emergency diesel generators and related equipment. The structure is composed of concrete slabs and load-bearing concrete walls. The walls surrounding the diesel generator units are supported by strip footings bearing on soil at El. 9'-0". Soil was backfilled between these walls up to the slab on grade at El. 24'-6". The diesel generator pedestals bear on this backfilled soil, but are separated from the slab on grade by one-inch-thick compressible material. Walls enclosing the fuel oil tank vault were cast integrally and are supported by a base mat.

Resistance to the initiation of sliding provided by static friction between the concrete strip footings and base mat and the soil below, shearing resistance of the soil entrapped by the EGE walls through the horizontal shear plane at the bottom of the strip footings, and concrete-on-soil friction introduced by lateral earth pressure. As noted in Section 4.1.1.7, initiation of structure sliding does not necessarily imply failure. Should the EGE slide in the south direction, the one inch expansion joints separating the pedestrian walkway slab from the EGE and the control building may close. However, this impact is expected to cause damage only to the walkway slab since the EGE and control building walls are much more heavily reinforced. The only important potential failure mode resulting from sliding is failure of attached piping. For an estimated median sliding displacement capacity of four inches, the median bedrock acceleration capacity for sliding-induced failure was found to be approximately 1.3g. Median factors of safety and variabilities for this failure mode are listed in Table 4-13.

Under N-S seismic response, the E-W walls are subjected to out-of-plane loading from the adjacent soil outside the structure and entrapped within the walls and from inertial forces associated with the slab on grade and the walls themselves. The out-of-plane wall reactions are transmitted to the strip footings. Any horizontal loading on the footings in excess of the concrete-on-soil frictional resistance must be

transmitted by the E-W footings acting as horizontal beams to the vault base mat and the strip footing below the west exterior wall. The strip footings are reinforced as horizontal beams with reinforcement concentrated at the vertical faces. Evaluation of the footings for conservatively determined lateral earth pressure loading determined a median acceleration capacity of approximately 0.88g. Median factors of safety and variabilities are listed in Table 4-14. Failure of the wall footings is not expected to lead to gross structural failure. However, some damage in terms of loss of anchorage may be expected to equipment mounted on the slab near the walls at El. 24'-6" and on the walls between El. 24'-6" and El. 51'-0". Other failure modes for the EGE that were evaluated included failure of the slab on grade (analyzed similar to the wall footings) and shear wall failure. Median acceleration capacities of approximately 1.0g and 1.9g, respectively, were determined.

4.2.5 Engineered Safety Features Building

The engineered safety features (ESF) building is composed of reinforced concrete floor slabs and load-bearing walls. It is founded on two base mats bearing on bedrock located at different elevations, one at El. 4'-6" and the other at El. (-)34'-9". The structure is partially embedded down into bedrock on the north, south, and east sides and separated from the rock faces by 1/4" thick protection board and concrete fill. The west side of the structure is separated from the containment structure by a four inch thickness of compressible material except for the base mat at El. (-)34'-9" which butts up against the containment base mat. The ESF building houses equipment related to the containment recirculating, quench spray, residual heat removal, safety injection, and the auxiliary feedwater systems.

The controlling failure mode for the ESF building is a combined base mat - shear wall failure. Under loading in the west direction, in-plane shears from the E-W shear walls are transmitted to the base mat at El. 4'-6". Resistance to sliding in the west direction is provided by a thickened portion of the base mat beneath the east exterior wall. This

thickened portion performs as a shear key and transmits the base shear into bedrock. Calculations indicate that friction developed on the inclined key face are sufficient to prevent the key from sliding up and out of the rock trench. Capacity of the key is limited by the ability of the base mat to transmit the west direction shears into the key through direct tension. Once yielding of the base mat initiates, additional resistance is provided by the shear walls spanning from the base mat at El. (-)34'-9" to El. 4'-6". Shear from these walls is transmitted from the ESF bulding base mat to the containment base mat. The median acceleration capacity for this failure mode was estimated to be approximately 1.7g. Median factors of safety and variabilities are listed in Table 4-15.

Other potential ESF building failure modes evaluated included shear wall failure and diaphragm failure. These failure modes were found to have median acceleration capacities of approximately 2.4g and 2.7g, respectively. The structure sliding displacements in the north, south, and east directions are limited to the thickness of the protection board separating the structure from concrete fill poured to the vertical bedrock faces. Displacements of this magnitude are insufficient to fail piping attached to the structure.

4.2.6 Pumphouse

The pumphouse is a reinforced concrete structure housing both the service water and circulating water pumps. The structure is founded on a base mat bearing on either excavated rock or fill concrete overlying bedrock. Below the floor at El. 14'-6", the structure is essentially open to Long Island Sound with transverse guide walls channeling the water flow.

Capacity of the pumphouse is expected to be controlled by structure sliding in the west direction with subsequent damage to the water lines. Resistance to sliding in the N-S direction is enhanced by shear keys opposing imposed shears. Sliding in the east direction is

restricted by adjacent bedrock which is separated from the structure by fill concrete. No such condition exists against shear in the west direction, however, and only resistance provided by the static friction of the base mat bearing against the excavated/fill concrete surface is available. Sliding in the west direction is expected to initiate at a median acceleration capacity of approximately 0.48g. As noted in Section 4.1.1.7, initiation of structure sliding does not necessarily imply failure. Sufficient sliding displacement to damage the attached piping or electrical duct banks is expected to occur at a median acceleration capacity of approximately 1.3g. Median factors of safety and variabilities are listed in Table 4-16. Other pumphouse failure modes investigated included diaphragm and shear wall failure. Median acceleration capacities of approximately 1.5g and 1.6g, respectively, were found for these failure modes. Median factors of safety and variabilities for these failure modes are listed in Tables 4-17 and 4-18.

4.3.7 Demineralized Water Storage Tank

The demineralized water storage tank (DWST) is essentially a reinforced concrete structure with a steel liner. It serves as part of the auxiliary feedwater system. The concrete walls of the DWST are supported by an octagonal base mat approximately ten feet thick. Inspection of field reports indicated that this base mat was poured on a fill concrete leveling mat overlying bedrock.

The median acceleration corresponding to the initiation of sliding was estimated to be approximately 0.63g. The sliding resistance is controlled by the base mat-concrete fill interface. Capacity of the tank is expected to be governed by the failure of attached piping due to sliding-induced relative displacements. The median acceleration capacity for this failure mode is estimated to be approximately 1.6g. Median factors of safety and variabilities are listed in Table 4-19. Other failure modes, including failure of the concrete walls and failure of the liner, were found to be well in excess of this 1.6g capacity.

4.2.8 REFUELING WATER STORAGE TANK

The refueling water storage tank (RWST) is fabricated from SA 240-304 stainless steel. It has a radius of 29'-6" and stands 59'-0" to the top of the side wall with plate thicknesses varying from 3/16" to 1/2". A total of fifty 3" diameter anchor bolts are provided around the tank perimeter at the base mat. The RWST serves as part of the quench spray system.

Capacity of the RWST was found to be governed by buckling of the lowest shell course due to overall structure overturning moment. The median acceleration capacity for this tank was estimated to be approximately 0.88g. Median factors of safety and variabilities are listed in Table 4-20. Buckling of the tank wall is assumed to lead to loss of contents due to the potential for cracking at a weld.

TABLE 4-1

RESULTS OF CONCRETE COMPRESSIVE STRENGTH TESTING

Structure	Specified Design Strength (psi)	Age at Testing (days)	Average Test Strength (psi)	Test Strength Standard Deviation (psi)
Containment Wall	3000	28	4380	350
Containment Internal Structure	5000	60	6510	670
Auxiliary Building	3000	28	4180	460
Auxiliary Building	5000	60	6180	350
Control Building	3000	28	3720	280
Emergency Generator Enclosure	3000	28	4590	730
Engineered Safety Features Building	3000	28	4200	450
Pumphouse	4000	28	4930	460

TABLE 4-2

MEDIAN CONCRETE COMPRESSIVE STRENGTHS AND VARIABILITIES

Structure	Specified Design Strength (psi)	Median Strength, $\tilde{f}'_c$ (psi)	Logarithmic Standard Deviation, β
Containment Wall	3000	5200	0.13
Containment Internal Structure	5000	7200	0.11
Auxiliary Building	3000	5000	0.15
Auxiliary Building	5000	6800	0.08
Control Building	3000	4500	0.13
Emergency Generator Enclosure	3000	5400	0.19
Engineered Safety Features Building	3000	5000	0.15
Pumphouse	4000	5900	0.14

TABLE 4-3

MEDIAN REINFORCEMENT YIELD STRENGTH AND VARIABILITIES

Structure	Grade	Bar Sizes	Median Yield Strength (ksi)	Logarithmic Standard Deviation
Containment and Internal Structures	40	#4 to #8	51	0.11
	40	#9 to #11	49	0.11
	50	#14	59	0.05
	50	#18	56	0.04
	60	#7 to #9, #11	71	0.05
Auxiliary Building	40	#4 to #8	53	0.10
	40	#9 to #11	47	0.03
	50	#14	59	0.05
	60	#7 to #9, #11	69	0.05
Engineered Safety Features	40	#4 to #9, #11	51	0.07
	60	#7 to #9, #11	71	0.05
Pumphouse	40	#4 to #6	54	0.05
	60	#9 to #11	68	0.06
Emergency Generator Enclosure	40	#4 to #6	53	0.09
	60	#7 to #9, #11	69	0.05
Control Building	40	#4 to #11	51	0.14

TABLE 4-4

SCALE FACTORS NEEDED TO ACHIEVE $\mu = 1.85$

a) Due to 6.5 - 7.5 Richter magnitude earthquakes

Earthquake Record (Comp)	Model Structure Frequency			
	8.54 Hz	5.34 Hz	3.20 Hz	2.14 Hz
Olympia, WA., 1949 (N86E)	1.36	1.11	1.49	1.70
Taft, Kern Co., 1952 (S69E)	1.20	1.25	1.50	1.78
El Centro Array No. 12 Imperial Valley, 1979, (140)	1.34	1.56	1.29	1.48
Pacoima Dam San Fernando, 1971 (S14W)	1.25	1.38	1.26	2.19
Hollywood Storage PE Lot, San Fernando, 1971 (N90E)	1.45	1.65	1.58	1.39
El Centro Array No. 5 Imperial Valley, 1979, (140)	1.58	1.60	1.34	1.51

Mean = 1.47 Median = 1.47 Range = 1.11 - 2.19

b) Due to 4.5 - 6.0 Richter magnitude earthquakes

Earthquake Record (Comp)	Model Structure Frequency			
	8.54 Hz	5.34 Hz	3.20 Hz	2.14 Hz
UCSB Goleta Santa Barbara, 1978 (180)	1.35	1.65	1.41	1.49
Gilroy Array No. 2, Coyote Lake, 1979, (050)	1.36	1.93	2.00	1.86
Gavilan College Hollister, 1974 (S67W)	1.61	1.55	1.62	1.93
Melendy Ranch Barn, Bear Valley, 1972 (N29W)	1.45	1.96	2.18	1.98

Mean = 1.71 Median = 1.64 Range = 1.35 - 2.18

TABLE 4-5

SCALE FACTORS NEEDED TO ACHIEVE $\mu = 4.27$

a) Due to 6.5 - 7.5 Richter magnitude earthquakes

Earthquake Record (Comp)	Model Structure Frequency			
	8.54 Hz	5.34 Hz	3.20 Hz	2.14 Hz
Olympia, WA., 1949 (N86E)	1.56	1.54	2.67	3.75
Taft, Kern Co., 1952 (S69E)	1.25	1.65	2.05	3.38
El Centro Array No. 12 Imperial Valley, 1979, (140)	1.56	2.29	2.10	2.14
Pacoima Dam San Fernando, 1971 (S14W)	1.70	1.86	2.67	3.89
Hollywood Storage PE Lot, San Fernando, 1971 (N90E)	1.94	2.50	2.60	2.05
El Centro Array No. 5 Imperial Valley, 1979, (140)	2.38	2.66	2.33	3.45

Mean = 2.33 Median = 2.22 Range = 1.25 - 3.89

b) Due to 4.5 - 6.0 Richter magnitude earthquakes

Earthquake Record (Comp)	Model Structure Frequency			
	8.54 Hz	5.34 Hz	3.20 Hz	2.14 Hz
UCSB Goleta Santa Barbara, 1978 (180)	1.52	2.05	2.05	1.96
Gilroy Array No. 2, Coyote Lake, 1979, (050)	1.56	3.85	4.36	3.03
Gavilan College Hollister, 1974 (S67W)	2.84	2.97	2.71	8.49
Melendy Ranch Barn, Bear Valley, 1972 (N29W)	1.89	5.48	5.16	3.36

Mean = 3.33 Median = 2.91 Range = 1.52 - 8.49

TABLE 4-6

COMPARISON OF RECENT STUDIES (REFERENCE 22)
WITH AMENDED RIDDELL-NEWMARK PROCEDURE

		Reference 22		Amended Riddell-Newmark	
Magnitude Range	μ	Median	Range	Median	Range
$6.5 < M < 7.5$	4.27	2.22	1.25 - 3.89	2.24	1.28 - 3.92
$4.5 < M < 6.0$	4.27	2.91	1.52 - 8.49	2.89	1.41 - 5.94
$6.5 < M < 7.5$	1.85	1.47	1.11 - 2.19	1.49	1.14 - 1.92
$4.5 < M < 6.0$	1.85	1.64	1.35 - 2.18	1.84	1.21 - 2.69

TABLE 4-7

Structure: Containment Structure

Failure Mode: Shear Failure of Containment Wall

Factor	Median F. S.	β_R	β_U	β_C
Strength	11	0	0.21	0.21
Inelastic Energy Absorption	2.6	0.33	0.24	0.41
Spectral Shape	1.0	0.24	0.16	0.29
Damping	1.0	0.07	0.07	0.10
Modeling	1.0	0	0.16	0.16
Modal Combination	1.0	0.07	0	0.07
Combination of EQ. Components	1.0	0.10	0	0.10
Soil-Structure Interaction	1.0	0	0.05	0.05
TOTAL	29	0.43	0.40	0.59

Median Acceleration Capacity = 29 (0.17g) = 4.9g

TABLE 4-8

Structure: Containment Internal Structure

Failure Mode: Crane Wall Failure

Factor	Median F. S.	β_R	β_U	β_C
Strength	6.0	0	0.21	0.21
Inelastic Energy Absorption	2.2	0.27	0.20	0.34
Spectral Shape	1.0	0.24	0.16	0.29
Damping	1.0	0.07	0.07	0.10
Modeling	1.0	0	0.16	0.16
Modal Combination	1.0	0.07	0	0.07
Combination of EQ. Components	1.0	0.10	0	0.10
Soil-Structure Interaction	1.0	0	0.05	0.05
TOTAL	13	0.39	0.38	0.54

Median Acceleration Capacity = 13 (0.17g) = 2.2g

TABLE 4-9

Structure: Auxiliary Building

Failure Mode: Shear Wall Failure

Factor	Median F. S.	β_R	β_U	β_C
Strength	3.4	0	0.26	0.26
Inelastic Energy Absorption	2.4	0.30	0.23	0.38
Spectral Shape	1.0	0.20	0.13	0.24
Damping	1.0	0.05	0.05	0.07
Modeling	1.0	0	0.15	0.15
Modal Combination	1.0	0.04	0	0.04
Combination of EQ. Components	1.0	0.06	0	0.08
Soil-Structure Interaction	1.0	0	0.05	0.05
TOTAL	8.2	0.37	0.41	0.55

Median Acceleration Capacity = 8.2 (0.17g) = 1.4g

TABLE 4-10

Structure: Auxiliary Building

Failure Mode: Diaphragm Failure

Factor	Median F. S.	β_R	β_U	β_C
Strength	6.1	0	0.25	0.25
Inelastic Energy Absorption	1.2	0.06	0.05	0.08
Spectral Shape	1.0	0.17	0.11	0.20
Damping	1.0	0.04	0.04	0.06
Modeling	1.0	0	0.18	0.18
Modal Combination	1.0	0.09	0	0.09
Combination of EQ. Components	1.0	0.06	0	0.06
Soil-Structure Interaction	1.0	0	0.05	0.05
TOTAL	7.3	0.21	0.34	0.40

Median Acceleration Capacity = 7.3 (0.17g) = 1.2g

TABLE 4-11

Structure: Control Building

Failure Mode: Diaphragm Failure

Factor	Median F. S.	β_R	β_U	β_C
Strength	4.6	0	0.22	0.22
Inelastic Energy Absorption	1.3	0.09	0.07	0.11
Spectral Shape	1.0	0.21	0.14	0.25
Damping	1.0	0.05	0.05	0.07
Modeling	1.0	0	0.15	0.15
Modal Combination	1.0	0.01	0	0.01
Combination of EQ. Components	1.0	0.01	0	0.01
Soil-Structure Interaction	1.0	0.03	0.10	0.10
TOTAL	6.0	0.24	0.33	0.41

Median Acceleration Capacity = 6.0 (0.17g) = 1.0g

TABLE 4-12

Structure: Control Building

Failure Mode: Structure Impact Due to Sliding

Factor	Median F. S.	β_R	β_U	β_C
Strength	6.8	0	0.45	0.45
Inelastic Energy Absorption	1.0	0	0	0
Spectral Shape	1.0	0.19	0.12	0.22
Damping	1.0	0	0	0
Modeling	1.0	0	0	0
Modal Combination	1.0	0	0	0
Combination of EQ. Components	1.0	0.09	0	0.09
Soil-Structure Interaction	1.0	0.02	0.08	0.08
TOTAL	6.8	0.21	0.47	0.51

Median Acceleration Capacity = 6.8 (0.17g) = 1.2g

TABLE 4-13

Structure: Emergency Generator Enclosure

Failure Mode: Failure of Attached Piping Due to Structure Sliding

Factor	Median F. S.	β_R	β_U	β_C
Strength	7.4	0	0.42	0.42
Inelastic Energy Absorption	1.0	0	0	0
Spectral Shape	1.0	0.16	0.11	0.19
Damping	1.0	0	0	0
Modeling	1.0	0	0	0
Modal Combination	1.0	0	0	0
Combination of EQ. Components	1.0	0.17	0	0.17
Soil-Structure Interaction	1.0	0.04	0.15	0.16
TOTAL	7.4	0.24	0.46	0.52

Median Acceleration Capacity = 7.4 (0.17g) = 1.3g

TABLE 4-14

Structure: Emergency Generator Enclosure

Failure Mode: Failure of Wall Footing

Factor	Median F. S.	β_R	β_U	β_C
Strength	3.4	0	0.27	0.27
Inelastic Energy Absorption	1.1	0.03	0.02	0.04
Spectral Shape	1.4	0.18	0.12	0.22
Damping	1.0	0.01	0.01	0.02
Modeling	1.0	0	0.27	0.27
Modal Combination	1.0	0.03	0	0.03
Combination of EQ. Components	1.0	0.05	0	0.05
Soil-Structure Interaction	1.0	0.06	0.22	0.23
TOTAL	5.2	0.20	0.46	0.50

Median Acceleration Capacity = 5.2 (0.17g) = 0.88g

TABLE 4-15

Structure: Engineered Safety Features Building

Failure Mode: Base Mat/Shear Wall Failure

Factor	Median F. S.	β_R	β_U	β_C
Strength	7.2	0	0.25	0.25
Inelastic Energy Absorption	1.4	0.12	0.09	0.15
Spectral Shape	1.0	0.19	0.13	0.23
Damping	1.0	0.02	0.02	0.03
Modeling	1.0	0	0.31	0.31
Modal Combination	1.0	0.06	0	0.06
Combination of EQ. Components	1.0	0.01	0	0.01
Soil-Structure Interaction	1.0	0	0.05	0.05
TOTAL	10	0.23	0.43	0.49

Median Acceleration Capacity = 10 (0.17g) = 1.7g

TABLE 4-16

Structure: Pumphouse

Failure Mode: Failure of Attached Piping Due to Structure Sliding

Factor	Median F. S.	β_R	β_U	β_C
Strength	7.6	0	0.45	0.45
Inelastic Energy Absorption	1.0	0	0	0
Spectral Shape	1.0	0.17	0.12	0.21
Damping	1.0	0	0	0
Modeling	1.0	0	0	0
Modal Combination	1.0	0	0	0
Combination of EQ. Components	1.0	0.17	0	0.17
Soil-Structure Interaction	1.0	0.04	0.15	0.16
TOTAL	7.6	0.24	0.49	0.55

Median Acceleration Capacity = 7.6 (0.17g) = 1.3g

TABLE 4-17

Structure: Pumphouse

Failure Mode: Diaphragm Failure

Factor	Median F. S.	β_R	β_U	β_C
Strength	7.4	0	0.21	0.21
Inelastic Energy Absorption	1.2	0.07	0.06	0.09
Spectral Shape	1.0	0.19	0.13	0.23
Damping	1.0	0.04	0.04	0.06
Modeling	1.0	0	0.16	0.16
Modal Combination	1.0	0.08	0	0.08
Combination of EQ. Components	1.0	0.01	0	0.01
Soil-Structure Interaction	1.0	0	0.05	0.05
TOTAL	8.9	0.22	0.31	0.38

Median Acceleration Capacity = 8.9 (0.17g) = 1.5g

TABLE 4-18

Structure: Pumphouse

Failure Mode: Shear Wall Failure

Factor	Median F. S.	β_R	β_U	β_C
Strength	4.5	0	0.19	0.19
Inelastic Energy Absorption	2.1	0.25	0.19	0.32
Spectral Shape	1.0	0.19	0.13	0.23
Damping	1.0	0.04	0.04	0.06
Modeling	1.0	0	0.16	0.16
Modal Combination	1.0	0.08	0	0.08
Combination of EQ. Components	1.0	0.01	0	0.01
Soil-Structure Interaction	1.0	0	0.05	0.05
TOTAL	9.5	0.33	0.34	0.48

Median Acceleration Capacity = 9.5 (0.17g) = 1.6g

TABLE 4-19

Structure: Demineralized Water Storage Tank

Failure Mode: Failure of Attached Piping Due to Structure Sliding

Factor	Median F. S.	β_R	β_U	β_C
Strength	9.2	0	0.42	0.42
Inelastic Energy Absorption	1.0	0	0	0
Spectral Shape	1.0	0.17	0.11	0.20
Damping	1.0	0	0	0
Modeling	1.0	0	0	0
Modal Combination	1.0	0	0	0
Combination of EQ. Components	1.0	0.18	0	0.18
Soil-Structure Interaction	1.0	0	0	0
TOTAL	9.4	0.25	0.43	0.50

Median Acceleration Capacity = 9.2 (0.17g) = 1.6g

TABLE 4-20

Structure: Refueling Water Storage Tank

Failure Mode: Buckling of Shell Wall

Factor	Median F. S.	β_R	β_U	β_C
Strength	5.2	0	0.27	0.27
Inelastic Energy Absorption	1.0	0	0	0
Spectral Shape	1.0	0.27	0.18	0.32
Damping	1.0	0.05	0.05	0.07
Modeling	1.0	0	0.15	0.15
Modal Combination	1.0	0.01	0	0.01
Combination of EQ. Components	1.0	0.11	0	0.11
Soil-Structure Interaction	1.0	0	0.05	0.05
TOTAL	5.2	0.30	0.36	0.47

Median Acceleration Capacity = 5.2 (0.17g) = 0.88g

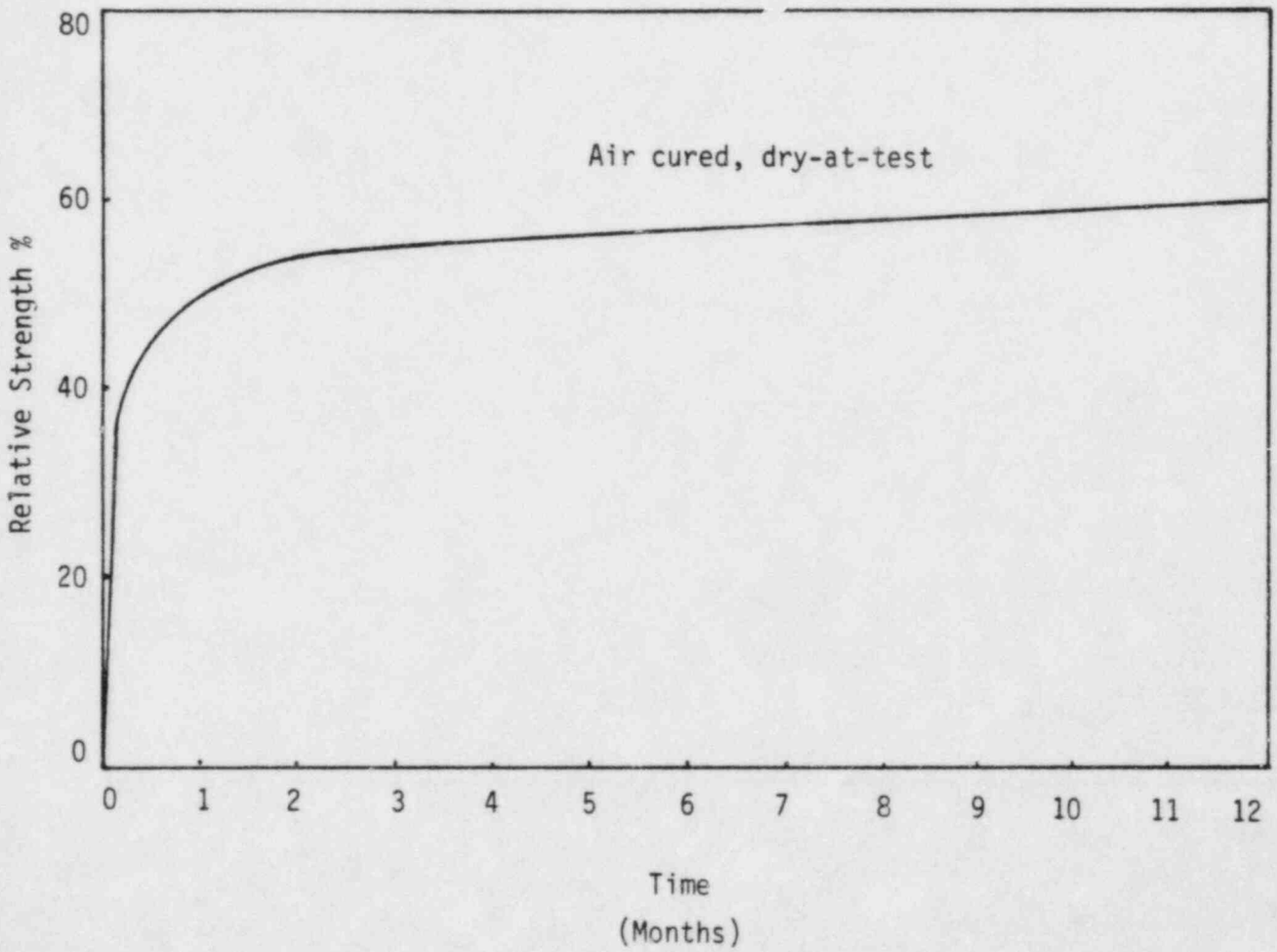

FIGURE 4-1. EFFECTS OF TIME AND CURING CONDITIONS ON CONCRETE STRENGTH (FROM REFERENCE 14)

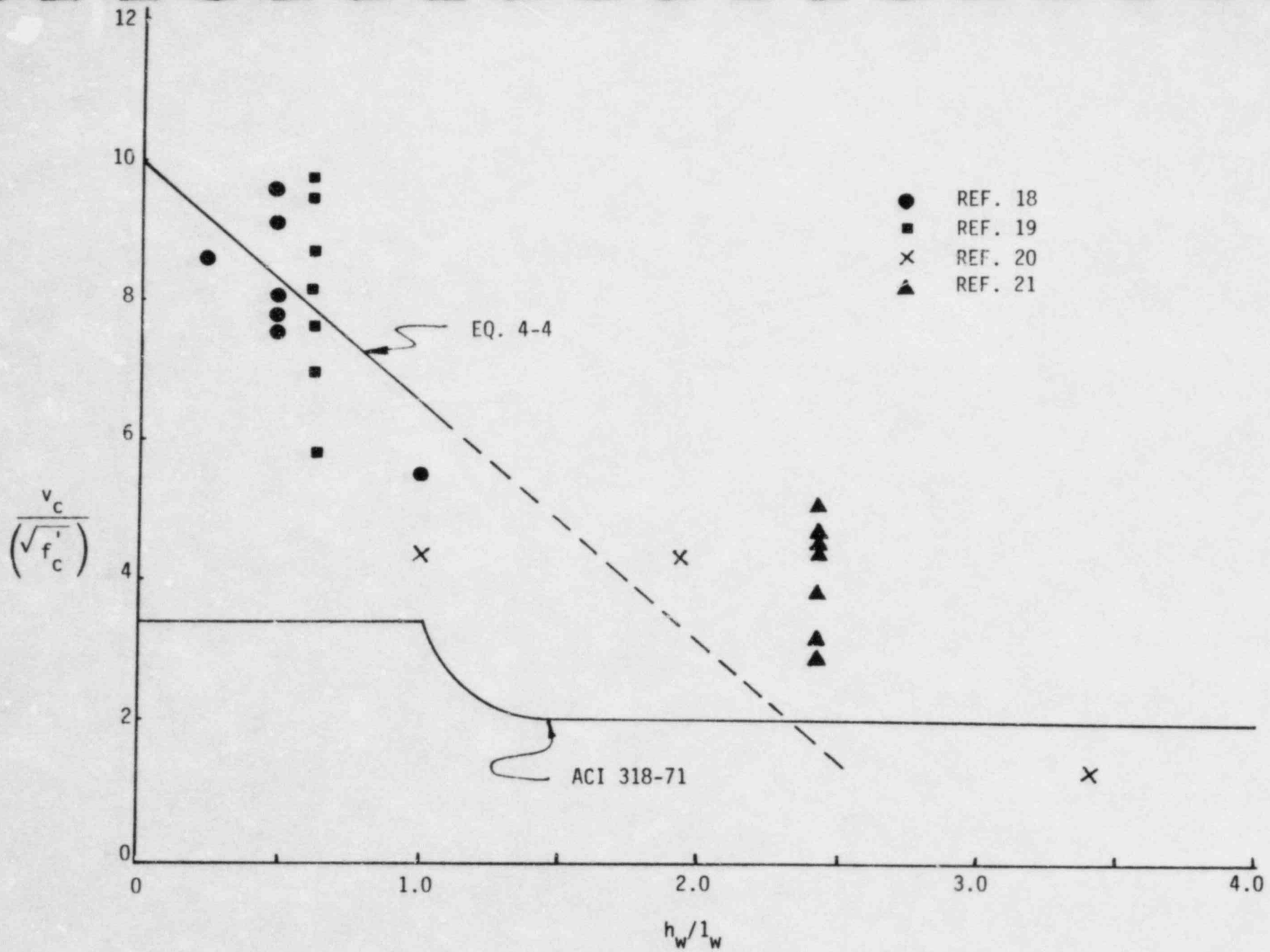

FIGURE 4-2. STRENGTH OF CONCRETE SHEAR WALLS

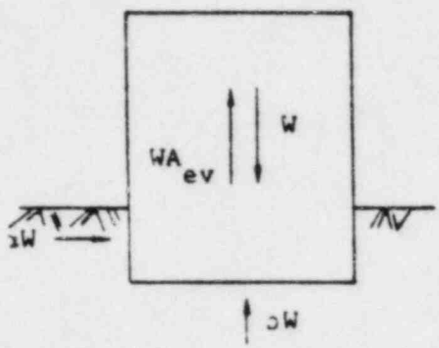

Effective vertical equivalent acceleration = A_{ev} g

Hydrostatic uplift = ρW

Net vertical contact force on base = $W (1-\rho-A_{ev})$

Static horizontal force = αW

Net horizontal resistance = NW = NMg

Coefficient of friction = u

Then $N = u(1-\rho-A_{ev}) - \alpha$

Consider a single pulse of horizontal acceleration Ag lasting for a time t_1, giving a velocity V

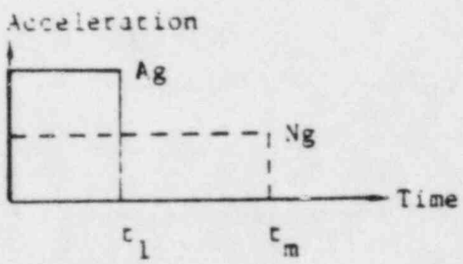

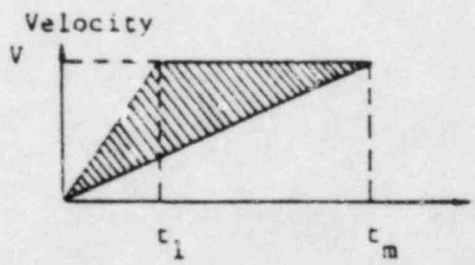

$$t_1 = \frac{V}{Ag}, \quad t_m = \frac{V}{Ng}$$

$$u_m = (t_m - t_1)\frac{V}{2} = \frac{V^2}{2g}\left(\frac{1}{N} - \frac{1}{A}\right)$$

$$= \frac{V^2}{2gN}\left(1 - \frac{N}{A}\right) \quad (4\text{-}9)$$

FIGURE 4-3. NEWMARK SLIDING APPROACH (FROM REFERENCE 15)

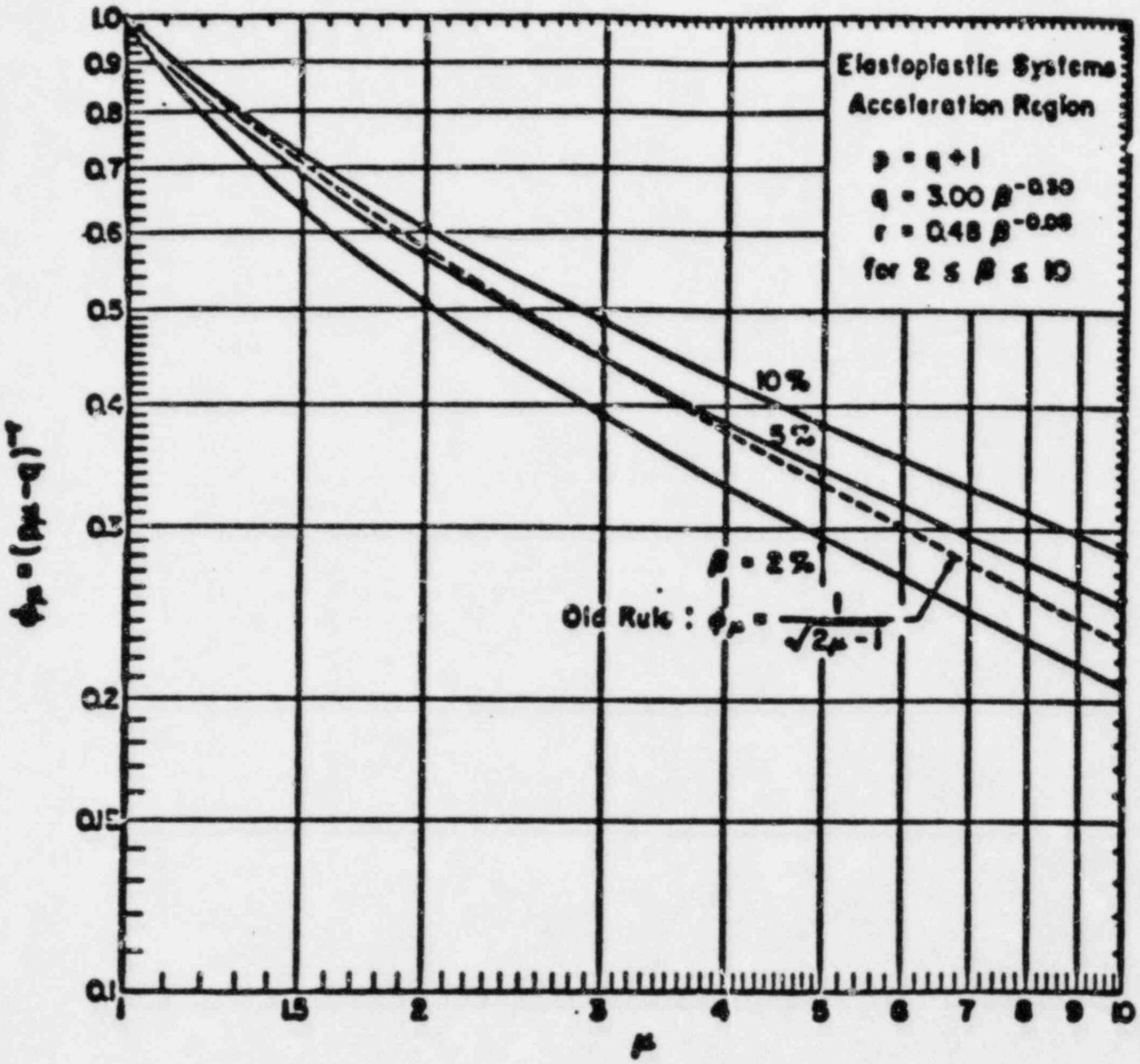

FIGURE 4-4. DEAMPLIFICATION FACTORS FOR ELASTIC-PERFECTLY PLASTIC SYSTEMS IN THE ACCELERATION AMPLIFIED RANGE (FROM REFERENCE 7)

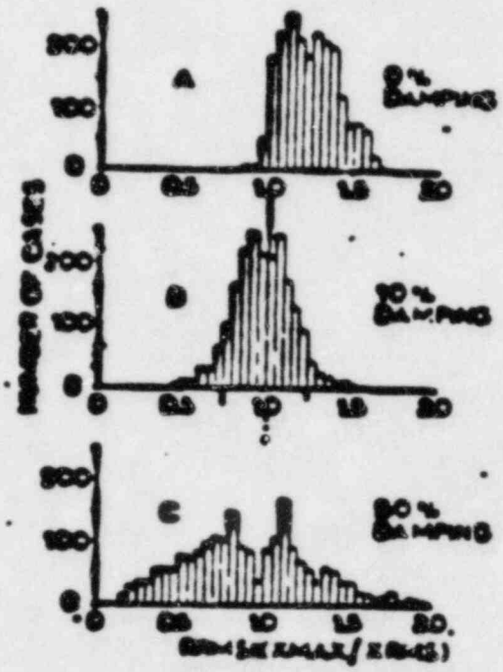

FIGURE 4-5. HISTOGRAMS OF RATIO OF PEAK RESPONSE TO SRSS COMPUTED RESPONSE FOR FOUR-DEGREE-OF-FREEDOM DYNAMIC MODELS (FROM REFERENCE 23)

5. EQUIPMENT FRAGILITY

This chapter describes the fragility development for the seismically critical equipment within the Millstone 3 Nuclear Power Plant. The scope of the equipment evaluation effort is limited and is based upon a preliminary evaluation of Millstone 3 equipment fragilities documented in Reference 34. SMA has conducted a cursory review of the approach and methodology used in the preliminary equipment evaluation and has judged the results to be generally conservative. As a result, the detailed site-specific reevaluation of equipment fragilities was conducted on only a selected set of components. Based upon systems information, it was judged that components exhibiting a median ground acceleration capacity (Ā) of 1.50g or greater will have negligible impact upon risk associated with the Millstone 3 Plant operation. Therefore, the reevaluation of equipment fragilities documented in this report was conducted on all components which, based upon the preliminary evaluation, exhibited a calculated acceleration capacity less than 1.50g. The resulting list of selected equipment used the seismic portion of the Millstone 3 PRA and is presented in Table 5-1. One additional component, the steam generator U-tubes, had a predicted median capacity greater than 2g in Reference 34. Because of the extremely severe consequence of a steam generator tube bundle failure, a reevaluation of the U-tubes was conducted. The median ground acceleration capacity was predicted to be greater than 5g, reconfirming the observed conservatism in fragility development in Reference 34.

Section 5.1 contains a general description of the equipment fragility methodology with a more in-depth treatment than that provided in Chapter 3. Section 5.2 presents a set of representative example fragility derivations which provide the reader with further insight into the equipment fragility determination process while Section 5.3 presents the resulting equipment fragilities for the selected Millstone 3 components.

5.1 EQUIPMENT FRAGILITY METHODOLOGY

Fragility as used in probabilistic seismic safety studies is defined as a conditional probability of failure for a given hazard input. In this case, the fragility of a component or system is defined as the frequency of failure as a function of effective peak ground acceleration. The development of these fragility levels combined with a discussion of the available information sources and the selection of equipment categories are the subject of this section.

5.1.1 Fragility Derivation

The procedure used in deriving fragility descriptions is similar to that used for structural fragility descriptions, wherein, factors of safety and their variability are first developed for equipment capacity and equipment response. These two factors, along with the factor of safety on structural response, are then multiplied together to obtain an overall factor of safety for the equipment item.

$$\check{F}_E = \check{F}_{EC} \cdot \check{F}_{ER} \cdot \check{F}_{SR} \qquad (5\text{-}1)$$

$\check{F}_{EC}$ is the capacity factor of safety for the equipment relative to the floor acceleration used for the design, $\check{F}_{ER}$ is the factor of safety inherent in the computation of equipment response, and $\check{F}_{SR}$ is the factor of safety in the structural response analysis that resulted in floor spectra for equipment design. Sections 5.1.1.1, 5.1.1.2, and 5.1.1.3 of this report contain a more thorough explanation of these three factors ($\check{F}_{EC}$, $\check{F}_{ER}$, and $\check{F}_{SR}$, respectively). The overall factor of safety, $\check{F}_E$, is then multiplied by the reference earthquake peak ground acceleration to obtain fragility in terms of peak ground acceleration.

$$\check{A} = \check{F}_E \cdot A_{SSE} \qquad (5\text{-}2)$$

where:

$\breve{A}$ = Median ground acceleration capacity

A_{SSE} = Peak ground acceleration of the safe shutdown earthquake

In most instances, the SSE was used as the reference earthquake; however, the OBE was used as a reference for those cases where the OBE acceptance criteria governed the equipment design.

The logarithmic standard deviation, β, for each of these factors is obtained using the logarithmic standard deviations for each of the above factors and based upon the lognormal model (Appendix A).

$$\beta_E = (\beta_{EC}^2 + \beta_{ER}^2 + \beta_{SR}^2)^{\frac{1}{2}} \qquad (5\text{-}3)$$

where β_{EC}, β_{ER}, and β_{SR} are the logarithmic standard deviations of the equipment capacity, equipment response and structural response, respectively. The logarithmic standard deviations are further divided into random variability, β_R, and uncertainty, β_U, as described in Chapter 3.

5.1.1.1 Equipment Capacity Factor

The equipment capacity factor is defined as the failure threshold divided by seismic design level. For the purposes of this study, the ultimate failure threshold is the acceleration level at which the component ceases to perform its intended function. This failure threshold could consist of a breaker tripping on a motor control center, excessive deflection of the control rod guide tubes or a support failure of the steam generator. Where several failure modes pertaining to the same component are found to have roughly the same capacity level, all significant failure modes are analyzed.

The factor of safety for the equipment seismic capacity consists of two parts:

1. The strength factor, F_S, based on the components static strength and
2. The ductility factor, F_μ, related to the equipment's inelastic energy absorption capability.

$$\breve{F}_{EC} = F_S \cdot F_\mu \tag{5-4}$$

The logarithmic standard deviation on the capacity can be derived by taking the SRSS of the logarithmic standard deviations on the strength factor and the ductility factor. The randomness and the uncertainty portion of the variability can each be derived individually from Equation 5-5, by substituting the random or the uncertainty β's for the strength factor and the ductility factor (i.e., β_{S_R} for β_S and β_{μ_R} for β_μ, etc.).

$$\beta_{EC} = \left(\beta_S^2 + \beta_\mu^2\right)^{1/2} \tag{5-5}$$

5.1.1.1.1 Strength Factor - The strength factor, F_S, is derived from the equation:

$$F_S = \frac{\frac{P_C}{P_D} - \frac{P_N}{P_D}}{\frac{P_T}{P_D} - \frac{P_N}{P_D}} \tag{5-6}$$

where P_C is the median limit state load or stress, P_N is the normal operating load or stress, P_T is the total normal plus seismic load or stress and P_D is the code design allowable load or stress.

Alternatively, this equation can be written:

$$F_S = \frac{P_C - P_N}{P_{SSE}} \qquad (5\text{-}7)$$

where P_{SSE} is the seismic load or stress corresponding to the safe shutdown earthquake. The normal and the seismic loads (P_N and P_{SSE}) are typically derived from the seismic qualification reports and the other information sources described in Section 5.1.2. The calculation of the capacity load, P_C, is a function of the failure mode for the specific equipment item. Equipment failures can be classified into three categories:

1. Elastic functional failures
2. Brittle failures
3. Ductile Failures.

Elastic functional failures involve the loss of intended function while the component is stressed below its yield point. Examples of this type of failure include:

1. Elastic buckling in tank walls and component supports.
2. Chatter and trip in electrical components.
3. Excessive blade deflection in fans.
4. Shaft seizure in pumps.

The limit state load for this type of a failure is defined as the load or stress level where functional failure occurs.

Brittle failures are defined in this study as those failure modes which have little or no system inelastic energy absorption capability. Examples of brittle type failures include:

1. Anchor bolt failures.
2. Component support weld failures.
3. Shear pin failures.

Each of these failure modes have the ability to absorb some inelastic energy on the component level, but the plastic zone is very localized and the system ductility for an anchor bolt or a support weld is very small. Thus, the collapse load for a brittle failure mode is defined as the median ultimate strength of the material. For example, consider a transformer structure whose anchor bolts have been determined to be the critical failure mode. Under seismic loading, the massive transformer will typically be stressed well below its yield level while the bolts are being stressed well above the bolt yield level. The amount of system inelastic energy absorption provided by the bolts' plasticity is negligible when compared to the seismically-induced kinetic energy of the transformer structure, and thus, these bolts will fail in a brittle mode once the ultimate bolt strength is reached.

Ductile failures coincide much more closely with the structure failures which were described in Chapter 4. Ductile failure modes are those in which the structural system can absorb a significant amount of energy through inelastic deformation. Examples of ductile failure modes include:

1. Pressure boundary failure of piping
2. Structural failure of cable trays
3. Structural failure of ducting
4. Polar crane failure.

The collapse load for ductile failure modes consists of the median yield strength of the material for tensile type loading conditions. For bending type failure modes, the yield point is defined as the limit load or stress to develop a plastic hinge. The ductility factor will then quantify the inherent safety factor above the yield strength to the failure threshold.

Each variable within Equations 5-6 and 5-7 has an associated lognormal probability distribution to express its combined randomness and uncertainty. To find the overall variance on the strength factor, a technique commonly referred to as the "Second Moment Method" is utilized. The mean and variance of a function comprised of lognormally distributed variables can be derived utilizing the moments (i.e., the mean and variances) of the logarithms of the distribution of each variable (Reference 27). The resulting equation for the logarithmic standard deviation on the strength factor derived from Equation 5-6 is given below:

$$\beta_S = \left[\frac{P_C^2}{(P_C - P_N)^2} \cdot \beta_C^2 + \frac{P_T^2}{(P_T - P_N)^2} \cdot \beta_T^2 + \frac{(P_C - P_T)^2 \cdot P_N^2}{(P_T - P_N)^2 \cdot (P_C - P_N)^2} \cdot \beta_N^2 \right]^{1/2} \quad (5\text{-}8)$$

where:

β_C = Logarithmic standard deviation on the capacity or limit load (stress).

β_T = Logarithmic standard deviation on the total load (stress).

β_N = Logarithmic standard deviation on the normal load (stress).

Similarily, the equation for the logarithmic standard deviation on the strength factor derived from Equation 5-7 is:

$$\beta_S = \left[P_C^2 \cdot \beta_C^2 + (P_N - P_C)^2 \cdot \beta_{SSE}^2 + P_N^2 \cdot \beta_N^2\right]^{1/2} \Big/ (P_C - P_N) \qquad (5\text{-}9)$$

where:

β_C and β_N have previously been defined, and

β_{SSE} = logarithmic standard deviation on the seismic load (stress).

5.1.1.1.2 Inelastic Energy Absorption Factor - The inelastic energy absorption capability of a piece of equipment is quantified by the inelastic energy absorption factor (or ductility factor). Brittle failure modes and functional failure modes typically have a ductility factor of 1.0, while ductile type failure modes have ductility factors which are a function of a deamplification factor. Section 4.1.2 of this report describes in great detail the methodology utilized in deriving an appropriate ductility factor for Millstone 3. The ductility factor is based on the Riddell-Newmark methodology presented in Reference 7, but is has been updated to reflect the correlation between earthquake magnitude and system ductility. The median ductility factors and their variabilities were established in Section 4.1.2 as a function of the component's natural frequency, and are summarized below:

a. For the 2 Hz to 8 Hz range,

$$F_\mu = \left[(q+1) \cdot \mu^{-q}\right]^r \qquad (5\text{-}10)$$

where

$q = 3.0 \times j^{-0.30}$

$r = 0.48 \times j^{-0.08}$

j = percent of critical damping to be used.

μ^* = effective ductility ratio
$= 1.0 + C_D (\mu - 1.0)$

C_D = factor accounting for the earthquake duration and equals 1.30 for Millstone 3.

b. For the rigid range,

$$F_\mu = \mu^{*-0.13} \qquad (5\text{-}11)$$

where μ^* is as previously defined.

c. For the range 8 Hz < f < rigid range.

A linear interpolation utilizing log-log paper is applicable for ductile equipment with natural frequencies in this range. A point at 8 Hz should be plotted using F_μ from Equation 5-10 and another point should be plotted at the lowest unamplified (rigid) frequency for the floor spectrum using Equation 5-11. A line drawn between these two points on log-log graph paper will uniquely determine the ductility factors within this frequency range.

The variabilities for these median ductility factor derivations are evaluated by estimating a 1% probability (-2.33β) that the actual ductility factor is less than 1.0. Thus, the following equations determine the composite variability, randomness and uncertainty, respectively.

$$\beta_{\mu_C} = \frac{1}{2.33} \ln(F_\mu)$$

$$\beta_{\mu_R} = 0.8 \times \beta_{\mu_C} \qquad (5\text{-}12)$$

$$\beta_{\mu_U} = 0.6 \times \beta_{\mu_C}$$

The ductility ratio, μ, itself is based upon the recommendations given in Reference 6. This reference gives a range of ductility values to be used for design. The upper end of this range is considered to be a median value. Engineering judgment was utilized to match the applicable category from Reference 6 to a particular failure mode for the equipment component.

5.1.1.2 Equipment Response Factor

The response factors are an estimate of the conservatism or unconservatism that may have existed in the computation of seismic response during the design process. In this section, individual response factors are described for both plant specific and generic equipment. These factors differ according to the seismic qualification procedure which was used in the equipment design.

There are three types of seismic qualifications which were performed for Millstone 3 plant equipment:

1. Dynamic Analysis
2. Static Analysis
3. Testing.

For equipment qualified by dynamic analysis, the important variables that affect the computed response and its dispersion are:

1. Qualification Method (F_{QM})
2. Spectral Shape (F_{SS})
3. Modeling (effects mode shape and frequency results) (F_M)
4. Damping (F_D)
5. Combination of Modal Responses (for response spectrum method) (F_{MC})
6. Combination of Earthquake Components (F_{ECC})

For equipment qualified by static analysis, two subdivisions must be considered. For rigid equipment, variabilities due to spectral shape, combination of modal responses, damping, and for the most part, modeling errors are eliminated. If the equipment is flexible and was designed via the static coefficient method, the dynamic characteristic variables and their variability must be considered. This involves estimating the range of frequency of the equipment and introduces a much larger uncertainty in quantifying the response factor.

Where testing is conducted for seismic qualification, the response factor must take into account:

1. Qualifiction Method (F_{QM})
2. Spectral Shape (F_{SS})
3. Boundary Conditions in the Test vs Installation (F_{BC})
4. Damping (F_D)
5. Spectral Test Method (sine beat, sine sweep, compex waveform, etc.) (F_{STM})
6. Multi-directional Effects (F_{MDE}).

The overall Equipment Response Factor is the product of each of these variables. The overall variabilities (uncertainty and randomness) are calculated by taking the SRSS of the individual logarithmic standard deviations for each of the variables. A brief description of each of the variables used to develop the equipment response factor is provided below. A more detailed discussion is contained within Reference (24).

5.1.1.2.1 Qualification Method Factor - The Qualification Method Factor is a measure of the conservatism/unconservatism involved in the seismic qualification method used to seismically qualify the component. Analytical qualifications can be separated into static analysis and dynamic analysis techniques. The inherent safety factor in using these

qualification techniques is discussed below, while the variability on this factor is generally accounted for within the Damping, Modeling and Mode Combination Factors (i.e., $\beta_{QM_R} = \beta_{QM_U} = 0.0$).

5.1.1.2.1.1 Static Analysis - The static coefficient method is intended to be a conservative upper bound method by which simple components may be qualified. Typically, the peak spectral acceleration is multiplied by a coefficient and this product is multiplied by the weight of the component to determine an equivalent static load to be applied at the subsystem center of gravity. If the component is comprised of more than one lumped mass, the same procedure may be applied at each lumped mass point in the static model or may be applied as a uniformly distributed load on the static model. If the component is rigid (i.e., its fundamental frequency is above the frequency where the response spectrum returns to the zero period acceleration), the degree of conservatism in the response level used for design is the ratio of the specified static coefficient divided by the zero period acceleration of the floor level where the equipment is mounted. If the equipment is flexible and responds predominantly in one mode, the degree of conservatism is the ratio of the static coefficient to the spectral acceleration at the equipment fundamental frequency.

5.1.1.2.1.2 Dynamic Analysis - Response spectrum, mode superposition time-history and direct integration time-history dynamic analysis methods may be applied in subsystem response analyses. If response for a single degree-of-freedom model with best estimate material properties and damping are computed by the response spectrum method, the mode superposition time-history method or the direct integration time-history method, we would expect to obtain equal median centered results assuming that the response spectrum and time-history inputs are compatible.

The response spectrum method, based upon a conservative ground time history, was extensively used for dynamic analysis of components and systems within the Millstone 3 plant. If the applicable Millstone 3

floor response spectra were utilized in the design analysis, the Qualification Method Factor, F_{QM}, is equal to unity and the variability is zero. If conservative generic spectrum were used to seismically qualify a component, F_{QM} is the ratio of the spectral acceleration from the generic spectrum divided by the spectral acceleration from the Millstone 3 site-specific spectra evaluated at the components' fundamental frequency.

5.1.1.2.1.3 Testing - In vibration testing, the test response spectrum generally envelopes the required response spectrum by approximately ten percent or more depending on the frequency range. If the test response spectra are available within the test report, the overtest safety factor will be accounted for in the Qualification Method Factor (F_{QM}) and its variability (β_{QM}). If the component fragility is being based on testing where the test response spectra are not available, F_{QM} and β_{QM} are used to account for the overtest safety factor and variability on a generic case-by-case basis.

5.1.1.2.2 Equipment Spectral Shape Factor - The Millstone 3 design floor response spectra were computed by means of a time-history (T/H) seismic analysis. The overall dynamic response of each of the critical buildings was modeled by lumping the mass of the structure and rigidly attached components generally at each of the floor levels. The synthesized time history accelerogram for the horizontal SSE normalized to 0.17g is shown in Figure 1-4 for 5% damping. This time history was used to generate the response spectra for 0.5, 1.0, 2.0, 4.0, and 8.0 percent damping. As depicted in Figure 1-4, this artificial time history was developed to envelope, as closely as possible, the ground response spectra for the Millstone 3 site. The combined conservatism/unconservatism involved in developing the floor response spectra from a time history representation of the ground response spectra and in using the specified Millstone 3 design response spectra in lieu of median Safe Shutdown Earthquake spectra is quantified in development of the Spectral Shape Factor associated with the Structural Response Factor (See Section 5.1.1.3).

The response spectrum method is often referred to as being conservative, however, the conservatism compared to a time-history analysis is primarily due to the method of developing the spectrum. Spectra used for design purposes are generally smoothed and the peaks are widened such that the resulting design spectrum is conservative.

5.1.1.2.2.1 Peak Broadening and Smoothing - The effect of smoothing and peak broadening varies with structure, elevation, frequency and damping. The criteria utilized in generating Millstone 3 floor response spectra was to broaden the peak resonant value by plus and minus 15%. Beyond this resonant range, the actual amplified response spectra are utilized exactly as shown. Figure 5-1 shows a typical example of the broadened versus unbroadened spectra comparison for the Auxiliary Building.

Factors of conservatism for peak broadening and smoothing were generated separately for specific frequency ranges within each of the Millstone 3 structures. Table 5-2 summarizes these factors together with their variabilities for most Millstone 3 structures. The frequency ranges were selected to reflect the portions of particular floor response spectra where the broadening was and wasn't undertaken. For any particular frequency, this peak broadening and smoothing safety factor can be computed from Equation 5-13 below.

$$F_{SS} = \frac{S_a \text{ (broadened and smoothed)}}{S_a \text{ (unbroadened and unsmoothed)}} \qquad (5\text{-}13)$$

where:

F_{SS} = Spectral shape factor due to peak broadening and smoothing

S_a = Spectral acceleration value

For the frequency range in question, the median ratio (F_{SS} from Equation 5-13) was computed with the minimum value of 1.0 considered to be a -2β extreme. Fragility parameters were determined at each floor elevation within the structures housing equipment to be evaluated. Table 5-2 shows the spectral shape factors for each of the building floors evaluated. The values of F_{SS} shown in Table 5-2 are for the case where all three earthquake components contribute to response. Since the variability, β_{SS}, is due to the shift in the frequency and the variation with floor elevation, it is considered to be all uncertainty.

5.1.1.2.3 Modeling Factor - In any dynamic analysis there is uncertainty in resonse due to assumptions made in modeling the structure, modeling boundary conditions and representing material behavior. Modeling of complex systems is usually conducted using nominal dimensions, weights, and material properties and is done in such a manner that further refinement of mesh size in a finite element representation will not significantly alter the calculated response. Representation of boundary conditions in a model may have a significant influence on the response. The misrepresentation of boundary conditions in the dynamic model by assuming greater or lesser stiffness or treating nonlinear gap effects linearly cannot be quantified generically and each model must be treated specifically to determine a response factor for modeling. Assuming that the analyst does his best job of modeling, modeling accuracy could be considered to be median centered (i.e., $F_M = 1.0$) with the variability in each of the modeling parameters amounting to variability in calculated mode shapes and frequencies. The error in calculation of mode shapes and frequencies then has an effect on the computed response.

For complex equipment which have been analyzed using state-of-the-art dynamic analysis, the logarithmic standard deviation on response is about 0.20. For simple single-frequency systems with fundamental frequencies in the amplified portion of the spectra, the variability is about 0.10. For single frequency systems with fundamental frequencies

out into the rigid range, the logarithmic standard deviation is 0.0. These variabilities are considered to be all uncertainty and are based on past experience and engineering judgment.

5.1.1.2.4 Damping Factor - The basis for the damping factor has been addressed in Section 3.4.2 of this report. Tables 3-1 and 3-2 show the damping values used for the SSE design analysis of Millstone 3 equipment. Median damping values and their variabilities are a function of the material, construction details, size and stress level. Reference 24 suggests that median damping for equipment at the SSE level is about five percent. Thus, for single-degree-of-freedom systems the damping factor for Millstone 3 equipment is:

$$F_D = \frac{S_a\ (qual)}{S_a\ (median)} \qquad (5\text{-}14)$$

where:

$S_{a(qual)}$ = Spectral acceleration using the qualification design analysis damping and evaluated at the equipment fundamental frequency

$S_{a(median)}$ = Spectral acceleration using the expected median damping and evaluated at the equipment fundamental frequency.

For multi-degree-of-freedom systems, Equation 5-14 can be altered to reflect the summation of the spectral accelerations at each of the frequencies multiplied by their associated mass participation factors.

There is variability in damping and associated response that must be considered. It is indicated within Reference 24 that for a median damping value of 5 percent, the minus one logarithmic standard deviation value is about 3.5 percent. The variability in damping results in a logarithmic standard deviation in response equal to:

$$\beta_{D_U} = \ln\left(\frac{S_{a_{\zeta = 3.5\%}}}{S_{a_{\zeta = 5.0\%}}}\right) \qquad (5\text{-}15)$$

where $S_{a_{\zeta = 5\%}}$ is the 5 percent damped spectral acceleration and $S_{a_{\zeta = 3.5\%}}$ is the 3.5 percent damped spectral acceleration taken at the equipment fundamental frequency using the applicable floor response spectra. The resulting logarithmic standard deviation on the damping response factor, from Equation 5-15 above, is considered to be all uncertainty. An additional randomness variability estimated at approximately 20 percent of the uncertainty variability reflects the earthquake time-histories' effect on the median damping value.

5.1.1.2.5 Mode Combination Factor - The modal combination technique utilized within the Millstone 3 seismic design analysis was described in general in Chapter 3 of this report. A square-root-of-the-sum-of-the-squares (SRSS) methodology was used for all Millstone 3 equipment. This SRSS method (allowing for absolute sum for closely spaced modes) is in accordance with current Regulatory Guide 1.92 (Reference 12) recommended practice and is considered median centered.

The response factor for combination of modes is then considered to be 1.0. The variability associated with mode combination depends upon the complexity of the model. For multi-degree-of-freedom systems, Reference 24 recommends that the logarithmic standard deviation due to mode combination is approximately 0.15. For single-degree-of-freedom flexible systems, the variability due to mode combination is estimated within Reference 24 to be approximately 0.10. For a single-degree-of-freedom rigid system, the variability is by definition zero. The variability due to mode combination is considered to be all random due to the random phasing of modes.

5.1.1.2.6 Earthquake Component Combination Factor - The majority of the equipment within Millstone 3 were designed based the SRSS combination of the two horizontal and the vertical earthquake components. Only the balance-of-plant piping was designed differently using the SRSS combination of the two horizontal plus the absolute sum combination of the vertical earthquake components. The square-root-of-the-sum-of-the-squares (SRSS) methodology is considered a median-centered approach and, thus, the factor is unity for components qualified in this manner. It should be noted a second method using a 100%, 40%, 40% combination is also considered to yield approximate median results . Reference 10 recommends that the response can be represented by combining the worst case horizontal response with 40 percent of the orthogonal horizontal response and 40 percent of the vertical response. The SRSS method must be applied to the end item of interest, while the 100%, 40%, 40% method can be applied at the input seismic load stage or at the stress intensity of interest stage with equivalent results. Both methods yield approximately the same factors of conservatism/unconservatism. In developing the Earthquake Component Combination Factors for Millstone 3 equipment, the SRSS combination was taken as the median. The magnitude of this Factor depends on the orientation, failure mode and response characteristics of the component under consideration.

A generic study was conducted to develop earthquake component combination response factors and their variabilities for common two- and three-dimensional equipment idealizations. The amount of conservatism/unconservatism and the associated variability on this factor are a function of the following:

1. The number and direction of earthquake components which affect the failure mode under consideration (e.g., piping failures can be influenced by all three directional responses, but a particular relay can fail due to a particular horizontal seismic excitation while remaining unaffected by the vertical and the other horizontal directions)

2. The amount of coupling that exists between directional response (i.e., does an x direction excitation cause a response in the y and z directions)

Table 5-3 contains the earthquake component combination response factors for those cases which were applicable to Millstone 3 equipment. The variability involved in the phasing of the three earthquake directional components was considered to be all random, while the variability due to the degree of coupling involved between directions was considered to be all uncertainty.

5.1.1.2.7 Boundary Conditions Factor (Testing) - The boundary conditions utilized in equipment seismic testing can be a significant source of variability that depends almost solely upon the diligence of the test laboratory and the qualification review organization. In general, a component that is bolted to the floor in a nuclear power plant and which is similarly bolted to a shake table for qualification testing, will experience little variability in response factor due to boundary conditions. Carelessness on the part of the various organizations involved in design, fabrication, testing and installation can result in a significant variability. For instance, the lack of a specified bolt torque at the mounting interface can result in a difference between the testing and installation condition which could have a pronounced impact on the response factor.

The variability of the subsystem response due to test boundary conditions would come primarily from any mode shape and frequency shift. The variability of mode shape and frequency and resulting response due to

boundary conditions varies considerably for different generic types of equipment. For a large majority of tests conducted by reputable testing laboratories, the Boundary Condition Factor is 1.0. Engineering judgment must be utilized in calculating Boundary Condition Factors for those cases where the component to test table attachment mechanism is not representative of the actual in-plant condition. The variability is all uncertainty and can be calculated based on spectral accelerations obtained from estimating a 90 percent confidence interval on the equipment frequency.

5.1.1.2.8 Spectral Test Method - Synthesized time-histories are currently developed directly from the Required Response Spectrum at most testing laboratories. A much better approach, as recommended in Reference 27, is to synthesize a time-history that corresponds to a power spectral density which closely envelopes the RRS rather than make the direct step from the RRS to the synthesized time-history. This approach tends to smooth out the input time-history, resulting in less chance for an equipment mode to coincide with a significant peak or valley. Reference 24 recommends a spectral test method factor of unity and a total variability of 0.11. This variability is entirely uncertainly since the use of better equipment and techniques could eliminate most of the uncertainty.

5.1.1.2.9 Multi-Directional Effects - The Multi-Directional Effects Factor is a measure of the conservative/unconservatism and corresponding variability involved in testing the three different earthquake directional components. Millstone 3 equipment fragilities were developed from plant specific and generic test data and are based on two types of testing: biaxial and uniaxial. Biaxial qualification tests are conducted by exciting the equipment in one horizontal direction at a time along with the vertical direction, using randomly phased input time-histories. Uniaxial qualification tests, on the other hand, are conducted in each of the three directions independently. Biaxial testing was conducted for most plant specific equipment qualified for the Millstone 3 plant. Thus,

multi-directional effect factors were developed for both biaxial testing and uniaxial testing and were applied based upon the test methodology employed.

5.1.1.2.9.1 Biaxial Testing - There is a slight unconservatism involved in biaxial testing in that the actual input during a seismic event is three-dimensional. This unconservatism along with its associated variability is a function of both the phasing and the coupling between earthquake directional components. Assuming that the median acceleration vector can be defined as recommended in Reference 10 as 100 percent of the acceleration in one direction plus 40 percent of the acceleration in the other two orthogonal directions, the degree of unconservatism associated with biaxial testing can be defined as the median response vector for biaxial testing divided by the median three-axis response. The resulting response factor based on both phasing and coupling is calculated to be 0.853. The variability due to phasing is a function of the earthquake, and thus, is all random. The phasing variability is identical to that which has been calculated for the general three-dimensional condition (Case No. 1 of Table 5-3) for the Earthquake Component Combination Factor and is equal to 0.12. The variability due to coupling is small since median coupling in testing exists by definition for the two input directional components. Using the uncoupled case and the 100 percent coupling case as $\pm 2.33\beta$ extremes on coupling, an uncertainty logarithmic standard deviation of 0.04 is calculated.

The Multi-Directional Effects Factor and its associated β's for random vibration biaxial testing is:

$$F_{MDE} = 0.853$$

$$\beta_{MDE_R} = 0.12$$

$$\beta_{MDE_U} = 0.04$$

5.1.1.2.9.2 Uniaxial Testing - A uniaxial test is, in general, unconservative in that coupling and phasing between the three-directional earthquake components is not accounted for. Again, assuming the median acceleration vector can be defined as recommended in Reference 10 as 100 percent of the acceleration in one direction plus 40 percent of the acceleration in the other two orthogonal directions, the degree of unconservatism associated with uniaxial testing can be defined as the median response vector for uniaxial testing divided by the median three-axis response. The resulting response factor based on both phasing and coupling is calculated to be 0.735. The phasing variability is random and is identical to that for the biaxial case, i.e., 0.12. The uncertainty variability due to coupling, based on the uncoupled case and the 100 percent coupling case being $\pm 2.33\beta$ extremes, is calculated to be 0.08.

Thus, the Multi-Directional Effects Factor and its associated β's for uniaxial testing is:

$$F_{MDE} = 0.735$$

$$\beta_{MDE_R} = 0.12$$

$$\beta_{MDE_U} = 0.08$$

5.1.1.3 Structural Response Factors

Structural response factors as they relate to structural capacity for the safety-related structures within Millstone 3 are derived in Chapter 4. The variables pertinent to the structural response analyses used to generate floor spectra for equipment design are the only variables of interest relative to equipment fragility. Time-history analyses, using the same structural models used to conduct structural response analyses for structural design, were used to generate floor spectra. The applicable variables for equipment from those analyses are:

1. Spectral Shape
2. Damping
3. Modeling
4. Soil-Structure Interaction.
5. Inelastic Energy Absorption of the Building

The explanation of each of these variables is contained in Chapter 4 and will not be repeated here. Note, the combination of earthquake components is not included in structural response since that variable is addressed for specific equipment orientation in the treatment of equipment response. As discussed in Chapter 4, a totally independent evaluation of the capacities of the important structures was undertaken in this effort. As a result, the generated median structural response factor was 1.0 and included its associated variabilities. This independent analysis employed the median ground spectra to define seismic input. In evaluating equipment acceleration capacities which are based upon design analysis results, a spectral shape factor associated with structural response must be computed which compares the 5% damped time history spectrum used for design with the appropriately damped median spectrum. The resultant structural response factors pertaining to the equipment fragility derivation are included in Table 5-4. Note that the structural response factors for each particular structure are broken up into two segments. Equipment with capacities less than the approximate building yield strength have Structural Response Factors in the "a" row, and equipment with capacities approximately equal to or greater than the structure yield strength have Structural Response Factors in the "b" row. The approximate yield level for each of the buildings was estimated by taking the ground acceleration capacity for the lowest structural failure mode (see Chapter 4) and dividing it by the inelastic energy absorption factor.

The structural response factors within Chapter 4 have been derived on the basis of the structure being at its failure threshold level. It should be noted that when the building goes inelastic, the actual floor level acceleration will be decreased over that which is predicted using the elastic structural model. At the same time, the displacement will increase over that which is predicted by the elastic model. Thus, acceleration sensitive equipment must have their capacities scaled up to reflect the actual lowering of the floor acceleration due to building ductility, while displacement sensitive equipment must have their capacities similarily scaled down. Reference 10 recommends ten percent median damping for reinforced concrete at or above the yield condition and five percent median damping for reinforced concrete at the one-half yield condition. In addition, the structures ductility does not modify the response of the equipment unless the equipment fragility is above the building's yield level. Thus, for the condition where the equipment capacity is less than the structure's yield level, 5% structural damping is considered median and the structure's ductility factor is effectively unity. For the case where the equipment capacity is approximately equal to or greater than the structure's yield level, 10% structural damping is considered median. As a result, a slight conservatism is introduced using the 5% structural damping for a component whose capacity is less than but is approaching the yield capacity of the structure.

5.1.2 Information Sources

Several sources of information are utilized in a PRA from which to develop plant specific and generic fragilities for equipment. Sources used in this evaluation of Millstone 3 equipment include:

1. Seismic Qualification Design Reports
2. Seismic Qualification Test Reports
3. Final Safety Analysis Report (FSAR)

4. Specifications for the Seismic Design of Equipment

5. Seismic Qualification Report Summaries

6. Past Earthquake Experience

Each of the information sources above are termed "plant specific" since they pertain to specific equipment within the Millstone 3 plant. Such plant specific sources are preferred since they have been generated for the specific items in question and their uncertainty level is reduced from those of potential generic sources of information.

5.1.3 Equipment Categories

Depending upon the uniqueness of the equipment, the failure mode, inelastic energy absorption capability and the dynamic characteristics of the equipment, a plant-specific or a generic derivation of the fragility description may be appropriate. The factors of safety relative to the Safe Shutdown Earthquake are widely variable. In general, flexible equipment such as piping, which possesses the ability to undergo large inelastic deformation, will have a factor of safety against failure of many times the Safe Shutdown Earthquake even if stressed to the maximum code allowable stress. Such equipment is a prime candidate for generic derivation of fragility descriptions. The increased uncertainty inherent in a generic derivation does not have much influence on the outcome of the seismic risk analysis if large safety factors can be demonstrated. On the other hand, if rigid equipment with relatively brittle failure modes are stressed to code allowable for the Safe Shutdown Earthquake, the factor of safety against failure may be considerably smaller and a generic treatment may result in unsatisfactory risk predictions.

Experience gained as to relative component fragility levels must also be utilized in deciding which components should be treated generically and which components should be treated specifically. As a result, those components which through experience have been shown to possess a high degree of resistance to seismic loading may often be

treated in more of a generic fashion while components which have been shown to possess low fragility levels are more thoroughly analyzed to provide as much accuracy as possible. Table 5-5 contains a listing of the relative fragility level for general equipment categories based on the data provided in Reference 32. The information provided within Table 5-5 is utilized within the PRA study to discern which equipment can be treated generically and which equipment should be treated on a plant specific basis.

5.2 EQUIPMENT FRAGILITY EXAMPLES

Because of the amount of equipment to be included within the risk model, it is impractical to describe the specific fragility derivation for each piece of equipment. This section contains selected examples of fragility derivations which are judged to be representative of the different types of analyses which had to be undertaken for Millstone 3 equipment. The equipment fragility derivation categories applicable to the Millstone reevaluation PRA are:

1. Equipment whose fragility descriptions are based on stress summaries.

2. Equipment whose fragility descriptions are based on a review of the component qualification stress report.

3. Equipment whose fragility descriptions are based on knowledge of the design specifications and the factors of safety inherent in the governing codes and standards.

4. Equipment whose fragility descriptions are based on component test data.

5. Equipment whose fragility descriptions are based on engineering judgment and past earthquake experience (non-seismically qualified components).

An example of Millstone 3 equipment whose fragility derivation stems from each of the above categories is included in this section.

5.2.1 Example of a Plant Specific Fragility Derivation Based Upon Summary Information

The evaluation of the majority of the equipment associated with the Nuclear Steam Supply System (NSSS) was based upon summary stress information provided by Westinghouse. The summary information generally included the faulted condition stress level for the critical regions of the components, failure modes, yield and/or code faulted allowable stress, and some measure as to what portion of the total stress was due to seismic response. Component fundamental frequencies were also provided in some cases. The example chosen to illustrate the derivation of fragility based upon summary information is the Residual Heat Removal Heat Exchanger.

5.2.1.1 RHR Heat Exchanger Capacity Factor

Three locations were identified by Westinghouse as being the most critical for RHR Heat Exchanger in terms of seismic stress. These were:

1. Anchor Bolts
2. Heat Exchanger Shell at the Intermediate Support Lugs
3. Baseplate

Based upon the supplied stress information, it was judged that the heat exchanger fragility would be governed by the shell stresses. The following information was provided.

1. Location: ESF Building at Elevation 4'-6" with horizontal restraints at Elevations 22'-0" and 46'-0".
2. Fundamental Frequency: Horizontal 21 Hz; Vertical 11 Hz.
3. Material: SA515-Gr 70: σ_y = 34,600 psi.
4. Design Seismic Accelerations: 1.5g (Horizontal); 1.0g (Vertical).
5. Faulted Condition Stress: 47,400 psi.
6. Portion Due to Seismic: 85%.

The failure mode consists of a local punching failure of the shell due to the horizontal restraint reactions. Failure is judged to occur at 1.5 times the median yield strength of the material and exhibit limited ductility. The factor of 1.5 is used to properly represent the actual load the shell can carry subsequent to first yield of the shell and accounts for both the section factor and strain hardening. Based upon the data presented in Reference 33, a lower bound factor of 1.25 is estimated to represent a 95% probability of exceedance value (-1.65β). Therefore, the logarithmic standard deviation for uncertainty is calculated as:

$$\beta_{1.5_u} = \frac{1}{1.65} \ln (1.50/1.25) = 0.11$$

In addition, Reference 38 reports that for soft steels the median yield strength is about a factor of 1.25 above the ASME code specified minimum yield strength. Again, considering the Code minimum yield strength to represent a 95% probability of exceedance value, the uncertainty variability becomes:

$$\beta_{1.25_u} = \frac{1}{1.65} \ln (1.25/1.00) = 0.14$$

The failure stress and its uncertainty can then be computed as:

$$P_C = (1.25)(1.50)(34,600) = 64,875 \text{ psi}$$

$$\beta_C = (.11^2 + .14^2)^{1/2} = 0.18$$

Using information items 5 and 6 above, the Strength Factor (F_S) is calculated in accordance with Equation 5-7.

$$F_S = \frac{(1.25)(1.50)(34,600) - (0.15)(47,400)}{(0.85)(47,400)} = 1.43$$

and the logarithmic standard deviation on strength uncertainty is calculated from Equation 5-9 as:

$$\beta_{S_U} = 64{,}875(.18)/(64{,}875-7{,}110) = 0.20$$

Computing the duration-modified Inelastic Energy Absorption Factor (Ductility Factor, F_μ) as discussed in Section 5.1.1.1.2, for a limited median ductility value of $\mu = 1.2$ at a frequency of 21 Hz and for a damping of 5% of critical, F_μ and its variabilities become:

$$F_\mu = 1.09$$

$$\beta_{\mu_R} = 0.03$$

$$\beta_{\mu_U} = 0.02$$

The overall Capacity Factor ($\check{F}_{EC}$) and its variabilities are then computed as the combination of the Strength and Ductility Factors and their associated variabilities as follows:

$$\check{F}_{EC} = F_S \bullet F_\mu = (1.43)(1.09) = 1.56$$

$$\beta_{EC_R} = \left(\beta_{S_R}^2 + \beta_{\mu_R}^2\right)^{1/2} = (.00^2 + .03^2)^{1/2} = 0.03$$

$$\beta_{EC_U} = \left(\beta_{S_U}^2 + \beta_{\mu_U}^2\right)^{1/2} = (.20^2 + .02^2)^{1/2} = 0.20$$

5.2.1.2 RHR Heat Exchanger Equipment Response Factor

The RHR Heat Exchanger was analyzed using a flexible static analysis approach based upon 1.5g horizontal and 1.0g vertical seismic static accelerations. The evaluation of the shell stresses included the effects of both seismic inertial forces and nozzle piping forces but the

division of stresses resulting from these two loading sources was not documented. However, since the portion of the stress level due to non-seismic sources is small, it is assumed that stresses resulting from nozzle forces and moments is small. Therefore, the derivation of response factors is based upon the vessel dynamic characteristics.

5.2.1.2.1 Qualification Method Factor - From the design SSE floor response spectra for the ESF Building at 5% damping, it was found that a horizontal acceleration vector of 0.335g was appropriate at the intermediate lugs. Therefore, the Qualification Method Factor (F_{QM}) is computed as a comparison of the qualification and actual design horizontal acceleration levels.

$$F_{QM} = 1.5/0.335 = 4.48$$

The horizontal acceleration at the upper restraints was found to be 0.419g. Since there is uncertainty as to whether the acceleration of the main support, the intermediate restraint, or the upper support contributes most to the seismic stress level at the intermediate lugs, the acceleration at the upper supsport is taken as the 95% non-exceedance probability value resulting in a logarithmic standard deviation of 0.14. This variability is all considered to be due to uncertainty.

$$F_{QM} = 4.48$$

$$\beta_{QM_R} = 0.00$$

$$\beta_{QM_U} = 0.14$$

5.2.1.2.2 Spectral Shape Factor - Since static acceleration coefficients were used in the design of the RHR Heat Exchanger and were compared with the appropriate design spectra at a frequency of 21 Hz, which is above the region of peak broadening, the Spectral Shape Factor (F_{SS}) is unity with logarithmic standard deviations on both randomness and uncertainty of zero.

$F_{SS} = 1.00$

$\beta_{SS_R} = 0.00$

$\beta_{SS_U} = 0.00$

5.2.1.2.3 Modeling Factor - Section 5.1.1.2.3 reflects a Modeling Factor (F_M) of 1.00 with an uncertainty variability of 0.15 for medium complex systems such as the RHR Heat Exchanger.

$F_M = 1.00$

$\beta_{M_R} = 0.00$

$\beta_{M_U} = 0.15$

5.2.1.2.4 Damping Factor - In determining the Qualification Method Factor (F_{QM}) the qualification seismic acceleration was compared with the horizontal acceleration vector from the design floor spectra at 5% damping which is considered median. Therefore, the Damping Factor (F_D) is unity. As described in Section 5.1.1.2.4, there is some uncertainty as to the actual level of damping associated with equipment failure. In accordance with Equation 5-15, 3-1/2% damping is taken as a one logarithmic standard deviation variation. However, at 21 Hz, which is approaching the rigid response range, the spectral acceleration difference between 3-1/2 and 5% damping is negligible and therefore the variabilities are taken to be zero.

$F_D = 1.00$

$\beta_{D_R} = 0.00$

$\beta_{D_U} = 0.00$

5.2.1.2.5 Mode Combination Factor - Section 5.1.1.2.5 specifies a median Mode Combination Factor (F_{MC}) of 1.00 with a logarithmic standard deviation on randomness of 0.10.

$$F_{MC} = 1.00$$

$$\beta_{MC_R} = 0.10$$

$$\beta_{MC_U} = 0.00$$

5.2.1.2.6 Earthquake Component Combination - The qualification of the RHR Heat Exchanger was based upon a horizontal seismic acceleration of 1.5g and a vertical acceleration of 1.0g with vertical component contribution to stress at the intermediate lug judged to be negligible. In determining the Qualification Method Factor (F_{QM}) the design horizontal seismic acceleration vector was computed from the design floor spectra using 100% of the highest horizontal global acceleration (North-South) combined with 40% of the lesser horizontal acceleration (East-West). The 100%/40% has been shown in Reference 10 to be approximately a median value and therefore the Earthquake Component Combination Factor (F_{ECC}) is taken to be unity. There is, however, some randomness variability on the actual phasing of the components which may occur at the Millstone 3 site. Taking 100% phasing and 0% phasing acceleration vectors as representing $\pm$ 3β variation at a median value for coupling, the randomness variability for the case in which the two horizontal seismic acceleration components contribute to failure is calculated to be 0.10 as shown in Table 5-3.

$$F_{ECC} = 1.00$$

$$\beta_{ECC_R} = 0.10$$

$$\beta_{ECC_U} = 0.00$$

5.2.1.2.7 Overall Equipment Response Factor - The combined Equipment Response Factor ($\check{F}_{ER}$) and the random and uncertainty variabilities then are:

$$\check{F}_{ER} = (4.48)(1.00)(1.00)(1.00)(1.00)(1.00) = 4.48$$

$$\beta_{ER_R} = (.10^2 + .10^2)^{1/2} = 0.14$$

$$\beta_{ER_U} = (.14^2 + .15^2)^{1/2} = 0.20$$

5.2.1.3 RHR Heat Exchanger Structural Response Factor

The ESF Building was found in Chapter 4 to exhibit yield and failure capacities of approximately 1.3 g's and 2.4 g's, respectively. Since the capacity of the RHR Heat Exchanger exceeds the yield strength of the ESF Building structure, the Structural Response Factor ($\check{F}_{SR}$) is calculated as the ratio of the design ground time history response spectral acceleration at the fundamental frequency of the ESF Building based upon the design analysis (11.4 Hz) and at 5% damping to the median-centered ground response spectral acceleration at the fundamental frequency of the ESF structure based upon the median analysis (12.9 Hz) and at 10% damping. Taken from Table 5-4 $\check{F}_{SR}$ and its variabilities are:

$$\check{F}_{SR} = 1.46$$

$$\beta_{SR_R} = 0.19$$

$$\beta_{SR_U} = 0.34$$

5.2.1.4 RHR Heat Exchanger Ground Acceleration Capacity

The ground acceleration capacity ($\check{A}$) for the RHR Heat Exchanger is calculated using Equations 5-1 and 5-2.

$$\check{A} = (1.56)(4.48)(1.46)(.17 \text{ g's}) = 1.73 \text{ g's}$$

The logarithmic standard deviations on randomness and uncertainty are calculated as the SRSS combination of the variabilities associated with the three factors contributing to overall capacity in accordance with Equation 5-3.

$$\beta_R = (.03^2 + .14^2 + .19^2)^{1/2} = 0.24$$

$$\beta_U = (.20^2 + .20^2 + .34^2)^{1/2} = 0.44$$

The combined variability, β_C, which is a measure of the overall variability contributed by earthquake randomness and uncertainty is obtained by taking the SRSS of β_R and β_U.

$$\beta_C = (.24^2 + .44^2)^{1/2} = 0.50$$

The three factors which make up the overall fragility of the RHR Heat Exchanger together with their logarithmic standard deviations on randomness and uncertainty are tabulated in Table 5-1 along with the remainder of the equipment addressed in this Millstone 3 PRA study. The various factors and variabilities calculated for the RHR Heat Exchanger are presented in Table 5-6.

5.2.2 Example of a Plant Specific Fragility Derivation Based Upon a Review of the Component Qualification Stress Report

The seismic qualification and stress reports were obtained for a majority of the components selected for reevaluation in this PRA study. The qualification reports generally contained the basic information necessary to determine critical failure modes and to calculate component capacities. As a result, most equipment responses based upon qualification parameters could accurately be converted to site-specific parameters thus reducing the associated variabilities. The example chosen to illustrate the derivation of fragility based on stress report information is the Containment Recirculation Cooler.

5.2.2.1 Containment Recirculation Cooler Capacity Factor

The Containment Recirculation Cooler is a vertical heat exchanger housed within the ESF Building but mounted on the Containment Structure Shell. Four locations were evaluated to determine that controlling the fragility of the Cooler. These were:

1. Upper Restraint Shoulder Pin
2. Upper Restraint Lug
3. Cooler Shell at the Main Support
4. Upper Tubesheet

Capacity Factors were calculated for each location, and it was found that the bending failure of the Upper Restraint Shoulder Pin governs. The evaluation of the fragility of the Recirculation Cooler is based upon the following information and assumptions:

1. Location: ESF Building, attached to the Containment Structure Shell. Main support at Elevation 28'-3" with horizontal restraints at Elevations 11'-4" and 47'-3".
2. Fundamental Frequency: 34.2 Hz
3. Design Seismic Accelerations: 0.65g horizontal
4. Pin Material: SA540-CL2; σ_y = 140,000 psi, σ_u = 155,000 psi
5. Pin Properties: Area = 0.785 in^2, Z = 0.098 in^3
6. Nozzle Loads: It is judged from previous experience that assuming 65% of the piping reactions to be from normal forces and 35% to be from seismic forces represents median values.
7. Worst Case Pin Stresses:

   σ_{Total} = 135,325 psi (88.7% = Nozzle; 11.3% = Inertia)

   σ_{Normal} = 78,115 psi

Since high strength steels exhibit only limited strength beyond yield, ultimate tensile strength is used to define failure. For high strength steels, Reference 33 reports the median ultimate to be about a factor of 1.1 times the ASME Code specified ultimate tensile strength with the Code value representing 95% probability of exceedance (-1.65β). The Strength Factor (F_S) is then computed from the information given above.

$$F_S = \frac{(1.1)(155,000) - 78,115}{135,325 - 78,115} = 1.62$$

The logarithmic standard deviation on the uncertainty of calculating the capacity strength as 1.1 times the Code ultimate is 0.06. In addition, there is further uncertainty in using the ultimate strength to define failure. The variability is based upon assessing the yield strength as representing a 95% lower bound confidence level which also results in a β_U of 0.06. Finally, there is also some uncertainty pertaining to the assumption on the breakdown between normal loads and seismic loads from the piping which is used to calculate σ_N. Here the case where 50% of the piping reactions are due to seismic forces (rather than 35%) is judged to represent 95% confidence upper bound level.

$$\beta_{N_U} = \frac{1}{1.65} \ln (.50/.35) = 0.22$$

Combining the capacity variabilities by SRSS and solving for the logarithmic standard deviation on the Strength Factor in accordanced with Equation 5-9, the uncertainty variability becomes 0.20. Since failure of the upper restraint pin, which is essentially a "brittle" failure mode, has been defined in terms of ultimate strength, the Ductility Factor (F_D) is unity and its variability is zero. Therefore, the overall Capacity Factor and its variabilities are equal to the Strength Factor and its corresponding variabilities.

$$F_{EC} = F_S = 1.62$$

$$\beta_{EC_R} = \beta_{S_R} = 0.00$$

$$\beta_{EC_U} = \beta_{S_U} = 0.20$$

5.2.2.2 Containment Recirculation Cooler Equipment Response Factors

The Recirculation Cooler Support was designed using a rigid static analysis approach based upon specified nozzle forces. It was assumed that the nozzle loads were defined from a response spectrum dynamic analysis of the attached piping using the appropriate 1% damped ESF Building floor spectra.

5.2.2.2.1 Qualification Method Factor - The response spectrum methodology used to evaluate the piping is considered median in terms of the Qualification Method Factor and therefore $F_{QM} = 1.00$. However, static acceleration coefficients of 0.65g in the two horizontal directions were used to define the inertial load. From the Containment Structure design spectra, the horizontal components of acceleration at the Cooler main support are 0.387 and 0.334g. As a result, the Qualification Method Factor for the inertial portion of the pin stress is:

$$F_{QM} = (.65^2 + .65^2)^{1/2} / \left[.387^2 + (.4x.334)^2\right]^{1/2} = 2.25$$

based upon using the 100%/40% earthquake component methodology. These two values of F_{QM} are combined as a weighted average based upon how the contributions of the seismic nozzle loads and the inertial loads bear on the total seismic load on the pin. This weighted average value of F_{QM} is calculatd as follows since the nozzle loads contribute most to the pin stresses.

$$F_{QM} = 1.00 \left[\frac{(.35)(.887)}{.4235}\right] + 2.25 \left[\frac{.113}{.4235}\right] = 1.33$$

Uncertainty exists as to whether the spectral acceleration vector at the main support (.409 g's) or the vector at the upper restraint (.473 g's) is a more significant contributor to the stresses in the pin. Using the upper restraint vector results in the calculation of a weighted Qualification Method Factor of 1.25. The variability is then calculated to be of 0.04 assuming the lower value to represent a 95% confidence lower bound. In addition, there is uncertainty that the weighted average accurately calculates the factor. This variability is calculated assuming that the F_{QM} value associated with the most significant contributor to pin stress (F_{QM} = 1.00 for nozzle forces in this case) represents a 95% confidence lower bound value (β = 0.17). Combining these two variabilities which are both due to uncertainty by SRSS, the overall Qualification Method Factor and its variabilities become:

$$F_{QM} = 1.33$$

$$\beta_{QM_R} = 0.00$$

$$\beta_{QM_U} = 0.17$$

5.2.2.2.2 Spectral Shape Factor - This factor which accounts for peak broadening is unity for the inertial analysis since the component is rigid. However, for the piping analysis, which is assumed to have at least one mode occurring in the peak broadened range for the ESF Building, a Spectral Shape Factor of 1.05 was calculated with a β on uncertainty of 0.02. Again, the overall Spectral Shape Factor is calculated as a weighted average.

$$F_{SS} = 1.05(.3105/.4235) + 1.00(.1130/.4235) = 1.04$$

The variability on this weighted average is also 0.02. The resulting overall Spectral Shape Factor and its logarithmic standard deviation which is all judged to be due to uncertainty becomes:

$F_{SS} = 1.04$

$\beta_{SS_R} = 0.00$

$\beta_{SS_U} = 0.03$

5.2.2.2.3 Modeling Factor - Section 5.1.1.2.3 gives a Modeling Factor of 1.00 with an uncertainty variability of 0.15 for medium complex systems such as the Containment Recirculation Cooler piping.

$F_M = 1.00$

$\beta_{M_R} = 0.00$

$\beta_{M_U} = 0.15$

5.2.2.2.4 Damping Factor - Similar to the calculation of F_{QM} and F_{SS}, the calculation of the Damping Factor (F_D) is based upon a weighted average of the relative contribution of piping and inertia to overall seismic stresses. F_D for the inertial portion of the defined load is unity with a variability of zero since the appropriate 5% damped design spectra were used as the basis for determining the inertial portion of the Qualification Method Factor. However, Reference 1 states that 1% damped spectra were used in the dynamic analysis of Balance-of-Plant Piping for the SSE loading. Based upon a comparison of the 1% and 5% (interpolated between 4% and 8%) damped floor spectra for the ESF Building in the frequency range between 5 and 20 Hz, a median Damping Factor for the piping portion of the pin loading was calculated to be 1.49 with a variability of 0.19. The weighted average Damping Factor is then calculated as:

$F_D = 1.49(.3105/.4235) + 1.00(.1130/.4235) = 1.36$

with a resultant uncertainty variability of 0.06. The variability due to the uncertainty as to the actual damping level associated with equipment failure is calculated in accordance with Equation 5-15. Taking 3-1/2% damping (interpolated between 2% and 4%) evaluated at a frequency of 7 Hz as a one logarithmic standard deviation variation, the variability on the damping level is computed to be 0.24. The three components of uncertainty variability are combined by SRSS and the variability on randomness is estimated to be equal to 20% of the uncertainty variability. The overall Damping Factor and its variabilities then become:

$$F_D = 1.36$$

$$\beta_{D_R} = 0.06$$

$$\beta_{D_U} = 0.31$$

5.2.2.2.5 Mode Combination Factor - Since the piping loads contribute most to the stresses in the pin, a median Mode Combination Factor of 1.00 with a logarithmic standard deviation on randomness of 0.15 is used based on the information included in Section 5.1.1.2.5.

$$F_{MC} = 1.00$$

$$\beta_{MC_R} = 0.15$$

$$\beta_{MC_U} = 0.00$$

5.2.2.2.6 Earthquake Component Combination - In determining the Qualification Method Factor, the median-centered 100%/40% combination method was used for the inertial portion and therefore, $F_{ECC} = 1.00$. However, Reference 1 states that the SRSS of the horizontals plus the absolute sum of the vertical method of earthquake component combination was used for the balance-of-plant piping. As a result, the Earthquake Component Combination Factor for Case 1 of Table 5-3 is applicable for

the piping portion of the loading. Again computing the overall Earthquake Component Combination Factor as the weighted average, F_{ECC} becomes:

$$F_{ECC} = 1.12(.3105/.4235) + 1.00(.1130/.4235) = 1.09$$

with a variability of 0.02. Taking the randomness variability from Table 5-3 and combining the uncertainty variabilities by SRSS, the overall Earthquake Component Combination Factor and its variabilities are:

$$F_{ECC} = 1.09$$

$$\beta_{ECC_R} = 0.12$$

$$\beta_{ECC_U} = 0.13$$

5.2.2.2.7 Overall Equipment Response Factor - The combined Equipment Response Factor ($\check{F}_{ER}$) and the randomness and uncertainty variabilities then are:

$$\check{F}_{ER} = (1.33)(1.04)(1.36)(1.00)(1.00)(1.09) = 2.05$$

$$= (.06^2 + .15^2 + .12^2)^{1/2} = 0.20$$

$$= (.20^2 + .03^2 + .31^2 + .15^2 + .13^2)^{1/2} = 0.42$$

5.2.2.3 Containment Recirculation Cooler Structural Response Factor

The Containment Structure Shell was found in Chapter 4 to exhibit yield and failure capacities of approximately 1.9 g's and 4.9 g's, respectively. Therefore, the Recirculation Cooler is more fragile than the structure to which it is mounted and will fail at an acceleration level at which the containment shell remains elastic. Therefore, the Structural Response Factor is calculated as the ratio of the design ground time history response spectral acceleration at the fundamental frequency

of the Containment Shell based upon the design analysis (4.7 Hz) and at 5% damping to the median-centered ground response spectral acceleration at the fundamental frequency of the Containment Shell based upon the median analysis (5.5 Hz) and at 5% damping. Table 5-4 gives the value of $\check{F}_{SR}$ and its variabilities as:

$$\check{F}_{SR} = 1.46$$

$$\beta_{SR_R} = 0.25$$

$$\beta_{SR_U} = 0.24$$

5.2.2.4 Containment Recirculation Cooler Ground Acceleration Capacity

The ground acceleration capacity (A) for the Containment Recirculation Cooler is computed from Equations 5-1 and 5-2.

$$\check{A} = (1.62)(2.05)(1.46)(.17\ g's) = 0.82\ g's$$

The logarithmic standard deviations on randomness and uncertainty are calculated as the SRSS combination of the variabilities associated with the three factors contributing to overall capacity in accordance with Equation 5-3.

$$\beta_R = (.00^2 + .20^2 + .25^2)^{\frac{1}{2}} = 0.32$$

$$\beta_U = (.20^2 + .42^2 + .24^2)^{\frac{1}{2}} = 0.52$$

The three factors which make up the overall fragility of the Containment Recirculation Cooler together with their logarithmic standard deviations on randomness and uncertainty are presented in Table 5-1 while the various factors and variabilities calculated for the Recirculation Cooler are shown in Table 5-7.

5.2.3 Example of Generic Fragility Derivation Based on Design Specifications

In the majority of cases in risk studies, detailed information regarding resulting stresses, deflections, bearing loads, etc., for safety-related equipment is not readily available to the risk analyst. Classes of equipment must then be treated generically and the fragility descriptions derived from knowledge of design criteria, analytical methods, service experience, etc. In this section, an example of a fragility description is developed which represents those items of equipment whose failure modes are structural and for which design reports or summaries were not reviewed. Balance-of-Plant (BOP) piping, cable trays, and ducting are typically addressed in this manner. Seismic capacities of Class 2 and 3 piping were derived in a generic manner and are chosen as the example for this section. Balance-of-Plant piping within the Auxiliary and Engineered Safety Features Buildings is specifically addressed.

5.2.3.1 BOP Piping Capacity Factor

There are three failure modes which typically are used to define the fragility level of the Balance-of-Plant (BOP) piping. The first pertains to rupture failure of the piping itself and is generally based upon the buckling capacity of standard weight piping (high energy piping generally fails at the tensile flow stress). The second failure mode pertains to rupture failure of the piping due to excessive movement of the structures relative to the ground or relative to other structures. This failure mode applies to buried or interconnecting piping and has been addressed in Chapter 4. The third mode pertains to failure of the piping supports due to weld failure or anchor bolt tearout. This third failure mode governs the fragility description of piping contained within the structures and is chosen as the example to illustrate the derivation of fragility based upon an understanding of the design criteria and the design specification.

Due to lack of specific data, the piping supports are evaluated generically. Piping supports are tyically fabricated from carbon steel (SA36, SA106-GrB, SA516-Gr70) and are at nearly room temperature. Since higher damping levels are allowed for faulted conditions, the upset conditions including the OBE typically govern the design of supports which carry only seismic loads (i.e., snubbers, horizontal restraints). Based upon significant experience, it is judged that a seismic stress level equal to 70% of the allowable represents a median value.

In the evaluation of piping supports, it has been found that the fillet welds represent the most critical construction area. For a typical fillet weld failure mode where both tensile and shear stresses are present in the throat, it can be shown from an interaction equation that the capacity of the fillet weld is equal to approximately 73% of the base material tensile capacity. For normal steels, References 33 and 35 report the median yield strength to be about a factor of 1.25 times the ASME Code specified minimum yield strength with the code value representing a 95% confidence lower bound. From the above information, the Strength Factor is computed as:

$$F_S = \frac{(1.25)(.73)(\sigma_y) - 0}{.70(.40)(\sigma_y)} = 3.26$$

based upon an AISC allowable stress of 0.4 σ_y for the OBE event.

The logarithmic standard deviation on the uncertainty of calculating the capacity strength as 1.25 times the Code yield is 0.14. There is also uncertainty in specifying the weld capacity as being 73% of the tensile capacity since for pure shear the capacity could be as low as 60% of the tensile capacity. Taking the case of pure shear as representing a 95% confidence lower bound value, the uncertainty variability is 0.12. In addition, there is some uncertainty pertaining to the assumption that the seismic stress is approximately equal to 70% of the allowable. The

case where the OBE stress level is equal to the allowable stress is taken as a + 1.65β variation resulting in an uncertainty variability of 0.22. Combining these uncertainty variabilities in accordance with Equation 5-9:

$$\beta_{S_U} = [(.14+.12)^2 + (.22)^2]^{\frac{1}{2}} = 0.34$$

Reference 6 recommends a ductility of 1.5 to 3 for design of critical piping systems. These are design recommendations; thus, the value of 3 is considered to be about a median value. A ductility of 1.0 represents the case where the support fails while the piping system remains elastic and is taken to be a 99% confidence lower bound or a minus 2.33 logarithmic standard deviation value. Using these assumptions and applying Equation 5-10, the median factor of safety for ductility was computed to be 2.46. The logarithmic standard deviations, β_{μ_R} and β_{μ_U}, are calculated from Equation 5-12 to be 0.31 and 0.23, respectively.

Combining all the factors and variabilities results in a median capacity factor of safety relative to the OBE and variability expressed in terms of logarithmic standard deviations of:

$$\breve{F}_{EC} = 8.01$$

$$\beta_{EC_R} = 0.31$$

$$\beta_{EC_U} = 0.41$$

5.2.3.2 Piping Equipment Response Factors

The equipment response factors for piping are contained within Table 5-8 and are explained briefly below. The bulk of the piping was qualified by response spectrum analysis; thus, a factor of unity and a variability of zero are applicable for the Qualification Method Factor. The Spectral Shape Factor (F_{SS}) was taken from Table 5-2 to account for peak broadening. The average value of the 5-20 Hz cases for all buildings was used.

$$F_{SS} = 1.06$$

$$\beta_{SS_R} = 0.00$$

$$\beta_{SS_U} = 0.03$$

The modeling of the piping systems is felt to be median-centered and of medium complexity, thus,

$F_M = 1.0$

$\beta_{M_R} = 0.0$

$\beta_{M_U} = 0.15$

The damping factor was computed by comparing response for a one-half percent damped spectrum to response for an expected median damping value of five percent at or near failure. One-half percent damping was utilized in designing the Balance-of-Plant piping for the OBE case. Since most critical piping systems are at least partially contained within the Containment Structure for which the Damping Factor was found to be the least, the Damping Factor (F_D) for all BOP piping is taken as:

$F_D = 1.57$

$\beta_{D_R} = 0.03$

$\beta_{D_U} = 0.14$

The Mode Combination Factor (F_{MC}) is unity with random variability of 0.15 as suggested in Section 5.1.1.2.5 for multiple-degree-of-freedom systems.

The Earthquake Component Combination Factor (F_{ECC}) for BOP piping is taken from Case 1 of Table 5-3 since the design of the BOP piping was based upon the SRSS of the horizontals plus the absolute sum of the vertical component combination methodology.

$F_{ECC} = 1.12$

$\beta_{ECC} = 0.12$

$\beta_{ECC} = 0.13$

The overall equipment response factor, $\check{F}_{ER}$ and the variability, β_R and β_U for piping are computed to be:

$\check{F}_{ER} = 1.86$

$\beta_{ER_R} = 0.19$

$\beta_{ER_U} = 0.24$

5.2.3.3 Piping Structural Response Factors

The structural response factors for piping are a function of the piping location (building and elevation). These structural response factors are shown in Table 5-4. The structural response factor used as an example in Table 5-8 for piping is that for the Auxiliary Building which exhibits the lowest yield capacity and a comparatively high median fundamental frequency of 9.6 Hz.

$\check{F}_{SR} = 1.62$

$\beta_{SR_R} = 0.21$

$\beta_{SR_U} = 0.21$

5.2.3.4 Piping Ground Acceleration Capacity

The ground acceleration capacity for piping was obtained by multiplying the three factors within Equation 5-1 by the OBE level of 0.09g's, since the Capacity Factor was developed based on the OBE and not the SSE as is generally the case.

$\check{A} = 2.17$ g's

$\beta_R = 0.42$

$\beta_U = 0.52$

The various factors and variabilities affecting the piping fragility are shown in Table 5-8.

5.2.4 Example of a Plant Specific Fragility Derivation Based Upon Component Test Data

Many components within a nuclear power plant must be shown to properly function during the course of a seismic event since failure to function might hinder safe shutdown of the plant. Mechanical equipment such as active values and pumps and electrical components such as switchgear, batteries and motor control centers fall into this classification. Frequently, such demonstrations of functionality is not related to stress level but to deflection or acceleration limitations. Component testing is generally employed to demonstrate satisfaction of the operability requirements. Both functional and structural failure modes must be evaluated to determine the controlling fragility level of active components. The example chosen to illustrate the derivation of fragility based upon component test information is the 480 VAC Motor Control Center.

5.2.4.1 480 VAC Motor Control Center Capacity Factor

The Motor Control Centers are subject to two functional failure modes which are related to chatter and tripping of the circuit breakers. The following information pertains to the fragility of the Motor Control Centers:

1. Location: Various - Auxiliary Building at Elevation 43'-6" is most critical.
2. Frequency: 5.2 Hz (S/S); 5.6 Hz (F/B).
3. Damping: Test at 1% damping.

Testing of active components is conducted to acceleration levels which envelope the required response spectrum (RRS) but are seldom carried to the point of failure which could be used to define fragility. Therefore, some basis must be used to define the "failure" capacity.

During the SSE test, a chatter failure occurred which was said to be due to a "loose bolt." The bolt was tightened and the test rerun without recurrence of the chatter failure. Therefore, the chatter fragility was taken to be 1.2 times the qualification level. From the test response spectrum (TRS), the spectral accelerations at the two fundamental frequencies is 5.2 and 7.5 g's. Since it is unclear which mode was excited causing the failure, the chatter capacity is taken as 1.2 times the average of the two or 7.62 g's. Comparing this value to the spectral acceleration between 5.2 and 5.6 Hz obtained from the 1% damped Auxiliary Building spectrum for floor Elevation 43'-6" which is 1.70 g's, the Strength Factor for chatter is calculated as:

$$F_S = 1.2(6.35)/1.70 = 4.48 \qquad \text{(chatter)}$$

The maximum and minimum spectral acceleration values at the fundamental frequencies of the Motor Control Centers are taken as $\pm$ 1.65β variation resulting in a logarithmic standard deviation on uncertainty of 0.11. Similarly, the uncertainty in specifying 1.2 times the qualification acceleration to be the chatter capacity is quantified by assuming that the qualification level represents a -1.0β variation since the chatter failure was not repeated after the bolt was tightened. The resulting logarithmic standard deviation is 0.18.

Based upon the Huntsville SAFEGUARD shock test data of generic equipment, the median acceleration defining trip failure is 7.7 g's at 5% damping. The resulting Strength Factor is:

$$F_S = 7.7/0.85 = 9.06 \qquad \text{(trip)}$$

The uncertainty associated with the 7.7 g level used to define trip failure is quantified by assuming that the chatter Strength Factor represents a -1.65β variation resulting in a logarithmic standard deviation of 0.43.

Since electrical equipment failure are judged to be "brittle", the Ductility Factor is unity with randomness and uncertainty variabilities equal to zero. As a result, the functional Capacity Factors for the Motor Control Centers are equivalent to the Strength Factors.

Chatter	Trip
$\breve{F}_{EC} = F_S = 4.48$	$\breve{F}_{EC} = F_S = 9.06$
$\beta_{EC_R} = \beta_{S_R} = 0.00$	$\beta_{EC_R} = \beta_{S_R} = 0.00$
$\beta_{EC_U} = \beta_{S_U} = (.18^2 + .11^2)^{\frac{1}{2}} = 0.21$	$\beta_{EC_U} = \beta_{S_U} = (.43^2 + .11^2)^{\frac{1}{2}} = .44$

5.2.4.2 480 VAC Motor Control Center Equipment Response Factor

The Equipment Response Factor for fragility parameters based upon testing methods were developed in detail for the Seismic Safety Margins Research Program (SSMRP) in Reference 24 and are briefly discussed in the following subsections.

5.2.4.2.1 Qualification Method Factor - The Qualification Method Factor and its variability quantifies the effects of using the superimposed multiple sine beat testing as opposed to using a spectral analyzer to generate a time history input. The median factor and variability have been calculated for the SSMRP Program (Reference 24) to be:

$F_{QM} = 1.04$

$\beta_{QM} = 0.05$

$\beta_{QM} = 0.11$

5.2.4.2.2 Spectral Shape Factor - The Spectral Shape Factor and its variability are obtained for the 5.2 to 5.6 Hz range of the Auxiliary Building which is outside the peak broadened range. The Strength Factor was based on floor spectra which were unbroadened and thus, the spectral shape factors for this case will be:

$$F_{SS} = 1.00$$

$$\beta_{SS} = 0.00$$

$$\beta_{SS} = 0.00$$

5.2.4.2.3 Boundary Conditions Factor - Difference in boundary conditions between the test lab and the actual plant installation can cause significant differences in the equipment responses. Reference 24 discusses this variability and provides estimates for different mounting conditions. The equipment under consideration is predominantly floor mounted, and is bolted or welded in both the laboratory plant installations. The response factor due to boundary conditions is considered to be unity and the estimated uncertainty variability, expressed as a logarithmic standard deviation, is 0.15.

5.2.4.2.4 Damping Factor - For chatter, F_D equals unity and the variabilities are zero since the test represents median damping. However, for trip failure there are two separate considerations in defining the variability in response due to damping. The first deals with the effect that variation in damping has upon response when the component is subjected to a seismic input, defined as an in-structure response spectrum (i.e., the applicable floor spectrum for the equipment location). The second deals with the conversion of undamped shock test spectra to damped shock spectra. The complete derivation is contained within Reference 31 with the resulting response factor of 1.0 and logarithmic standard deviation of 0.20. The variability is considered to be all uncertainty. Therefore,

Chatter	Trip
$F_D = 1.0$	$F_D = 1.0$
$\beta_{D_R} = 0.00$	$\beta_{D_R} = 0.00$
$\beta_{D_U} = 0.00$	$\beta_{D_U} = 0.20$

5.2.4.2.5 Spectral Test Methods Factor - The Spectral Shape Factor quantified the conservatism and variability involved in using an acceleration time history to develop the applicable floor response spectra. There also exists a variability in selecting a given time-history to represent a required response spectrum in vibration testing. Reference 31 states that a factor of unity with random and uncertainty logarithmic standard deviations of 0.14 and 0.10, respectively are applicable.

5.2.4.2.6 Multi-Directional Effects Factor - The multi-directional effects factor for biaxial testing is specified in Section 5.1.1.2.9.2 to be 0.853 with variabilities of $\beta_R = 0.12$ and $\beta_U = 0.04$.

5.2.4.2.7 Overall Equipment Response Factor - The overall equipment response factor was calculated to be 0.89 by taking the product of the individual response factors. The random and uncertainty β's are calculated to be 0.19 and 0.21, respectively, for chatter and 0.19 and 0.29, respectively, for trip and are determined by taking the SRSS of the individual random and uncertainty logarithmic standard deviations.

5.2.4.3 480 VAC Motor Control Center Structural Response Factor

The applicable Structural Response Factor for the Motor Control Centers is taken from Table 5-4 for the most critical location which is within the Auxiliary Building which reaches both its yield and failure capacities prior to failure of the Motor Control Centers. The Structural Response Factor and its variabilities are:

$\check{F}_{SR} = 1.62$

$\beta_{SR_R} = 0.21$

$\beta_{SR_U} = 0.21$

5.2.4.4 480 VAC Motor Control Center Acceleration Capacity

The ground acceleration capacities for both chatter and trip failure of the Motor Control Centers is calculated as the product of the three main fragility factors in Equation 5-1 by the SSE ground acceleration level of 0.17 g's. The overall randomness and uncertainty logarithmic standard deviations were calculated from Equation 5-3. The resulting acceleration capacities for the two functional failure modes is:

Chatter	Trip
$\check{A} = 1.09$ g	$\check{A} = 2.21$ g
$\beta_R = 0.28$	$\beta_R = 0.28$
$\beta_U = 0.36$	$\beta_U = 0.57$

The factors and variabilities contributing to the fragility descriptions of the Motor Control Centers are presented in Table 5-9.

5.2.5 Example of Fragility Based on Engineering Judgment and Earthquake Experience

There are several equipment items within the list of components for the Millstone PRA for which no seismic qualification was required. These components were not designed for seismic loading; thus, they will generally have a lower capacity and a higher uncertainty than seismically qualified components. The methodology which has been utilized on the previous four examples of developing capacity factors, response factors, duration factors, etc., is generally not applicable for unqualified components. The fragility levels for these unqualified components must

be derived based on earthquake experience and engineering judgment. The example which has been chosen in this category is the station off-site power.

5.2.5.1 Offsite Power Ground Acceleration Capacity

Failure of offsite power is governed primarily by failure of ceramic insulators. A review of insulator failure in six major earthquakes, ranging from 0.11g to 0.4g peak ground acceleration, resulted in a median capacity for ceramic insulators of:

$$\breve{A} = 0.20g$$

where $\breve{A}$ is the median peak ground acceleration capacity. The logarithmic standard deviation on this value is about 0.32 of which the estimated randomness, β_R, is about 0.20 and the uncertainty, β_U, is about 0.25.

5.3 EQUIPMENT FRAGILITY RESULTS

Table 5-1 contains fragility descriptions for all of the equipment which were selected for this PRA study. Fragility derivations were conducted for each of these components and are reported for those items which have a ground acceleration capacity less than 2.5 g's based on their Capacity and Equipment Response Factors only. It is judged that equipment with ground acceleration capacities greater than 1.5 g's will not significantly influence the Millstone 3 risk. Table 5-1 contains several components with ground acceleration capacities greater than 2.5 g's. These components did not have ground acceleration capacities above 2.5 g's based on their Capacity and Equipment Response Factors but their Structural Response Factors were sufficiently high so as to increase the final acceleration capacity ($\breve{A}$) above 2.5 g's.

Table 5-10 contains a list of those components which have ground acceleration capacities less than 1.5 g's. These components will all, to some degree, enter into the overall plant risk.

TABL

SUMMARY OF MILLSTONE 3

Component	Location	Equipment Characteristics	Seismic Qualification Method	Failure Mode	E
Reactor Vessel Core	CS, Various	Flexible, Passive	Dynamic Analysis	Upper Support Plate	
Control Rod Drives	CS, Atop RPV	Flexible, Active	Dynamic Analysis	Rod Travel Housing	
RPV In-Core Instrumentation	CS,-27'-3"	Flexible, Passive	Dynamic Analysis	Instrumentation Tube	
Pressurizer Relief Tank	CS,-27'-3"	Rigid, Passive	Static Analysis	Vessel Shell	
RHR Pump	ESF, 4'-6"	Rigid, Active	Dynamic Analysis	Nozzle Flange	
RHR Heat Exchanger	ESF, 4'-6"	Flexible, Passive	Static Analysis	Heat Exchanger Shell	
Reactor Trip Breaker	CB, 47'-0"	Flexible, Passive	Test	Anchor Bolt	
Off-Site Power	Yard	Flexible, Passive	None	Insulators	
Containment Recirculation	CS, 28'-3"	Rigid, Passive	Static Analysis	Upper Restraint Pin	
BOP Piping*	Various	Flexible, Passive	Dynamic Analysis	Supports	
Quench Spray Pump	ESF, 19'-6"	Rigid, Active	Static Analysis	Pump Hold Down Bolts	
Component Cooling Water Pump	Aux, 24'-6"	Rigid, Active	Static Analysis	Impeller Impact	
Component Cooling Surge Tank	Aux, 66'-6"	Rigid, Passive	Static Analysis	Anchor Bolt	
Motor Driven Aux Feed Pump	ESF, 19'-6"	Rigid, Active	Static Analysis	Impeller Impact	
ESF Logic Panel	CB, 47'-0"	Rigid, Passive	Test	Function	
4160 volt Switchgear	CB, 4'-6"	Flexible, Passive	Test	Chatter Trip	
Emergency Diesel Generator	EGE, 24'-6"	Flexible, Passive	Static Analysis	L.O. Cooler Anch[illegible]s	
125 VDC Batteries	CB, 4'-6"	Rigid, Passive	Test	Function	
125 VDC Distribution Switchgear	CB, 4'-6"	Flexible, Passive	Test	Trip	
120 VAC Converter	CB, 4'-6"	Flexible, Passive	Test	Function	
480 VAC Motor Control Center	Various	Flexible, Passive	Test	Chatter Trip	

*Does not apply to piping subject to building sliding
**Factor on OBE ground acceleration

1

PONENT FRAGILITIES

nt Capacity Factor		Equipment Response Factor			Structural Response Factor			Ground Acceleration Capacity			
β_{EC_R}	β_{EC_U}	$\bar{F}_{ER}$	β_{ER_R}	β_{ER_U}	$\bar{F}_{SR}$	β_{SR_R}	β_{SR_U}	$\bar{A}$	β_R	β_U	β_C
4 0.00	0.14	1.03	0.18	0.17	1.70	0.25	0.24	0.99	0.31	0.33	0.45
9 0.00	0.15	1.05	0.17	0.25	1.70	0.25	0.24	1.00	0.30	0.38	0.48
NA	NA	NA	NA	NA	NA	NA	NA	>2.50	NA	NA	NA
NA	NA	NA	NA	NA	NA	NA	NA	>2.50	NA	NA	NA
NA	NA	NA	NA	NA	NA	NA	NA	>2.50	NA	NA	NA
6 0.03	0.20	4.48	0.14	0.20	1.46	0.19	0.34	1.73	0.24	0.44	0.50
4 0.00	0.28	2.88	0.20	0.38	1.47	0.22	0.23	1.04	0.30	0.53	0.60
NA	NA	NA	NA	NA	NA	NA	NA	0.20	0.20	0.25	0.32
2 0.00	0.20	2.05	0.20	0.42	1.46	0.25	0.24	0.82	0.32	0.52	0.61
1** 0.31	0.41	1.86	0.19	0.24	1.62	0.21	0.21	2.17	0.42	0.52	0.67
5 0.00	0.47	1.70	0.13	0.35	1.46	0.19	0.34	2.93	0.23	0.68	0.72
9 0.00	0.17	1.00	0.13	0.19	1.62	0.21	0.21	1.13	0.25	0.33	0.11
7 0.00	0.27	1.00	0.03	0.10	1.62	0.21	0.21	3.16	0.21	0.36	0.41
1 0.00	0.17	1.00	0.01	0.16	1.46	0.19	0.34	3.30	0.19	0.41	0.45
0 0.00	0.38	4.62	0.00	0.29	1.47	0.22	0.23	1.39	0.22	0.38	0.44
0 0.00	0.08	2.89	0.20	0.35	1.49	0.21	0.17	0.88	0.29	0.40	0.49
6 0.00	0.74	0.89	0.18	0.32	1.49	0.21	0.17	3.09	0.28	0.81	0.86
2 0.00	0.31	0.92	0.12	0.10	1.60	0.21	0.28	0.91	0.24	0.42	0.49
0 0.00	0.11	8.53	0.19	0.24	1.00	0.21	0.17	1.74	0.29	0.31	0.43
0 0.00	0.08	6.82	0.15	0.24	1.23	0.21	0.17	1.71	0.26	0.30	0.40
0 0.00	0.08	5.15	0.19	0.30	1.30	0.21	0.17	1.37	0.28	0.35	0.45
0.00	0.21	0.89	0.19	0.21	1.62	0.21	0.21	1.09	0.28	0.36	0.46
0.00	0.22	0.89	0.19	0.29	1.62	0.21	0.21	2.21	0.28	0.57	0.63

TABLE 5-2

EQUIPMENT SPECTRAL SHAPE FACTORS

Building	Elevation	Frequency Range (Hz)	F_{SS}	$\beta_{SS_R}^*$	β_{SS_U}
Control Building	24'-6"	6-9 5-20	1.11 1.04	0.00	0.05 0.02
Auxiliary Building	24'-6"	6.5-10 5-20	1.15 1.05	0.00	0.07 0.02
	43'-6"	6.5-10 5-20	1.24 1.09	0.00	0.11 0.04
	66'-6"	6.5-10 5-20	1.27 1.10	0.00	0.12 0.05
Reactor Containment Internal Structures	24'-6"	4-6.5 5-20	1.18 1.06	0.00	0.08 0.03
Engineered Safety Features Building	19'-6"	9.5-15.5 5-20	1.13 1.05	0.00	0.06 0.02
	36'-6"	9.5-15.5 5-20	1.21 1.07	0.00	0.10 0.04

*NOTE: All variability from peak broadening is due to uncertainty

TABLE 5-3

EARTHQUAKE COMPONENT COMBINATION FACTORS

Case	Description	Design = SRSS(H,V)		Design = SRSS(H)+(V)		β_R
		F_{ECC}	β_U	F_{ECC}	β_U	
1	3D Case - Median Coupling - All directional components contribute to failure	1.00	0.00	1.12	0.13	0.12
2	2D Case - Median Coupling - Both horizontal contribute to failure	1.00	0.00	1.17	0.08	0.10
3	2D Case - No Coupling - Both horizontals contribute to failure	1.00	0.00	1.00	0.00	0.06
4	2D Case - Median Coupling - 1 horizontal and the vertical contribute to failure	1.00	0.00	1.25	0.04	0.09
5	2D Case - No Coupling - 1 horizontal and the vertical contribute to failure	1.00	0.00	1.00	0.00	0.03
6	1D Case - Any one of the directional components alone is responsible for the failure	1.00	0.00	1.00	0.00	0.00

TABLE 5-4

STRUCTURAL RESPONSE FACTORS FOR EQUIPMENT

Building	Ground Acceleration Range (g)*	$\overset{v}{F}_{SR}$	β_{SR_R}	β_{SR_U}
Control Building	a) < 0.78 b) ≥ 0.78	1.26 1.47	0.22	0.23
Auxiliary Building	a) < 0.58 b) ≥ 0.58	1.38 1.62	0.21	0.21
Containment Structure	a) < 1.87 b) ≥ 1.87	1.46 1.70	0.25	0.24
Containment Internal Structure	a) < 1.02 b) ≥ 1.02	1.46 1.70	0.25	0.24
Engineered Safety Features Building	a) < 1.29 b) ≥ 1.29	1.40 1.46	0.19	0.34
Emergency Generator Enclosure**	a) < 0.80 b) ≥ 0.80	1.23 1.47	0.21	0.28

* Acceleration value shown reflects yield capacity of structure
**Based on pedestal model

TABLE 5-5

NUCLEAR POWER PLANT EQUIPMENT CATEGORIES

Relative Capacity Level	Equipment Category
High	1. Piping, Ducting, Cable Trays and Electrical Conduit 2. All Valves (Except small motor operated valves)
Medium-High	3. Small Vessels and Heat Exchangers 4. Horizontal Pumps, Compressors and Turbines 5. Fans and Air Conditioning Units 6. Diesel Generator 7. Reactor Coolant Loop Components
Medium	8. Small Motor Operated Valves 9. Large Vessels and Heat Exchangers 10. Batteries and Racks 11. Vertical Pumps 12. Reactor Internals and Control Rod Drive Mechanism
Low-Medium	13. Motor Control Centers, Switchgear, Control Panels, Instrument Racks 14. Non-seismically Qualified Components (e.g. Offsite Power System)

TABLE 5-6

FRAGILITY DERIVATION OF RHR HEAT EXCHANGER

Factors	Median Safety Factor	Randomness Variability β_R	Uncertainty Variability β_U
Capacity Factor ($\breve{F}_{EC}$)			
1. Strength	1.43	0.00	0.20
2. Ductility	1.09	0.03	0.02
Combined ⟶ $\breve{F}_{EC}$	1.56	0.03	0.20
Equipment Response Factor ($\breve{F}_{ER}$)			
1. Qualification Method	4.48	0.00	0.14
2. Spectral Shape	1.00	0.00	0.00
3. Modeling	1.00	0.00	0.15
4. Damping	1.00	0.00	0.00
5. Mode Combination	1.00	0.10	0.00
6. Earthquake Component Combination	1.00	0.10	0.00
Combined ⟶ $\breve{F}_{ER}$	4.48	0.14	0.20
Structural Response Factor ($\breve{F}_{SR}$)	1.46	0.19	0.34
Ground Acceleration Capacity ($\breve{A}$)	1.73	0.24	0.44

TABLE 5-7

FRAGILITY DERIVATION OF CONTAINMENT RECIRCULATION COOLER

Factors	Median Safety Factor	Randomness Variability β_R	Uncertainty Variability β_U
Capacity Factor ($\breve{F}_{EC}$)			
1. Strength	1.62	0.00	0.20
2. Ductility	1.00	0.00	0.00
Combined ⟶ $\breve{F}_{EC}$	1.62	0.00	0.20
Equipment Response Factor ($\breve{F}_{ER}$)			
1. Qualification Method	1.33	0.00	0.20
2. Spectral Shape	1.04	0.00	0.03
3. Modeling	1.00	0.00	0.15
4. Damping	1.36	0.06	0.31
5. Mode Combination	1.00	0.15	0.00
6. Earthquake Component Combination	1.09	0.12	0.13
Combined ⟶ $\breve{F}_{ER}$	2.05	0.20	0.42
Structural Response Factor ($\breve{F}_{SR}$)	1.46	0.25	0.24
Ground Acceleration Capacity ($\breve{A}$)	0.82	0.32	0.52

TABLE 5-8

FRAGILITY DERIVATION OF BALANCE-OF-PLANT PIPING

Factors	Median * Safety Factor	Randomness Variability β_R	Uncertainty Variability β_U
Capacity Factor ($\breve{F}_{EC}$)			
1. Strength	3.26	0.00	0.34
2. Ductility	2.46	0.31	0.23
Combined ⟶ $\breve{F}_{EC}$	8.01	0.31	0.41
Equipment Response Factor ($\breve{F}_{ER}$)			
1. Qualification Method	1.00	0.00	0.00
2. Spectral Shape	1.06	0.00	0.03
3. Modeling	1.00	0.00	0.15
4. Damping	1.57	0.03	0.14
5. Mode Combination	1.00	0.15	0.00
6. Earthquake Component Combination	1.12	0.12	0.13
Combined ⟶ $\breve{F}_{ER}$	1.86	0.19	0.24
Structural Response Factor ($\breve{F}_{SR}$)	1.62	0.21	0.21
Ground Acceleration Capacity ($\breve{A}$)	2.17	0.42	0.52

*Factor on OBE ground acceleration of .09g's

TABLE 5-9

FRAGILITY DERIVATION OF 480 VAC MOTOR CONTROL CENTERS

Factors	Median Safety Factor	Randomness Variability β_R	Uncertainty Variability β_U
Capacity Factor ($\breve{F}_{EC}$)			
1. Chatter	4.48	0.00	0.21
2. Trip	9.06	0.00	0.44
Equipment Response Factor ($\breve{F}_{ER}$)			
1. Qualification Method	1.04	0.05	0.11
2. Spectral Shape	1.00	0.00	0.00
3. Boundary Conditions	1.00	0.00	0.15
4. Damping	1.00	0.00	0.00/0.20
5. Spectral Test Method	1.00	0.14	0.10
6. Multi-Directional Effects	0.85	0.12	0.04
Combined ⟶ $\breve{F}_{ER}$	0.89	0.19	0.21/0.29
Structural Response Factor ($\breve{F}_{SR}$)	1.62	0.21	0.21
Ground Acceleration Capacity ($\breve{A}$)			
1. Chatter	1.09	0.28	0.36
2. Trip	2.21	0.28	0.57

TABLE 5-10

MILLSTONE 3 EQUIPMENT EXHIBITING GROUND ACCELERATION

CAPACITY LESS THAN 1.5 g's

Component	$\overset{v}{A}$ (g)	β_R	β_U
Off-Site Power	0.20	0.20	0.25
Containment Recirculation Cooler	0.82	0.32	0.52
4160 Volt Switchgear (Chatter)	0.88	0.29	0.40
Emergency Diesel Generator	0.91	0.24	0.43
Reactor Vessel Core	0.99	0.31	0.33
Control Rod Drives	1.00	0.30	0.38
Reactor Trip Breakers	1.04	0.30	0.53
480 VAC Motor Control Center (Chatter)	1.09	0.29	0.43
Component Cooling Water Pump	1.13	0.25	0.33
120 VAC Converter	1.37	0.28	0.35
ESF Logic Panel	1.39	0.22	0.38

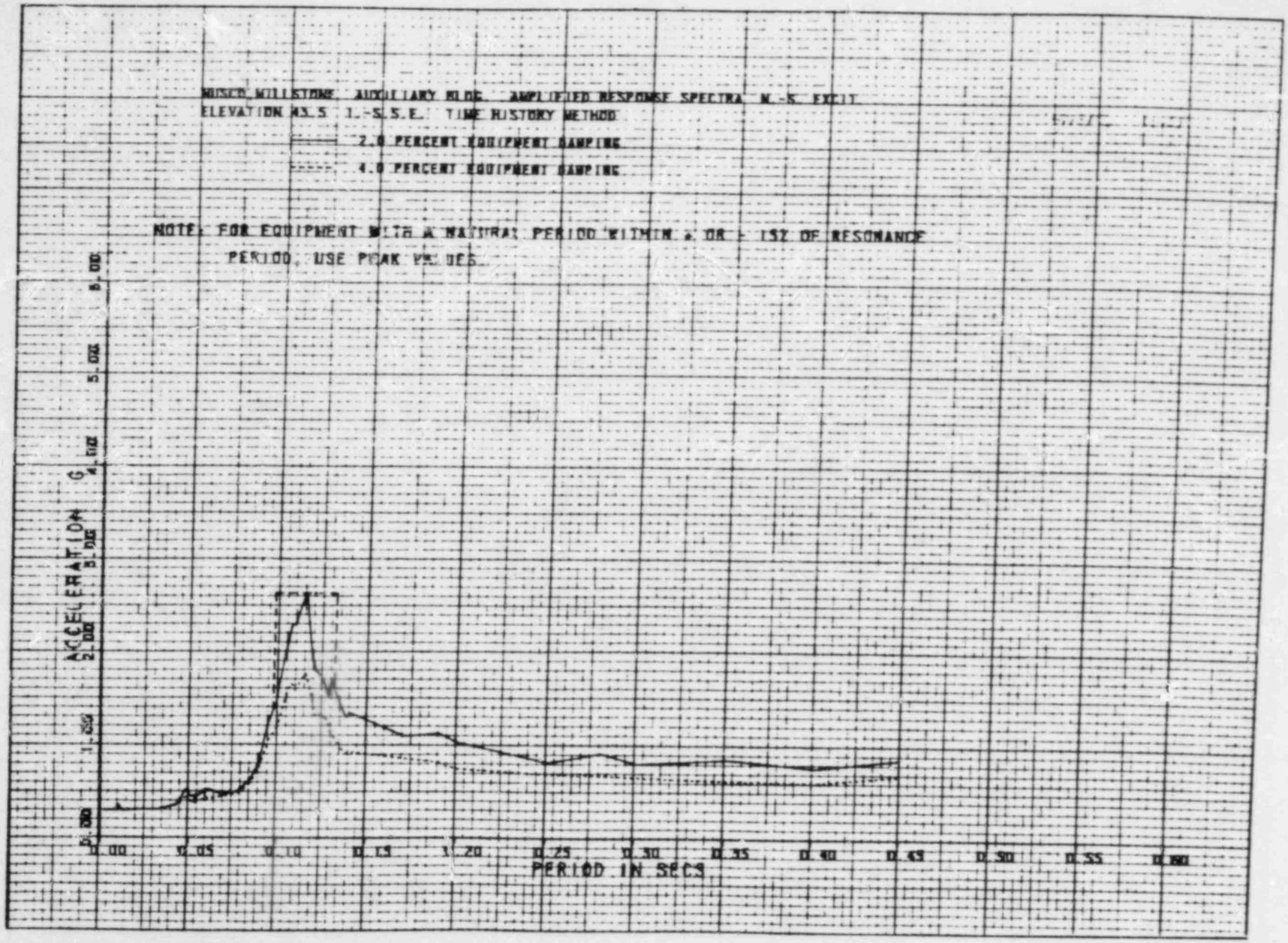

FIGURE 5-1. TYPICAL COMPARISON OF BROADENED AND UNBROADENED FLOOR RESPONSE SPECTRA

REFERENCES

1. Millstone Nuclear Power Station - Unit 3 Final Safety Analysis Report, Long Island Lighting Company.

2. USNRC, "Design Response Spectra for Seismic Design of Nuclear Power Plants", USNRC Regulatory Guide 1.60, Revision 1, December, 1973.

3. Freudenthal, A. M., J. M. Garrelts, and M. Shinozuka, "The Analysis of Structural Safety", Journal of the Structural Division, ASCE, ST 1, pp. 267-325, February, 1966.

4. Kennedy, R. P., A Statistical Analysis of the Shear Strength of Reinforced Concrete Beams, Technical Report No. 78, Department of Civil Engineering, Stanford University, Stanford, California, April, 1967.

5. Newmark, N. M., "A Study of Vertical and Horizontal Earthquake Spectra", WASH 1255, Nathan M. Newmark Consulting Engineering Services, prepared for USAEC, April, 1973.

6. Newmark, N. M., "Inelastic Design of Nuclear Reactor Structures and Its Implications on Design of Critical Equipment", SMiRT Paper K 4/1, 1977 SMiRT Conference, San Francisco, California.

7. Riddell, R., and N. M. Newmark, "Statistical Analysis of the Response of Nonlinear Systems Subjected to Earthquakes", Department of Civil Engineering, Report UILU 79-2016, Urbana, Illinois, August, 1979.

8. Bernreuter, D. L., "Seismic Hazard Analysis, Application of Methodology, Results, and Sensitivity Studies", NUREG/CR-1582, Vol. 4, Lawrence Livermore National Laboratory, October, 1981.

9. USNRC, "Damping Values for Seismic Design of Nuclear Power Plants", USNRC Regulatory Guide 1.61, October, 1973.

10. Newmark, N. M., and W. J. Hall, "Development of Criteria for Seismic Review of Selected Nuclear Power Plants", NUREG/CR-0098, May, 1978.

11. Kennedy, R. P., et al., "Probabilistic Seismic Safety Study of an Existing Nuclear Power Plant", Nuclear Engineering and Design, Vol. 59, No. 2, pp. 315-338.

12. USNRC, "Combining Modal Responses and Spatial Components in Seismic Response Analysis", USNRC Regulatory Guide 1.92, Rev. 1, February, 1976.

13. Stone and Webster calculation #12179-NiS(B)-092, Revision 0.

REFERENCES (Continued)

14. Troxell, G.E., H.E. Davis and J.W. Kelly, Composition and Properties of Concrete, McGraw-Hill, 1968.

15. Letter correspondence, N. M. Newmark to A. J. Bingaman, et al, Subject: Factor of Safety Against Sliding, June 10, 1975.

16. Mirza, S. A., M. Hatzinikolas, and J. G. MacGregor, "Variability of Mechanical Properties of Reinforcing Bars", Journal of Structural Division, ASCE, May, 1979.

17. ACI 318-71, "Building Code Requirements for Reinforced Concrete", American Concrete Institute, 1971.

18. Barda, F., J. M. Hanson and W. G. Corley, "Shear Strength of Low-Rise Walls with Boundary Elements", ACI Symposium, "Reinforced Concrete Structures in Seismic Zones", ACI, Detroit, Michigan, 1976.

19. Shiga, T., A. Shibata and J. Tabahashi, "Experimental Study on Dynamic Properties of Reinforced Concrete Shear Walls", 5th World Conference on Earthquake Engineering, Rome, Italy, 1973.

20. Cardenas, A. E., et al., "Design Provisions for Shear Walls", ACI Journal, Vol. 70, No. 3, March, 1973.

21. Oesterle, R. G., et al., "Earthquake Resistant Structural Walls - Tests of Isolated Walls - Phase II", Construction Technology Laboratories (Division of PCA), Skokie, Illinois, October, 1979.

22. "Kennedy, R. P., et al, "Engineering Characterization of Ground Motion. Effects of Characteristics of Free-Field Motion on Structural Response", SMA 12702.01, prepared for Woodward-Clyde Consultants, April, 1983.

23. Merchant, H. C., and T. C. Golden, "Investigations of Bounds for the Maximum Response of Earthquake Excited Systems", Bulletin of the Seismological Society of America, Vol. 64, No. 4, pp. 1239-1244, August, 1974.

24. NUREG/CR-1706, UCRL-15216, "Subsystem Response Review, Seismic Safety Margin Research Program", October, 1980.

25. Amplified Response Spectra for Equipment Qualification, Millstone Nuclear Power Station Unit 3, by Stone and Webster Engineering Corporation.

26. Smith, P. D. and O. R. Maslenikov, "LLNL/DOR Seismic Conservatism Program, Part III: Synthetic Time Histories Generated to Satisfy NRC Regulatory Guide 1.60", UCID-17964 (draft report), Lawrence Livermore Laboratory, Livermore, California, April, 1979.

27. "Seminar on Understanding Digital Control and Analysis in Vibration Test Systems", sponsored by Goddard Space Flight Center, Jet Propulsion Laboratory and The Shock and Vibration Information Center held at Goddard Space Flight Center on 17-18 June 1975 and at the JPL on 22-23 July 1975.

28. HNDDSP-72-156-ED-R, "Subsystem Hardness Assurance Report, Volumes I and II", U.S. Army Corps of Engineers, Huntsville Division, 30 June 1975.

29. HNDDSP-73-161-ED-R, "Subsystem Hardness Assurance Analysis, Volumes I and II", U.S. Army Corps of Engineers, Huntsville Division, 30 June 1975.

30. HNDDSP-72-151-ED-R, "Shock Tests Program Plan, Volume I, Management and Technical Plan", U.S. Army Corps of Engineers, Huntsville Division, 1 October 1973.

31. NUREG/CR-2405, UCRL-15407, Kennedy, R. P., R. D. Campbell, G. S. Hardy and H. Banon, "Subsystem Fragility - Seismic Safety Margins Research Program (Phase 1)", Structural Mechanics Associates, Inc., prepared for U.S. Nuclear Regulatory Commission, February, 1982.

32. Hardy, G.S. and R. D. Campbell, "Development of Fragility Descriptions of Equipment for Seismic Risk Assessment of Nuclear Power Plants", paper to be presented at the ASME Pressure Vessel and Piping Conference in Portland, June, 1983.

33. NUREG/CR-2137, "Realistic Seismic Design Margins of Pumps, Valves and Piping", by E.C. Rodabaugh and K. D. Desai, June, 1981.

34. Seismic Fragility Evaluation of Millstone Unit 3 Structures and Equipment, Stone and Webster Engineering Corporation, May 1983.

35. ASTM DS-552 "An Evaluation of the Yield, Tensile, Creep and Rupture Strengths of Wrought 304, 316, 321 and 347 Stainless Steels at Elevated Temperatures", American Society of Testing Materials.

36. Sargent and Lundy Report, "Evaluation of the Functional Capability of ASME Section III, Class 1, 2 and 3 Piping Components, MARK I Containment Program, Task 3.1.5.4", September 21, 1978.

37. Witt, F. J., W. H. Bamford and T. C. Esselman, "Integrity of the Primary Piping Systems of Westinghouse Nuclear Power Plants During Seismic Events", WCAP No. 9283, Westinghouse Electric Corporation, March, 1978.

38. NUREG/CR0261, ORNL/SUB-2913/8, Evaluation of the Plastic Characteristics of Piping Products in Relation to ASME Code Criteria, by E. C. Rodabaugh and S. E. More, Battelle Columbus Laboratories, July, 1978.

39. HNDDSP-72-74-ED-R, Hardness Program-Non-Emp. Test Specification and Procedure, Electric Motor Control Center Fragility Test, U.S. Army Corps of Engineers, Huntsville Division, 20 November 1972.

40. "San Fernando Earthquake of February 9, 1971: Effects on Power System Operation and Electrical Equipment", Prepared by the Design and Construction Division of the Department of Water and Power of the City of Los Angeles, October, 1971.

APPENDIX

CHARACTERISTICS OF THE LOGNORMAL DISTRIBUTION

APPENDIX

CHARACTERISTICS OF THE LOGNORMAL DISTRIBUTION

Some of the characteristics of the lognormal distribution which are useful to keep in mind when generating estimates of $\check{A}$, β_R, and β_U are summarized in References A1 and A2. A random variable X is said to be lognormally distributed if its natural logarithm Y given by:

$$Y = \ln (X) \tag{A-1}$$

is normally distributed with the mean of Y equal to $\ln \check{X}$ where $\check{X}$ is the median of X, and with the standard deviation of Y equal to β, which will be defined herein as the logarithmic standard deviation of X. Then, the coefficient of variation, COV, is given by the relationship:

$$COV = \sqrt{\exp(\beta^2)-1} \tag{A-2}$$

For β values less than about 0.5, this equation becomes approximately:

$$COV \approx \beta \tag{A-3}$$

and COV and β are often used interchangeably.

For a lognormal distribution, the median value is used as the characteristic parameter of central tendency (50 percent of the values are above the median value and 50 percent are below the median value). The logarithmic standard deviation, β, or the coefficient of variation, COV, is used as a measure of the dispersion of the distribution.

The relationship between the median value, $\breve{X}$, logarithmic standard deviation, β, and any value x of the random variable can be expressed as:

$$x = \breve{X} \cdot \exp(\eta \cdot \beta) \qquad \text{(A-1)}$$

where η is the standardized Gaussian random variable, (mean zero, standard deviation one). Therefore, the frequency that X is less than any value x' equals the frequency that η is less than η' where:

$$\eta' = \frac{\ell n\ (x'/\breve{X})}{\beta} \qquad \text{(A-5)}$$

Because η is a standardized Gaussian random variable, one can simply enter standardized Gaussian tables to find the frequency that η is less than η' which equals the probability that X is less than x'. Using cumulative distribution tables for the standardized Gaussian random variable, it can be shown that $\breve{X} \cdot \exp(+\beta)$ of a lognormal distribution corresponds to the 84 percentile value (i.e., 84 percent of the data fall below the $+\beta$ value). The $\breve{X} \cdot \exp(-\beta)$ value corresponds to the value for which 16 percent of the data fall below.

One implication of the usage of the lognormal distribution is that if A, B, and C are independent lognormally distributed random variables, and if

$$D = \frac{A^r \cdot B^s}{C^t}\ q \qquad \text{(A-6)}$$

where q, r, s and t are given constants, then D is also a lognormally distributed random variable. Further, the median value of D, denoted by $\check{D}$, and the logarithmic variance β_D^2, which is the square of the logarithmic standard deviation, β_D, of D, are given by:

$$\check{D} = \frac{\check{A}^r \cdot \check{B}^s}{\check{C}^t} \, q \qquad \text{(A-7)}$$

and

$$\beta_D^2 = r^2 \beta_A^2 + s^2 \beta_B^2 + t^2 \beta_C^2 \qquad \text{(A-8)}$$

where $\check{A}$, $\check{B}$, and $\check{C}$ are the median values, and β_A, β_B, and β_C are the logarithmic standard deviations of A, B, and C, respectively.

The formulation for fragility curves given by Equation 2-1 and shown in Figure 2-1 and the use of the lognormal distribution enables easy development and expression of these curves and their uncertainty. However, expression of uncertainty as shown in Figure 2-1 in which a range of peak accelerations are presented for a given failure fraction is not very usable in the systems analyses for frequency of radioactive release. For the systems analyses, it is preferable to express uncertainty in terms of a range of failure fractions (frequencies of failure) for a given ground acceleration. Conversion from the one description of uncertainty to the other is easily accomplished as illustrated in Figure A-1 and summarized below.

With perfect knowledge (i.e., only accounting for the random variablity, β_A), the failure fraction, f(a), for a given acceleration a can be obtained from:

$$f(a) = \phi\left(\frac{\ln(a/\check{A})}{\beta_R}\right) \qquad \text{(A-9)}$$

in which $\Phi(\bullet)$ is the standard Gaussian cumulative distribution function, and β_R is the logarithmic standard deviation associated with the underlying randomness of the capacity.

For simplicity, denote $f = f(a)$. Similarly, f' is the failure fraction associated with acceleration a', etc. Then, with perfect knowledge (no uncertainty in the failure fractions), the ground acceleration a' corresponding to a given frequency of failure f' is given by:

$$a' = \tilde{A} \exp\left[\beta_R \Phi^{-1}(f')\right] \tag{A-10}$$

The uncertainty in ground acceleration capacity corresponding to a given frequency of failure as a result of uncertainty of the median capacity can then be expressed by the following probability statement:

$$P\left[A > a'' | f'\right] = 1 - \Phi\left[\frac{\ell n(a''/A)}{\beta_U}\right] \tag{A-11}$$

in which $P[A > a'' | f']$ represents the probability that the ground acceleration A exceeds a'' for a given failure fraction f'. This probability is shown shaded in Figure A-1. However, it is desirable to transform this probability statement into a statement on the probability that the failure fraction f is less than f' for a given ground acceleration a'', or in symbols $P[f \leq f' | a'']$. This probability is also shown shaded in Figure A-1. It follows that:

$$P[f \leq f' | a''] = P[A > a'' | f'] \tag{A-12}$$

Thus, from Equations A-10 and A-11:

$$P[f \leq f' | a''] = 1 - \Phi\left[\frac{\ell n\left(a''/\tilde{A} \exp\left[\beta_R \Phi^{-1}(f')\right]\right)}{\beta_U}\right] \tag{A-13}$$

from which:

$$P[f > f' | a''] = \Phi\left(\frac{\ln\left(a''/\check{A}\ \exp\left[\beta_R\ \Phi^{-1}\ (f')\right]\right)}{\beta_U}\right) \qquad \text{(A-14)}$$

which is the basic statement expressing the probability that the failure fraction exceeds f' for a ground acceleration a" given the median ground acceleration capacity $\check{A}$, and the logarithmic standard deviations β_R and β_U associated with randomness and uncertainty, respectively.

As an example, if:

$$\check{A} = 0.77, \qquad \beta_R = 0.36, \qquad \beta_U = 0.39$$

then from Equation A-14 for typical values of f and a",

$$P[f > 0.5 | a'' = 0.40g] = 0.05$$

which says that there is a 5 percent probability that the failure frequency exceeds 0.5 for a ground acceleration of 0.40g.

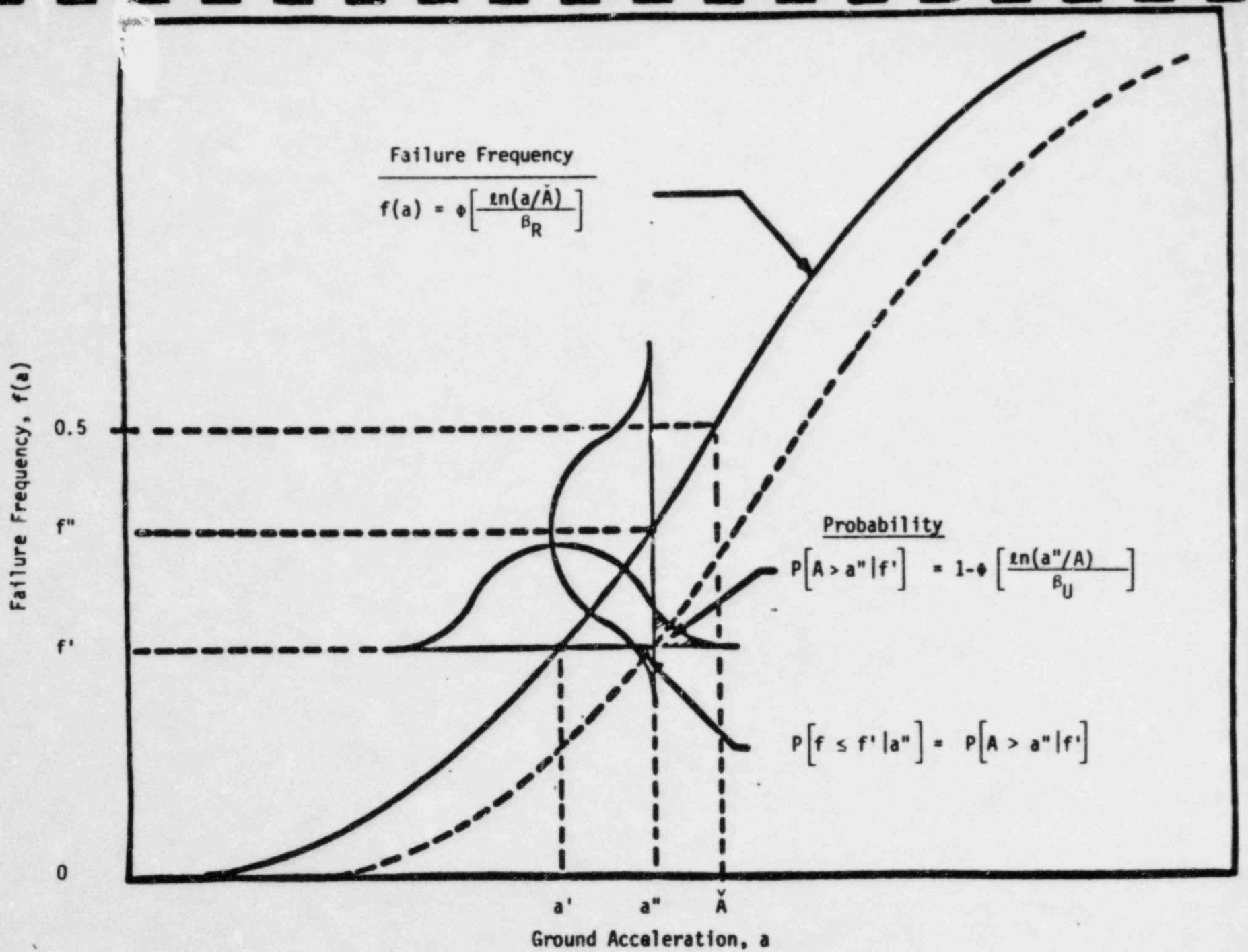

FIGURE A-1. RELATIONSHIP BETWEEN UNCERTAINTY IN GROUND ACCELERATION FOR A GIVEN FAILURE FRACTION AND UNCERTAINTY IN FAILURE FRACTION FOR A GIVEN GROUND ACCELERATION

REFERENCES

A.1 Benjamin, J. R., and Cornell, C. A., Probability, Statistics and Decision for Civil Engineers, McGraw Hill Book Company, New York, 1970.

A.2 Kennedy, R. P., and Chelapati, C. V., "Conditional Probability of a Local Flexural Wall Failure of a Reactor Building as a Result of Aircraft Impact", Holmes and Narver, Inc., prepared for General Electric Company, San Jose, California, June, 1970.